Comparison of conventional activated sludge and aerobic granular sludge reactors for microplastics removal during municipal wastewater treatment

By

Omolola Racheal Odunola

Submitted to the graduate degree program in Civil & Environmental and Architectural Engineering and the Graduate Faculty of the University of Kansas in partial fulfillment of the requirements for the degree of Master of Science.

_____

Chairperson: Belinda S.M. Sturm

_____

Edward Peltier

_____

Justin Hutchison

Date Defended: January 14, 2020

The Thesis Committee for **Omolola Racheal Odunola**

certifies that this is the approved version of the following thesis:

Comparison of conventional activated sludge and aerobic granular sludge reactors for microplastics removal during municipal wastewater treatment

_____

Chairperson: Belinda S.M. Sturm

Date approved: January 30, 2020

Abstract

The objective of this study was to investigate the performance of the conventional activated sludge (CAS) process and the relatively new biofilm process, aerobic granular sludge (AGS) for microplastics removal. In addition, the likely influence of aggregate extracellular polymeric substances on microplastics removal was assessed.

Two lab-scale sequential batch reactors were operated for both processes for two experimental phases: an organic loading rate (OLR) of 0.9 and 0.6 kg COD m^{-3} day^{-1} with sodium acetate as the sole carbon source. The microplastics removal efficiency obtained in both phases was then compared. Microplastics removal was quantified using epi-fluorescent microscopy while adsorption to EPS was observed through EPS staining and confocal microscopy.

The results showed that larger sized microplastics (100 – 150 μm) generally had higher removal efficiencies than smaller sized microplastics (40 – 90 μm). Overall, microplastics removal efficiencies obtained in the 0.6 kg COD m^{-3} day^{-1} phase (96% and 94% in CAS and AGS respectively) were higher than those measured in the 0.9 kg COD m^{-3} day^{-1} phase (69% and 77% in CAS and AGS respectively). This difference was likely due to the presence of more loosely bound EPS fractions and smaller-sized aggregates in the 0.6 kg COD m^{-3} day^{-1} phase. Furthermore, confocal microscopy investigations demonstrated that microplastics were mostly located either close to the surface of granules or at the edge of flocs suggesting that microplastics were adsorbed to the outer parts of aggregates. Therefore, both CAS and AGS technologies can effectively remove microplastics with small aggregate size and a disperse morphology.

ACKNOWLEDGEMENTS

I would like to sincerely appreciate my advisor and committee chair, Dr. Belinda Sturm for her continuous support, patience, and encouragement throughout the duration of my graduate study at the University of Kansas. Her guidance was key to the successful completion of my study.

I am thankful to the National Science Foundation (NSF #1707069) for generously funding this research.

My gratitude goes to my thesis committee members: Dr. Edward Peltier and Dr. Justin Hutchison for taking time out of their busy schedule to review my research and give constructive criticisms.

To every person that has trained me and helped with my research, I express utmost gratitude. The list includes but is not limited to: Dr. Qiang Ye, Heather Shinogle, Noraida Martinez-Rivera, Rasha Faraj, Abdullah Ibrahim, Devinda Hiripitiyage and Tyler Mayo.

In addition, I wish to thank, especially, my best friend, Peter Adigun for his unceasing willingness to lend a listening ear, and his words of encouragement. I appreciate my good friends, Wole and Cha-cha for the helpful science discussions, for always making me laugh when I am stressed and for making my graduate study a fun ride.

Last but not least, my appreciation goes to my family for their immense support, prayers, and for cheering me on regardless.

TABLE OF CONTENTS

LIST OF TABLES

LIST OF FIGURES

NOMENCLATURE

Acronym / symbol	Description
mm	Millimeter
WWTPs	wastewater treatment plants
CAS	conventional activated sludge
AGS	aerobic granular sludge
EPS	extracellular polymeric substance
PCBs	polychlorinated biphenyls
PAHs	polycyclic aromatic hydrocarbons
POPs	persistent organic pollutants
PE	polyethylene
PP	polypropylene
PS	polystyrene
PET	polyethylene terephthalate
PVC	polyvinyl chloride
SBR	sequencing batch reactor
α	alpha
g	gram
L	liter
LB	loosely bound
TB	tightly bound
f/m	food to microorganism ratio
OLR	organic loading rate
EDTA	ethylene diamine tetra acetic acid
CER	cation exchange resins
NaCl	sodium chloride
ALE	alginate-like extracellular polymers
ESEM	environmental scanning electron microscopy
AFM	atomic force microscopy

CLSM	confocal laser scanning microscopy
FT-IR	fourier transform infrared spectroscopy
rbCOD	readily biodegradable chemical oxygen demand
COD	chemical oxygen demand
VSS	volatile suspended solids
MLSS	mixed liquor suspended solids
ESS	effluent suspended solids
SVI	sludge volume index
cm	centimeter
mL	milliliter
min	minute
HRT	hydraulic retention time
m	meter
kg	kilogram
µm	micrometer
nm	nanometer
FITC	fluorescein-isothiocyanate
Con A	concanavalin A
WGA	wheat germ agglutinin
PBS	phosphate-buffered saline
rpm	revolutions per minute
w/v	weight to volume ratio
µL	microliter
PAOs	phosphorus accumulating organisms
DPAOs	denitrifying phosphate accumulating organisms
DGAOs	denitrifying glycogen accumulating organisms
SND	simultaneous nitrification/denitrification

1. INTRODUCTION

The production of plastics has grown rapidly since its invention in the 1900s (Cole et al. 2011). These synthetic organic polymers are being used in an endless spectrum of applications, ranging from shipping or packaging, household appliances, electronics, construction, automotive and airplane components to medicine (Goodship 2007), with the United States of America being a major plastic producer (Nuelle et al. 2014). The breakdown of large plastics into minuscule sizes less than 5 mm called microplastics has brought about increased scientific concern in recent years. This is due to their ubiquitous distribution, potential for bioaccumulation and biomagnification, resistance to degradation, hydrophobicity, and small size, which makes them difficult to detect (Cole et al. 2011; Rochman, Kross, et al. 2015; Nizzetto, Futter, and Langaas 2016).

Microplastics originate from personal care products such as cosmetics, sunscreen, toothpaste, body and face washes (Rochman, Kross, et al. 2015; Derraik 2002; Fendall and Sewell 2009), cleaning supplies (Browne et al. 2011), household and laundry dust, industrial processes, automobile tire wear, and plastic surface deterioration (Nizzetto, Futter, and Langaas 2016; Gregory 1996). These microplastics can be transported to wastewater treatment plants (WWTPs). Although over 90% of microplastics have been reported to be retained in sewage sludge during primary and secondary treatment (Nizzetto, Futter, and Langaas 2016; Carr, Liu, and Tesoro 2016), effluent release into the environment is evident (Magnusson and Norén 2014; Mintenig et al. 2017; Ziajahromi et al. 2017). Increase in urbanization and population growth globally implies an increasing quantity of wastewater produced, and subsequently more microplastics release from WWTPs into the environment (Browne et al. 2011; Ziajahromi, Neale, and Leusch 2016). Hence,

an understanding of the effectiveness and mechanism of microplastics removal by WWTPs might help in reducing their contribution to microplastics pollution.

The most common biological wastewater treatment method used for both municipal and industrial plants is the conventional activated sludge (CAS) process (Wei et al. 2003; Ahmed et al. 2017), which utilizes the use of microbial aggregates to remove solids and nutrients. A relatively new treatment technology, aerobic granular sludge (AGS), involves the use of denser granules with higher settling velocities than CAS (McSwain et al. 2005). The properties of microbial aggregates have been shown to depend largely on their extracellular polymeric substance (EPS) (Sheng, Yu, and Li 2010; Liu, Liu, and Tay 2004). Properties including adsorption ability, settling, surface charge, flocculation, and granulation can influence the removal of microplastics in wastewater. It was therefore determined that an investigation of the role of EPS in microplastics removal would be required to select an effective biological wastewater treatment technology.

2. BACKGROUND

2.1 Microplastics pollution in the environment: impacts, sources and transport

The environmental contamination of microplastics is well established. Microplastics have been detected in both aquatic and terrestrial habitats (Eerkes-Medrano, Thompson, and Aldridge 2015; Ziajahromi et al. 2017), and the impact of their presence on aquatic organisms has been reported by many studies (Cole et al. 2011; Andrady 2011). Because of their hydrophobicity, microplastics can accumulate persistent organic pollutants such as polychlorinated biphenyls (PCBs) and polycyclic aromatic hydrocarbons (PAHs) (Teuten et al. 2009). Frias et. al. (2010) identified and quantified persistent organic pollutants (POPs) that had been adsorbed to stranded microplastics pellets obtained from two beaches (Frias, Sobral, and Ferreira 2010). Aquatic organisms readily ingest microplastics due to their small size, creating a route for possible accumulation of hydrophobic contaminants and negative health consequences (Browne et al. 2011). Microplastics can also be transferred along the food web through predator-prey relationship (bio-magnification), making it very likely to be ingested by humans through contaminated sea-food consumption (Rochman, Tahir, et al. 2015; Miranda and de Carvalho-Souza 2016). A study by Setälä et al. (2014) showed the transfer of polystyrene microspheres from mesozooplankton to macrozooplankton using planktonic organisms (Setälä, Fleming-Lehtinen, and Lehtiniemi 2014), while Miranda and Freire de Carvalho-Souza (2016) identified microplastics in the stomachs of two species of important edible fish (Miranda and de Carvalho-Souza 2016).

Microplastics can be manufactured (primary sources) as microbeads used in cleaning or personal care products (Cole et al. 2011; Fendall and Sewell 2009), or they can be produced due to disintegration of macroplastics (secondary sources) (Browne et al. 2011; Cole et al. 2011). Common classes of plastics found in the marine environment include polyethylene (PE),

polypropylene (PP), polystyrene (PS), polyethylene terephthalate (PET), and polyvinyl chloride (PVC) (Andrady 2011). Although locating all sources of microplastics release into the environment can be challenging, some land-based and aquatic-based pathways have been identified (Hammer, Kraak, and Parsons 2012), of which urban runoff and effluent disposal from wastewater treatment plants are prominent (Ziajahromi et al. 2017; Eerkes-Medrano, Thompson, and Aldridge 2015; Wagner et al. 2014).

2.2 Microplastics in water and resource recovery facilities

The detection of microplastics in the marine environment by several studies in recent years led to the suspicion that wastewater effluent is a potential source of contamination (Gallagher et al. 2016; Ziajahromi et al. 2017; McCormick et al. 2014). Moreover, several studies such as those carried out by Ziajahromi et al. (2017), Mintenig et al. (2017), Michielssen et al. (2016), and Talvitie et al. (2015) have identified microplastics in municipal wastewater treatment plant effluents (Ziajahromi et al. 2017; Mintenig et al. 2017; Michielssen et al. 2016; Talvitie et al. 2015). Ziajahromi et al. (2017) found an average concentration between 0.2 and 1.5 microplastics per liter of treated effluent. Although the concentration of microplastics in treated effluent seem to be small, Murphy et al. (2016) calculated a daily release of 6.5×10^7 microplastics into receiving waters from a municipal WWTP effluent despite a retention capacity of 98.41%. Mintenig et al. (2017) showed that between 9×10^7 and 4×10^9 microplastic particles were discharged annually from each of twelve sampled WWTPs in Lower Saxony, Germany. In a study of microplastic pollution from 17 municipal wastewater treatment plants, Mason et al. (2016) reported a daily release of over 4 million microplastics per facility, despite an average of 0.05 ± 0.024 microplastics found per liter of effluent across the facilities. Hence, wastewater effluent is a significant pathway for microplastics release into the aquatic environment.

Microplastics are conveyed to municipal WWTPs through microbeads in personal care products and cleaners, and microplastic fibers from synthetic textiles released during laundry. With the increasing human population growth, microbead-containing products and synthetic textile is increased, and more microplastics will be conveyed to domestic wastewater infrastructures (Browne et al. 2011). Although an overall microplastics retention efficiency of over 99% has been recorded in a WWTP using a combination of treatment processes including biological treatment (Talvitie et al. 2017), it is probable that due to small size, the removal of microplastics by WWTPs is ineffective (Browne et al. 2011; Fendall and Sewell 2009; McCormick et al. 2014; Murphy et al. 2016). The removal efficiency is probably influenced by the treatment technology and operating conditions employed. An understanding of the wastewater treatment process would most likely give insight into microplastics removal mechanism.

2.3 Biological wastewater treatment process

In biological wastewater treatment; dissolved and particulate organic contaminants are transformed to biomass and evolved gases, suspended and colloidal solids are captured within a biological floc or biofilm, and nutrients such as nitrogen and phosphorus are removed (Tchobanoglous et al. 2014; Wei et al. 2003). The most commonly used biological treatment process is the activated sludge process (Wei et al. 2003) which involves the use of mostly flocculent sludge (CAS). However, the use of sludge containing self-immobilized granular shaped microbial aggregates (AGS) has been reported to be a promising method of wastewater treatment (Chen et al. 2019; Adav et al. 2008).

2.3.1 Conventional activated sludge process

The activated sludge process requires the presence of dissolved oxygen to produce an activated mass of microorganisms efficient in stabilizing wastewater (Buttiglieri and Knepper 2007; Ahmed et al. 2017; Klatt and LaPara 2003). The formation of floc particles ranging between 50 to 200 µm is critical to the activated sludge process (Tchobanoglous et al. 2014). A schematic of a full-scale activated sludge treatment plant is shown in figure 2-1. After preliminary treatment e.g. grit, sand and oil removal, incoming wastewater and biomass are mixed and aerated in the aeration tank to allow for the biodegradation of the dissolved organic content in the wastewater (Blackall et al. 2002; Klatt and LaPara 2003). This is followed by a separation of the sludge from the treated effluent by gravity clarification. The separated biomass is then either returned back to the aeration tank or removed from the system as a waste byproduct (Klatt and LaPara 2003). The CAS treatment is often designed to eliminate or reduce pathogens and bulk organic and inorganic compounds to prevent pollution and subsequent eutrophication of receiving waters (Buttiglieri and Knepper 2007).

A sequencing batch reactor (SBR) system can combine the functions of biological transformations and solids separation as described above in a single unit (Jenkins, Richard, and Daigger 2003) allowing for less space requirements, less operator attention, and smaller footprints, compared to the flow scheme. The SBR system is a fill-and-draw activated sludge system involving recurring cycles in the following time-based sequence: fill, react, settle, decant, and idle (Ab Halim et al. 2016). During the react phase, the reactor is aerated and transformation of pollutants by a mixed population of microorganisms occurs. During the settling phase, activated sludge flocculate and is separated from treated wastewater by gravity sedimentation, which allows for the effluent to be decanted during the decant phase (Jenkins, Richard, and Daigger 2003; Ab

Halim et al. 2016). Biomass retention depends on the sedimentation step which subsequently depends on the flocculation or granulation property of the sludge (Dutta et al. 2014).

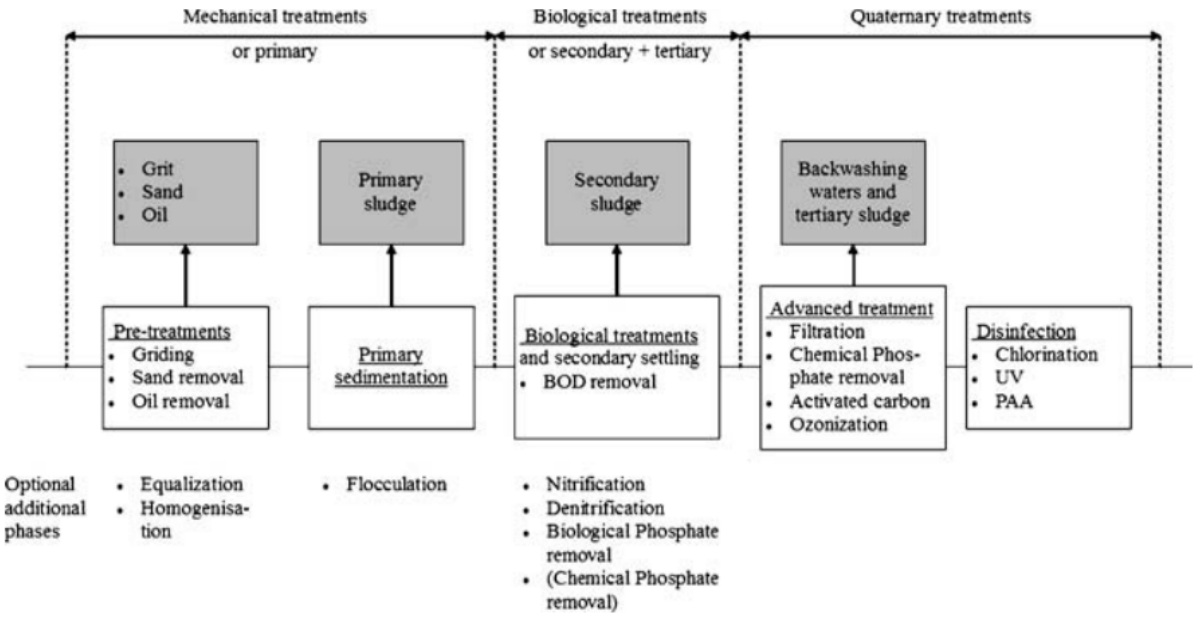

Figure 2-1: Scheme of a full-scale conventional activated sludge treatment plant. Materials produced in each section are indicated in grey boxes. Diagram obtained from Buttiglieri and Knepper (2007)

2.3.2 Aerobic granular sludge process

Aerobic granular sludge is considered to be a special case of biofilm, which researchers have shown to be more efficient for water purification than suspended activated sludge (Adav et al. 2008). The AGS technology was developed in the Netherlands at laboratory scale (Heijnen and Van Loosdrecht 1998). The first full-scale application of the process was reported in 2011 (Van der Roest et al. 2011; van Dijk, Pronk, and van Loosdrecht 2018). In the AGS process, granulation is achieved in SBRs by reducing the settling time such that poor settling flocs are washed out, and fast-settling granules are retained in the biomass (Bassin et al. 2019). Aerobic granules are more compact and dense, with a higher settling velocity and lower sludge volume index compared to

flocculent sludge (Bassin et al. 2019; Tay, Liu, and Liu 2001b). Hence, the aerobic granular sludge process is considered an efficient substitute for conventional activated sludge technology in biological wastewater treatment (Adav et al. 2008). Sludge granules are usually spherical with an average size of 0.3 – 8.0 mm and density of 1.004 – 1.065 g/L (Tay, Liu, and Liu 2001b; Mishima and Nakamura 1991). Microbial aggregates are comprised mainly of water, biomass and extracellular polymeric substances (EPS) (Keiding, Wybrandt, and Nielsen 2001). EPS has been shown to play a significant role in the formation, structure, and stability of biofilms and aerobic granules (Schmidt and Ahring 1994; Liu and Tay 2001).

2.4 Extracellular polymeric substances (EPS)

EPS consists mostly of high molecular weight secretions from microorganisms and products derived from cell lysis and hydrolysis of macromolecules (Sheng, Yu, and Li 2010). EPS can be categorized into bound EPS and soluble EPS (Liu and Fang 2003; Nielsen and Jahn 1999), with both forms capable of being separated by centrifugation. The structure of bound EPS shown in figure 2-2 is usually a two-layer model consisting of a stable inner layer – tightly-bound EPS (TB-EPS), and a loose outer layer – loosely-bound EPS (LB-EPS) (Sheng, Yu, and Li 2010).

EPS is composed primarily of carbohydrates and proteins (Sheng, Yu, and Li 2010; Bura et al. 1998; Frølund et al. 1996; Nouha et al. 2018), with humic substances also suggested as a key component in activated sludge (Frølund et al. 1996). However, other polymers like phospholipids, glycoproteins, nucleic acids, and uronic acids have been found in EPS obtained from different matrices (Adav and Lee 2008; Tsuneda et al. 2001). The production of EPS by microorganisms plays a significant role in the activated sludge and granular sludge treatment technologies.

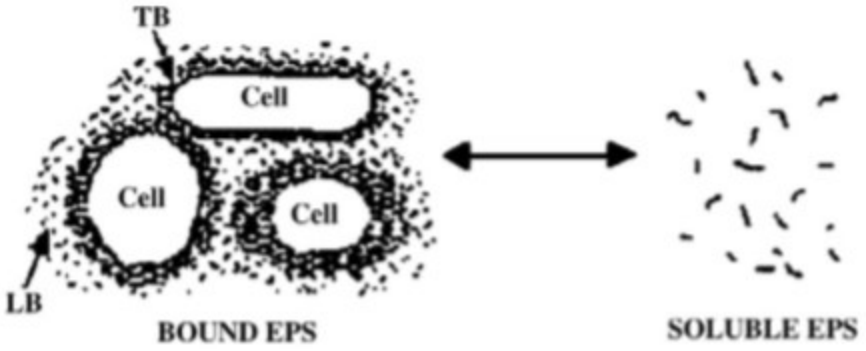

Figure 2-2: EPS structure; obtained from (Sheng, Yu, and Li 2010)

2.4.1 Production of EPS and role in microbial aggregates

The production of EPS is affected significantly by organic loading (Sheng, Yu, and Li 2010; Durmaz and Sanin 2001; Liu and Fang 2003). Janga et al. (2007) showed that increases in the food to microorganism ratio (f/m) ratio in a submerged membrane bioreactor led to an increase in the total EPS content. Other factors such as substrate type, cultivation time, presence of toxic pollutants (e.g. heavy metals), and operating conditions (reactor shear rate, pH, temperature, aerobic or anaerobic conditions) can also influence EPS production (Sheng, Yu, and Li 2010; Nouha et al. 2018). Flocculation and aggregation of bacteria cells and suspended solids is enhanced through interactions between EPS and biomass such as ion bridging, electrostatic interactions, hydrogen bonding, and Van der Waal's forces (Nouha et al. 2018). As a result, EPS affects sludge settling, dewatering, metal complexation, and toxic organic contaminant removal (Chien, Lin, and Wu 2013; Nouha et al. 2016).

EPS provides structure for both activated sludge and granular sludge (Seviour et al. 2018) by cohesive and adhesive interactions between cells, and binding with divalent cations such as Ca^{2+} and Mg^{2+} (Mayer et al. 1999; Sheng, Yu, and Li 2010). Structure plays an important role in

the stability of microbial aggregates, which is crucial for the efficient separation of biomass from water (Mayer et al. 1999). Quarmby and Forster (1995) showed that granules became weaker with increasing surface negative charge of cells, and extracellular polymers of weak granules had lower polysaccharide content compared to strong granules. Mikkelsen and Nielsen (2001) found that a higher sludge EPS content resulted in greater sludge stability. Furthermore, microorganisms can utilize EPS as carbon and energy reserves during starvation, and as protective layer against harsh external conditions (Liu and Fang 2002).

EPS contains both hydrophilic and hydrophobic groups, which can serve as sorption sites for organic pollutant adsorption (Späth, Flemming, and Wuertz 1998). The composition of EPS can influence the relative ratio of the two groups (Sheng, Yu, and Li 2010). Jorand, Boue-Bigne, et al. (1998) separated the hydrophilic and hydrophobic fractions of EPS extracted from activated sludges from a variety of sources using XAD resin and discovered that the hydrophobic fraction consisted mainly of proteins, while carbohydrates were a major composition of the hydrophilic fraction. The hydrophobicity of microbial aggregates might be influenced by the hydrophobic properties of EPS (Liu and Fang 2003). This property is also likely to influence the adsorption or removal of microplastics in activated sludge given the hydrophobicity of plastics.

2.4.2 EPS extraction

EPS can be extracted through physical processes such as centrifugation, ultrasonication and heating; chemical methods such as alkaline treatment, ethylene diamine tetra acetic acid (EDTA), cation exchange resins (CER), and ethanol extraction; or a combination of both methods (Sheng, Yu, and Li 2010). It is near impossible to completely extract all the components of EPS through a single method due to their complexity (Felz et al. 2016). The extraction efficiency of each method varies from one to another, with chemical methods generally reported to be more

efficient than physical methods (Comte, Guibaud, and Baudu 2006). Ideally, an EPS extraction method should cause minimal cell lysis and maintain EPS structure (Frølund et al. 1996). However, McSwain et al. (2005) reported that it might be necessary to breakup granules mechanically before chemical extraction due to the large size of the aggregates.

Different components of EPS can be extracted using suitable methods of extraction. For instance, centrifugation is usually used for soluble EPS (Sheng, Yu, and Li 2010) and loosely-bound EPS. For bound EPS, several methods have been employed (Nielsen and Jahn 1999; Felz et al. 2016). Li and Yang (2007) used a modified heat extraction method which involved a mild step of centrifugation and NaCl dilution, and a harsh step of heat and centrifugation for extracting LB-EPS and TB-EPS, respectively. Extraction methods specific for gel-forming polymers known as alginate-like extracellular polymers (ALE) were developed by Felz et al. (2016). Alginate is a heteropolysaccharide composed of D-mannosyl and L-glucuronosyl residues, produced by *Pseudomonas aeruginosa* and *Azotobacter vinelandii* (Nouha et al. 2018). Since each method has its own advantages and disadvantages, it would be best to compare the methods and choose the most efficient one for the specific EPS fraction desired. It might become necessary to use a combination of methods to extract different EPS fractions (Sheng, Yu, and Li 2010).

2.4.3 EPS quantification methods

The contents of EPS can be quantified using conventional chemical colorimetric analyses. Methods for quantifying carbohydrates include the Anthrone method (Gaudy 1962) and the phenol-sulfuric acid method (Dubois et al. 1956b). For measuring protein content, common methods are the Lowry method (Lowry et al. 1951), the Bradford method (Bradford 1976), or the total N-content method (Sheng, Yu, and Li 2010). Raunkjær et al. (1994) compared methods for analyzing carbohydrate, protein, and lipid content in domestic wastewater and found that the

Anthrone method and the Lowry method were most suitable for measuring carbohydrate and protein content respectively (Raunkjær, Hvitved-Jacobsen, and Nielsen 1994). However, Frolund et al. (1996) in a comparison of analytical methods for measuring sludge and EPS extracts, showed that although the Anthrone method yielded similar results to the phenol-sulfuric acid method for carbohydrate quantification, the Anthrone method had a lower coefficient of variation compared to the phenol-sulfuric method. Moreover, the Lowry method for protein measurement had a higher recovery than the Bradford method (Frølund et al. 1996). The total N-content method is very effective but has complex procedures (Frølund et al. 1996). Thus, the Lowry method is often used for protein quantification (Sheng, Yu, and Li 2010). Rao and Pattabiraman (1989) indicated that both the Anthrone and Phenol-sulfuric methods generate different absorbance maxima and intensity for different saccharide structures. Hence, the total sugar content of exopolysaccharides can be underestimated especially with non-hexose sugars (Seviour et al. 2012). All the above methods would require EPS to be extracted from sludge first before quantification.

Another approach of quantifying EPS is to directly observe microbial aggregates using microscopy, such as environmental scanning electron microscopy (ESEM) (Beech et al. 1996), atomic force microscopy (AFM) (Li and Logan 2004), or confocal laser scanning microscopy (CLSM) (Zhang and Fang 2001; McSwain et al. 2005). This approach coupled with fluorescent staining allows the original shapes and structure of EPS to be directly observed in fully hydrated samples (Sheng, Yu, and Li 2010), and has been reported to be the most flexible method for biofilm EPS imaging (Neu and Lawrence 2014). Many studies have used fluorescein isothiocyanate (FITC) to stain extracellular proteins (Chen et al. 2007; McSwain et al. 2005). The widely used lectin, concanavalin A, binds with α-mannopyranosyl and α-glucopyranosyl, while calcofluor white stains β-polysaccharides (Baird, Wadsworth, and Hill 2012; Chen et al. 2007). Another

lectin, wheat germ agglutinin (WGA), binds to N-acetyl-D-glucosamine and sialic acid, thus interacts with membrane glycoproteins (Strathmann, Wingender, and Flemming 2002). The attachment of pollutants such as microplastics within the EPS structure can be observed using the microscopy and fluorescent staining technique.

2.5 Microplastics identification and quantification in wastewater samples

Currently, there is no standardized procedure for isolating, detecting, identifying, and quantifying microplastics in environmental samples. For isolating microplastics from sediments, methods such as density separation using salt-saturated solutions, filtration, sieving and elutriation (Claessens et al. 2013; Imhof et al. 2012; Nuelle et al. 2014; Van Cauwenberghe et al. 2013) have been used successfully. However, for wastewater samples which contains high organic matter, methods involving removal of organic matter such as wet peroxidation is often used (Sutton et al. 2016; Mason et al. 2016; Sun et al. 2019). The National Oceanic and Atmospheric Administration (NOAA) recommends a combination of wet peroxidation and density separation to isolate microplastics from water samples (Masura et al. 2015). After separation from labile particles, microplastics have been identified and quantified through visual sorting (Talvitie et al. 2015; Carr, Liu, and Tesoro 2016; Murphy et al. 2016), optical microscopy (Magnusson and Norén 2014), Fourier Transform Infrared Spectroscopy (FT-IR) (Browne et al. 2011), Raman spectroscopy (Lenz et al. 2015), and fluorescent staining (Shim et al. 2016).

A study carried out by Song et al. (2015) compared stereomicroscope and FT-IR spectroscope methods of identifying microplastics in environmental samples. The authors determined that although identification using microscope method was easier and faster than FT-IR, microplastic abundance may be under- or overestimated. The spectroscope method was found to be more accurate than the stereomicroscope (Song et al. 2015). The FT-IR and Raman

spectroscope technique has been reported to be generally reliable but requires expensive equipment, a well-trained operator, and lots of time consumption (Rocha-Santos and Duarte 2015; Shim et al. 2016). Microplastics have been identified by staining with lipophilic dyes, such as Nile Red, and visualized under a fluorescence microscope (Shim et al. 2016). Fluorescent staining has the advantage of fast processing time and lower cost but specific plastic identity is not known. In FT-IR spectroscopy, the polymeric composition of unknown microplastics are identified by comparing their IR spectra with a database of known polymers (Rocha-Santos and Duarte 2015). It is suggested that chemical identification be conducted to confirm the results obtained through visual inspection, optical analysis and fluorescent staining (Rocha-Santos and Duarte 2015).

Fluorescent microbeads have been used by some studies for controlled laboratory and bench-scale studies (Carr, Liu, and Tesoro 2016). This approach makes for easy quantification of microplastics, as the microbeads fluoresces a unique color under fluorescent light. Also, chemical identification can be by-passed since the polymer type is known.

2.6 Scope of study

In this study, the microplastics removal efficiency of both CAS and AGS was investigated and compared at an organic loading rate (OLR) of 0.9 kg COD m^{-3} day^{-1} and at a lower OLR of 0.6 kg COD m^{-3} day^{-1}, with food to microorganism ratios (F/M) ranging from 0.26 – 0.44 g rbCOD / g VSS-day. This approach is based on the expectation that the production of EPS would increase with an increase in organic load, as determined in literature (Basuvaraj, Fein, and Liss 2015; Janga et al. 2007; Wang, Liu, and Tay 2005). The purpose was to determine the role that EPS play in microplastics entrainment or adsorption by microbial aggregates.

The first phase of the study involved the operation of two lab scale sequential batch reactors (CAS and AGS) at the same OLR (0.9 kg COD m^{-3} day^{-1}) and F/M (0.3 g rbCOD / g VSS-day).

Microplastics were fed into both reactors during steady state operation for a duration of three weeks. The aim was to accept or reject the hypothesis that AGS would retain more microplastics compared to CAS because AGS releases more EPS. In the second experimental phase, microplastics were fed into both reactors at the same OLR of 0.6 kg COD m^{-3} day^{-1} but at different F/M ratios (0.26 and 0.44 g rbCOD / g VSS-day for AGS and CAS respectively), and the results for each process were compared to the results obtained in the first phase of the experiment. The aim here was to check how EPS production influenced by low substrate concentration affects microplastics removal.

3. METHODS AND PROCEDURES

3.1 Reactor operation

3.1.1 Sequencing batch reactor design

For each treatment process, a reactor of 3L working capacity was used. A figure of the reactor setup is shown in figure 3-1. Both reactors have identical parameters; an internal diameter of 6.4 cm, external diameter of 10 cm and a 96 cm height. The sequential phases were programmed on a timer (ChronTrol, San Diego, California), and consisted of anoxic/anaerobic fill, aeration, settling, and decant periods. The reactors were operated on a 4-hour cycle time. The cycle profile used for both experimental phases is reported on table 3-1. A settling time of 6 minutes was set for AGS to select for dense, fast settling granules. Wastewater was pumped into and out of the reactors with the aid of peristaltic pumps (Cole-Primer model 7524, Illinois) set at flowrates of 25 mL/min for influent and 33 mL/min for effluent pumps. Effluent wastewater was extracted at the middle of the reactor yielding an exchange ratio of approximately 50%.

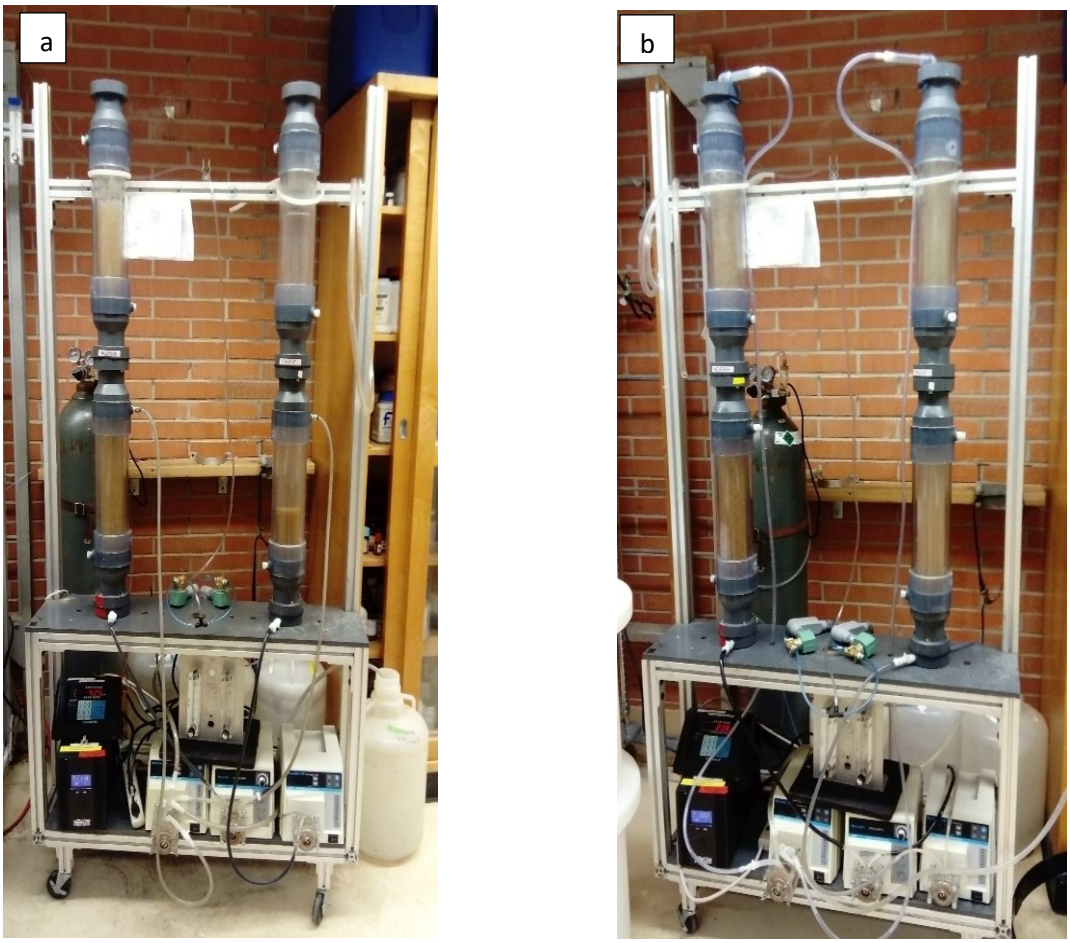

Figure 3-1: Aerobic granular sludge and conventional activated sludge reactor setup a) initial setup b) effluent setup changed on day 173 during the first experimental phase

For the first 172 days of operation during the first phase of study, the setup used for extracting effluent was as shown in figure 3-1a. However, loss of biomass was experienced, which was probably due to biomass getting stuck in the effluent port. This concern led to a change in effluent setup on day 173, shown in figure 3-1b. Initially, the effluent was discharged through tubing connected to a port at the middle of the reactor, but the setup change involved closing the effluent port and connecting effluent tubing to a PVC pipe placed directly in the reactors. The PVC pipe was long enough to withdraw effluent from the middle of the reactor. This setup was

maintained for the rest of the first experimental phase and throughout the second phase of this study. Aeration and mixing in both reactors were achieved by passing air from a pressurized service connection through air stones placed strategically at the bottom of each reactor. A flow meter was used to maintain air flow rate at 2.5 L/min for each reactor, creating a superficial upflow gas velocity of approximately 1.3 cm/s as suggested in literature for compact granule formation (Adav, Lee, and Lai 2007; McSwain et al. 2005; Tay, Liu, and Liu 2001a).

Table 3-1: SBR phase configuration for experimental stages

		0.9 kg COD m^{-3} day^{-1}	0.6 kg COD m^{-3} day^{-1}
Reactor	SBR phase	Duration (minutes)	Duration (minutes)
AGS	Aeration	168	168
	Settling	6	6
	Decant	6	6
	Feed	60	60
	Cycle time	240	240
CAS	Aeration	141	133
	Settling	33	41
	Decant	6	6
	Feed	60	60
	Cycle time	240	240

Reactor operation was initiated with seed sludge obtained from the Kansas River Wastewater Treatment Plant (WWTP) in Lawrence, Kansas for the first phase of the experiment (OLR of 0.9 kg COD m^{-3} day^{-1}). During the second experimental phase (OLR of 0.6 kg COD m^{-3} day^{-1}), seed sludge was obtained both from the Kansas River WWTP and the Wakarusa plant in Lawrence.

3.1.2 Wastewater constituents

Synthetic wastewater was prepared using the stock solution recipe shown in table 3-2 and diluted in 40 liters tap water, enough for a two-day feed. A single influent tub was used for feeding both reactors. Sodium acetate was used as the only carbon source during both phases of this study, but the chemical oxygen demand (COD) concentration differed according to the F/M targeted during each phase. The composition of trace metals solution was prepared based on the study by Smolders, van Loosdrecht, and Heijnen (1995). The recipe used is reported in Appendix I. The composition of synthetic wastewater used was determined based on the required C:N:P ratio for aerobic wastewater treatment, which is typically between the range of 100:10:1 and 100:5:1 (Tchobanoglous et al. 2014; Benefield and Randall 1981). For the first experimental phase, both reactors were operated at a hydraulic retention time (HRT) of 8 h and an organic loading rate of 0.9 kg COD m^{-3} day^{-1}. However, an organic loading rate of 0.6 kg COD m^{-3} day^{-1} was employed for the second experimental phase. The OLR was adjusted for the second phase by changing the final carbon concentration based on COD calculations for a target F/M of 0.18 g rbCOD / g VSS-day as shown in table 3-2.

Table 3-2: Synthetic wastewater composition[1]

Influent chemical	Stock Concentration (g/L)	Final[2] concentration for 0.9 kg COD m^{-3} day^{-1} (g/L)	Final[3] concentration for 0.6 kg COD m^{-3} day^{-1} (g/L)
CH_3COONa	200	0.3850	0.2564
$MgSO_4$*7H2O	50	0.1001	0.1001
KCl	50	0.0500	0.0500
NH_4Cl	100	0.0856	0.0588
K_2HPO_4	30	0.0148	0.0131
KH_2PO_4	20	0.0058	0.0051

[1] 1 ml of trace metals solution per liter of influent solution was used

[2] COD:TN:TP equals 100.00 : 7.50 : 1.30

[3] COD:TN:TP equals 100.00 : 7.70 : 1.70

3.1.3 Physical tests

Measurements including mixed liquor suspended solids (MLSS), mixed liquor volatile suspended solids (MLVSS), effluent suspended solids (ESS), and sludge volume index (SVI) were performed two to three times weekly according to *Standard methods for the examination of water and wastewater* (AWWA 2005). The purpose of these measurements was to monitor biomass production and ensure the sludge had good settling characteristics. Weekly samples of sludge were also passed through a 300 μm sieve to determine the percentage of flocs or granules present in sludge. Solids retained on the sieve were classified as granules.

3.1.4 Chemical tests

The biochemical conversion performance of the aggregates was monitored through COD, ammonia, total nitrogen and total phosphorus removal measurements. Grab influent and effluent samples were taken weekly for analysis. The COD measurements was carried out using

high range COD digestion vials (HACH, product #2125915, Colorado). Samples were added to vials, 2 ml each, digested for two hours in a digital digester block (Hach DRB200, Colorado), and photometric measurements were read. High range and ultra-low range Ammonia vials (Hach, TNT 831, Colorado) were used for influent and effluent ammonia measurements respectively. Samples were added to the vials, allowed to incubate for a minimum of 15 minutes, then photometric measurements were read. Nitrate, nitrite and orthophosphate measurements were carried out using ion chromatography IC 2000 equipped with IonPac AS18 Analytical Column and IonPac AG18 Guard Column. Appendix II shows the IC operating conditions used for the measured anions.

3.1.5 Image analysis of aggregates

During each experimental stage, sludge samples were obtained weekly from each reactor for image analysis. The purpose of this was to monitor if there were any changes in floc and granule morphology throughout the duration of the experiment. Images of sludge structure were obtained with a Stereomaster microscope (Fisher Scientific) and analyzed with image-j software (https://imagej.nih.gov/ij/). Parameters such as particle area, roundness, feret's diameter and aspect ratio were measured using this software.

3.2 Microplastics quantification

For both experimental phases (OLR of 0.9 kg COD m^{-3} day^{-1} and 0.6 kg COD m^{-3} day^{-1}), microplastics dosing was carried out for a period of three weeks. The microplastics used were fluorescent red polyethylene microspheres (Cospheric product, ID: UVPMS-BR-1.20) in two size fractions: 40 – 90 µm and 100 – 150 µm. A visual of the microplastics used is shown in figure 3-2. The plastics have a density of 1.2 g cm^{-3}, and 0.015 g of each size fraction was dosed per liter of influent wastewater. Because of the hydrophobicity of microplastics used, they were immersed in 1% tween-80 solution for at least one week before dosing. In addition, the influent and effluent

plastic tubs were also coated with the surfactant for a minimum of 24 hrs before the start of the experiment. Moreover, an electric mixer (Arrow Engineering model 1750, Pennsylvania) at a speed of 2 rev/min was used to provide continuous mixing of influent so that the microplastics remained in solution.

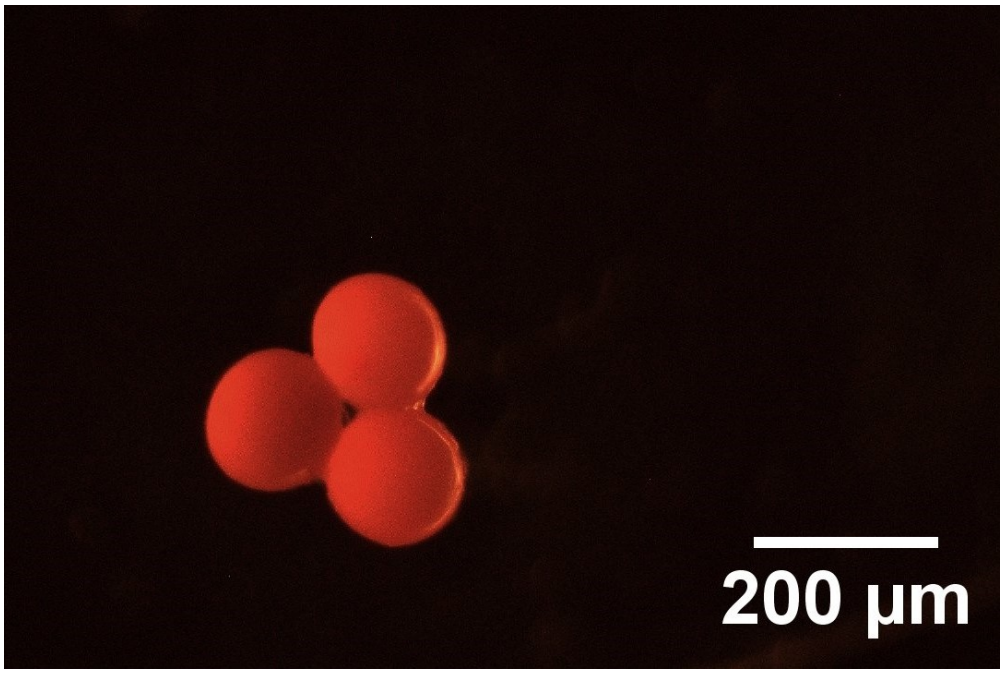

Figure 3-2: Fluorescent red microplastics

3.2.1 Sample preparation

Percentage microplastics removal was quantified for both reactors by obtaining single representative 40 ml samples from the influent and effluent per day, and then counting the number of microplastics present in the samples. Each sample obtained was ran through a glass fiber filter (Whatman 1827-047 TISCH Scientific, Ohio) and allowed to dry in the oven at 60°C for one hour.

After drying, each filter was attached between a glass slide and a gridded petri-sticker (Electron Microscopy Sciences, Pennsylvania) as shown in figure 3-3 for microscopic imaging.

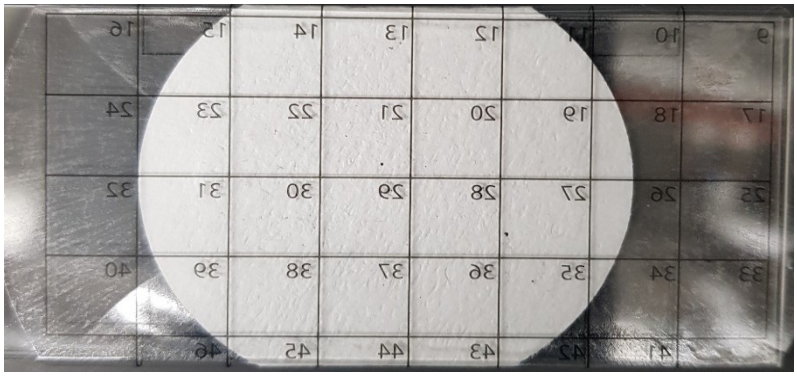

Figure 3-3: Sample prepared for fluorescent microscope imaging

3.2.2 Subsample area determination

To save processing time and reduce cost, the entire filter was not imaged under the microscope, rather, targeted sections were analyzed. A rarefaction curve was used to determine the minimum number of grids sufficient for analyzing microplastics concentration per sample. Rarefaction is a statistical technique commonly used in ecological contexts to estimate minimum representative sample size. The curve was constructed by plotting the number of grids or subsample area measured against the corresponding microplastics concentration estimated from the selected area. The results are presented in section 4.1.2.2. A subsample area that will give a reasonable estimate of the concentration is determined when the curve converges. Moreover, to avoid bias, the same cross-section of grids was imaged and analyzed for all samples.

3.2.3 Epi-fluorescent microscopy and image analysis

Selected sub-sample areas were viewed under the epi-fluorescent microscope (Olympus scientific solutions, Waltham, Massachusetts) with fluorescent light. Plastics fluoresced in the Texas-red channel at excitation and emission wavelengths of 561 - 581 nm and 607 - 627 nm

respectively. The fluorescent images were then exported as TIF files and analyzed with image-j software (https://imagej.nih.gov/ij/). Data derived from image-j for each grid include the number of microplastics present and the area of each particle. The diameter of the beads was calculated from the given area using excel. This enabled the classification of beads into the expected size range (i.e. 40 – 90 μm and 100 – 150 μm).

3.2.4 Test for loss of microplastics' fluorescent coating

Since the microbeads used for this study were manufactured with a fluorescent coating to enable fluorescence under fluorescent light, three effluent samples obtained during microplastics dosing were analyzed to investigate the possibility that microbeads lost their fluorescent coating while in the reactor. Fluorescent control microplastics were quantified in all the samples, then the same samples were stained with Nile red, a lipophilic dye that stains hydrophobic materials, and has been used to stain microplastics (Shim et al. 2016). All stained microplastics within the expected size range, and also within the typical aspect ratio (1 – 1.3) and roundness (0.8 – 1) of the control fluorescent microbeads were quantified. The results obtained were compared with the number of control microbeads counted before staining to determine the presence of microbeads that lost its coating and probably did not fluoresce without Nile red staining. The microplastics present in one of the effluent samples was then identified using FTIR spectroscopy.

3.3 EPS staining and extraction

3.3.1 EPS staining

During the experiment, 10 ml of biomass was obtained from each reactor twice weekly and fixed using 4% paraformaldehyde in 20x phosphate-buffered saline solution (ThermoFisher Scientific, catalog #28348, Waltham, Massachusetts) diluted twenty-fold in water. The purpose of doing this was to preserve bacterial cell morphology so that EPS distribution can be viewed under

the microscope with the aid of fluorescent dyes. The fate of microplastics within the EPS structure can also be ascertained through this means.

From literature, EPS has been found to be composed mostly of proteins and polysaccharides. Hence, it was determined to use fluorescein-isothiocyanate (FITC) (ThermoFisher Scientific, catalog #PI46425, Waltham, Massachusetts) – a fluorescent dye reactive towards amine and sulfhydryl groups (Schmid et al. 2003) – for probing proteins, Concanavalin A (ConA) (Biotium, catalog #29075, California) – a lectin which probes α-polysaccharides (Goldstein and Hayes 1978), and Wheat Germ Agglutinin (WGA) (Biotium, catalog #29022-1, California) – a carbohydrate-binding lectin which stains glycoproteins (Goldstein and Hayes 1978).

The staining procedure used was adapted from Chen et al. (2007), with two of the selected stains being used at a time. Hydrated flocs in 2ml centrifuge tubes were placed on a shaker table rotating at 160 rpm. Dilute stain solution (50 μg/mL for ConA and FITC, and 1 μg/mL for WGA) was added, 200 μL each to the aggregates and allowed to incubate for 30 mins in the dark by wrapping foil around centrifuge tubes. After incubation, the aggregates were rinsed twice with 1x PBS solution before the next stain was added. The incubation and rinsing procedure were repeated after the second stain addition. Stained aggregates were then mounted on glass slides for microscopic imaging (Microscopy and Analytical Imaging Laboratory, University of Kansas). Because of how large granules were, they were embedded in optimal cutting temperature compound (Fisher scientific catalog number: 23-730-571) at a -80°C freezer and sectioned into 20 or 30 μm slices with a cryostat (Thermo scientific Microm HM550, Walldorf, Germany) before staining was carried out. In this case, dilute stains were applied directly to granule sections placed on glass slides, incubated in the dark and rinsed accordingly.

EPS distribution and plastics attachment within aggregates were obtained by viewing stained aggregates under a confocal laser scanning microscope (Olympus scientific solutions, Americas, Waltham, Massachusetts). The flocs and sectioned granules were imaged using a 10x or a 40x objective, and images were acquired using Slidebook 6.0 (Intelligent Imaging Innovation, Denver, Colorado). The excitation and emission spectra of the stains and fluorescent microplastics dosed are shown in figure 3.4. Dosed microplastics were detected in the Texas-red channel at an excitation wavelength of 561 - 581 nm and emission of 607 – 627 nm (red). The FITC fluorescence was detected using an excitation of 475 – 500 nm and emission of 510 – 530 nm (green). ConA was detected in the DAPI channel with an excitation of 384 - 404 nm and emission of 420 – 440 nm (blue), while WGA was also detected in the FITC channel with an excitation wavelength of 475 - 495 nm and emission of 500 – 520 nm (bright green). The acquired images were analyzed with Image-j.

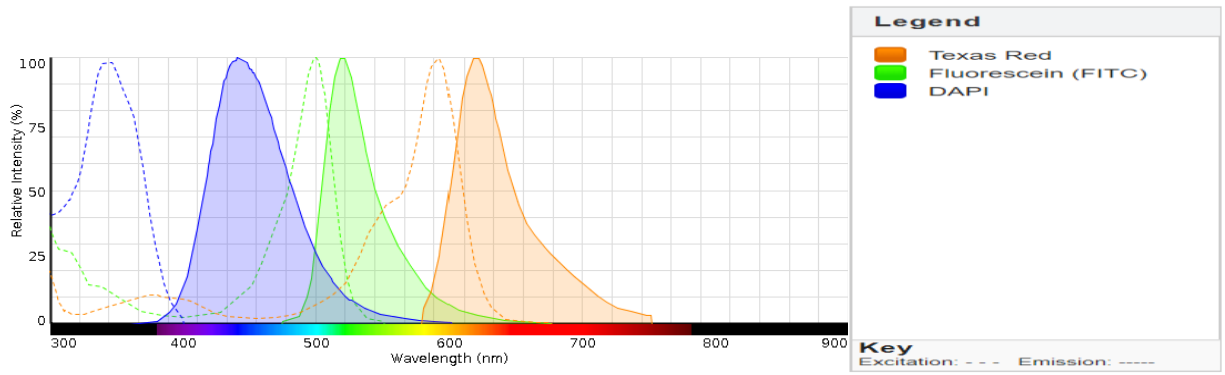

Figure 3-4: Excitation and emission spectra of channels used for confocal microscopy (obtained from ThermoFisher Scientific, SpectraViewer)

3.3.2 EPS extraction and analysis

3.3.2.1 EPS extraction

At the end of the duration of the experiment, loosely bound (LB-EPS) and tightly bound EPS (TB-EPS) fractions were extracted from biomass contained in each reactor. The method used for extraction was the high temperature-sodium carbonate (Na_2CO_3) extraction method adapted from Li and Yang (2007) and Felz et al. (2016). The extraction procedure for both LB-EPS and TB-EPS is shown in figure 3-5. Biomass volume corresponding to 0.3 – 0.35 g VSS was collected from each reactor before the end of the cycle. The samples collected were centrifuged at 4°C and 4,000 rpm for 20 mins to separate the bulk liquid (supernatant) from bound EPS (pellets). The pellets for each sample were resuspended in 30 ml heated milli Q water (80°C) with a vortex mixer and centrifuged at 4000 rpm for 20 mins. The supernatant contained the loosely bound EPS. Tightly bound EPS was extracted from the pellets by adding Na_2CO_3 anhydrous to pellets to obtain a 0.5% (w/v) Na_2CO_3 concentration, heating this mixture at 80°C for 35 mins while stirring at 400 rpm with a stir bar. The mixture was then centrifuged for 20 mins at 4000 rpm and 4°C. The supernatant obtained was then placed in dialysis bags (Fisher Scientific catalog #2115214, Waltham, Massachusetts) and allowed to rotate in MQ water for a day to enable molecules less than 3,500 Da molecular weight to diffuse through the pores of the bag into the water. The dialyzed water was changed after 12 hours to enhance the effect of the dialysis. The dialyzed extract was the tightly bound EPS fraction. The extracted EPS fractions were stored at -20°C for protein and carbohydrate analyses. Solids measurements were carried out on the day of EPS extraction because EPS content was eventually normalized to the MLVSS of biomass.

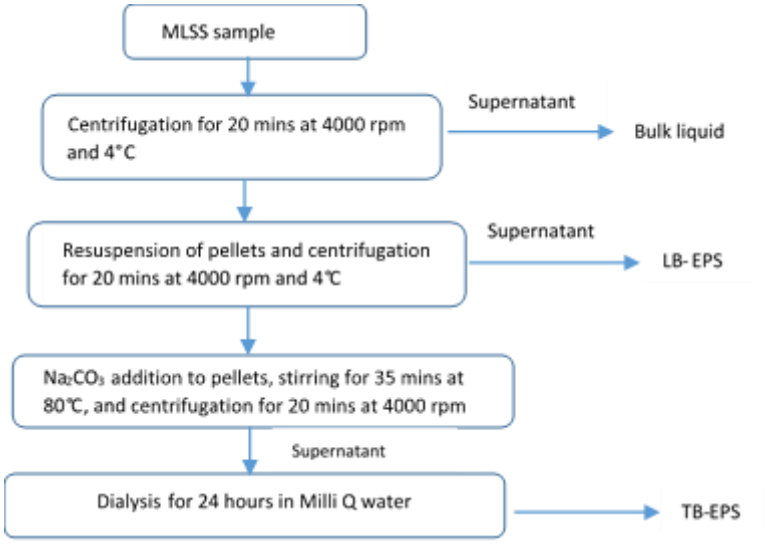

Figure 3-5: Extraction procedure for LB-EPS and TB-EPS fractions

3.3.2.2 EPS analysis

Carbohydrate content of EPS samples was analyzed using the Phenol-sulfuric assay (Dubois et al. 1956b) with some modifications. The standard operating procedure used for this analysis is presented in appendix III. Stored samples were transferred to room temperature, and triplicate 400 µL volume of each sample were placed in glass tubes. Sulfuric acid and phenol were added to each sample and mixed to achieve a sample: sulfuric acid: phenol volumetric ratio of 40:1:100. These mixtures were then digested at 90°C for 5 mins in a thermoblock, after which they were incubated in the dark for 30 mins. The samples were then pipetted into microplate wells, and the absorbance at 490 nm was read with the aid of a microplate reader (Biotek uQuant model MQX200). Glucose was used to prepare standard solutions on the day of analysis. A standard curve was constructed from the measured absorbance of standard solutions, and this was used to estimate the unknown concentrations.

Protein analysis for extracted EPS samples was carried out using the Bicinchoninic acid (BCA) assay (Smith et al. 1985). A BCA protein assay kit consisting of BCA reagent A and B, and 2 mg/ml albumin standard ampules was purchased from ThermoScientific, USA (Product number 23227). One albumin standard ampule was used to prepare a set of diluted standards. A BCA working reagent was prepared from reagent A and B in a 50:1 volumetric ratio, and 200 µL was added to triplicate EPS and standard samples in a microplate. The mixture was mixed, and incubated for 30 mins at 37°C. The plate was then allowed to cool to room temperature and the absorbance at 562 nm wavelength was measured with a microplate reader. Absorbance readings of standard solutions were used to prepare a standard curve. The protein content of EPS samples was then calculated from the standard curve and normalized per mass of MLVSS.

3.3.3 Chemical identification

To verify the presence of dosed microplastics within the aggregate structure, some floc and granule samples viewed under fluorescent light were also scrutinized under Infrared light using Fourier transform Infrared spectroscopy (Institute of Bioengineering Research Laboratories, University of Kansas). First, absorption spectra were obtained from the control fluorescent polyethylene microbeads. These spectra were then used to create a database that was subsequently compared with absorption spectra obtained from floc and granule samples. A minimum spectra match of 70% was considered positive for microplastics presence using spectragryph software (version v1.2.6, http://spectroscopy.ninja).

3.4 Statistical analysis

The error level between measurements was represented by standard error. The student's t-test was carried out to determine if there were significant differences between reactor performance parameters, while the Mann-Whitney U test in the R studio environment was performed to check

for significant differences between microplastics removal efficiencies. Normality was tested by comparing a histogram of sample data to a normal probability curve. A 95% confidence interval ($\alpha = 0.05$) was used as the level of significance. A difference was concluded as significant at $p < 0.05$.

4. RESULTS

4.1 Microplastics removal for OLR of 0.9 kg COD m^{-3} day^{-1}

For this phase of the study, an f/m ratio of 0.3 g rbCOD/g VSS-day was targeted for both CAS and AGS reactors. The experiment was carried out to study the microplastics removal efficiency of both processes and how EPS possibly influences this performance.

4.1.1 Reactor operation

Both reactors were operated identically with the same feed concentration of 300 mg COD L^{-1}, providing a daily organic loading rate of 0.9 kg COD m^{-3} day^{-1}. The difference in reactor operation between both systems was in the settling time: CAS had a 33 mins settling time, while AGS settled for 6 mins.

4.1.1.1 Sludge characteristics

The size of aggregates was analyzed from sludge images captured with a stereomicroscope. Granule and floc images captured after steady state has been achieved are shown in figure 4-1. AGS contained mostly large compact granules. The flocs developed in CAS were unlike the typical irregularly shaped filamentous flocs found in many full-scale wastewater treatment plants. Flocs were more spherical in shape and compact.

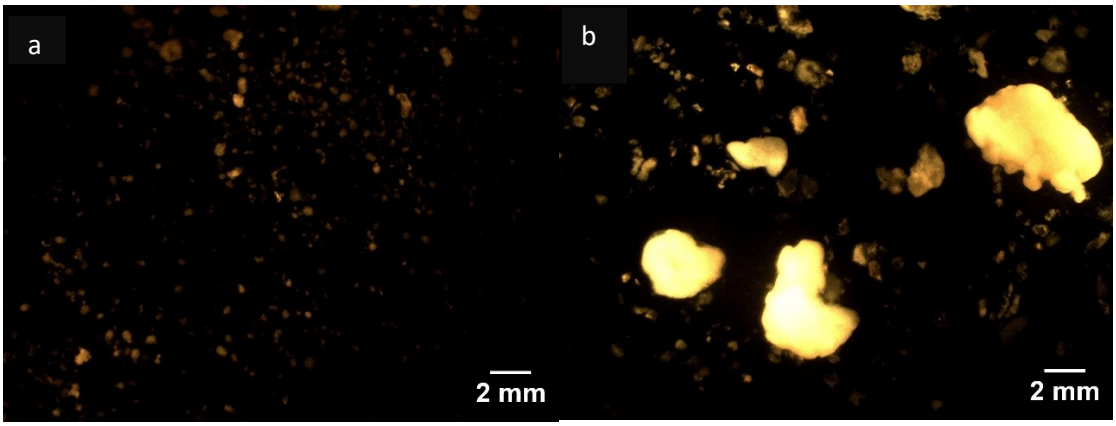

Figure 4-1: Steady state sludge structure in (a) CAS and (b) AGS during the 0.9 kg COD m^{-3} d^{-1} experimental phase. Scale bar represents 2 mm.

A summary of the average diameter, aspect ratio (ratio of particle width to particle height), and roundness estimated using image j is reported in table 4-1, and histograms showing size distributions are shown in figure 4-2. The average diameter of biomass particles in CAS (0.1 ± 0.2 mm) varied significantly ($p < 0.05$) from that in AGS (0.40 ± 0.9 mm). The roundness, which describes how spherical the solids are, was 0.8 ± 0.2 and 0.6 ± 0.2 for CAS and AGS, respectively, with 1 being perfectly round. Also included in table 4-1 is the percentage particle size distribution derived from sieve analysis. Flocs are defined as particles < 0.3 mm, while granules are defined as particles > 0.3 mm. Results of sieve analysis showed that approximately 44% of the sludge particles in CAS were flocs, while AGS contained about 4% flocs.

Table 4-1: Average aggregate size analyzed on day 224 of the 0.9 kg COD m^{-3} d^{-1} experimental phase. Particles < 0.3 mm were estimated through sieve analysis.

	CAS	AGS
Average diameter (mm)	0.1 ± 0.2	0.4 ± 0.9
Average aspect ratio (unitless)	1.5 ± 0.7	1.9 ± 0.9
Average roundness (unitless)	0.8 ± 0.2	0.6 ± 0.2
Number of particles	786	579
Percentage particles < 0.3 mm (From sieve analysis)	44 ± 5	4 ± 2

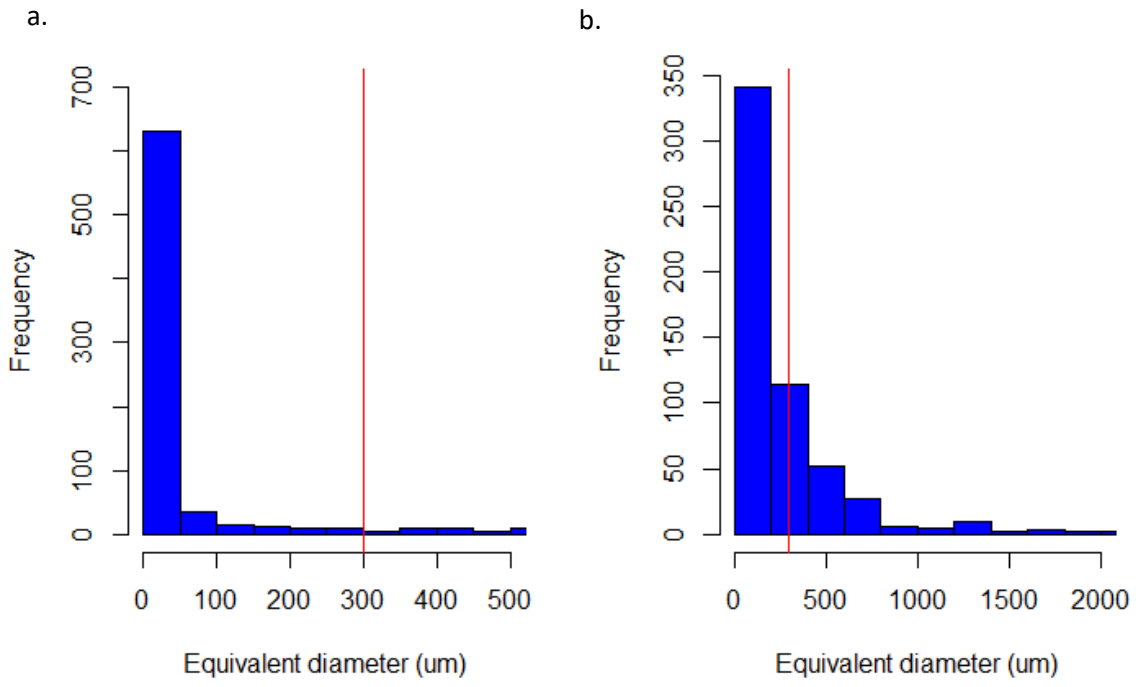

Figure 4-2: Steady state size frequency of sludge particles in (a) CAS and (b) AGS during 0.9 kg COD m^{-3} d^{-1} experimental phase, determined through image analysis. Red line shows the size limit of flocs (300 μm).

4.1.1.2 Physical measurements

For both reactors, suspended solids properties (MLSS, MLVSS, SVI_5 and SVI_{30}) were measured thrice every week. Results varied significantly ($p < 0.05$) between both reactors for MLSS, MLVSS and SVI_5. During the first three months of reactor operation, the mixed liquor volatile suspended solids (MLVSS) concentration for both AGS and CAS reactors fluctuated greatly (figure 4-3). MLVSS in CAS underwent a decline between days 120 and 165, then an increasing trend in the 6th month. Eventually, steady state was arrived at in the last month of operation and MLVSS did not change significantly during microplastics dosing. Between days 120 and 200, the MLVSS in AGS was consistently higher than that in CAS, so daily wasting of biomass in AGS was carried out to force the MLVSS concentration close to CAS and to maintain the f/m ratio at 0.3 g rbCOD/g VSS-day. There was no significant difference ($p > 0.05$) in the MLVSS measured between both reactors during steady state operation.

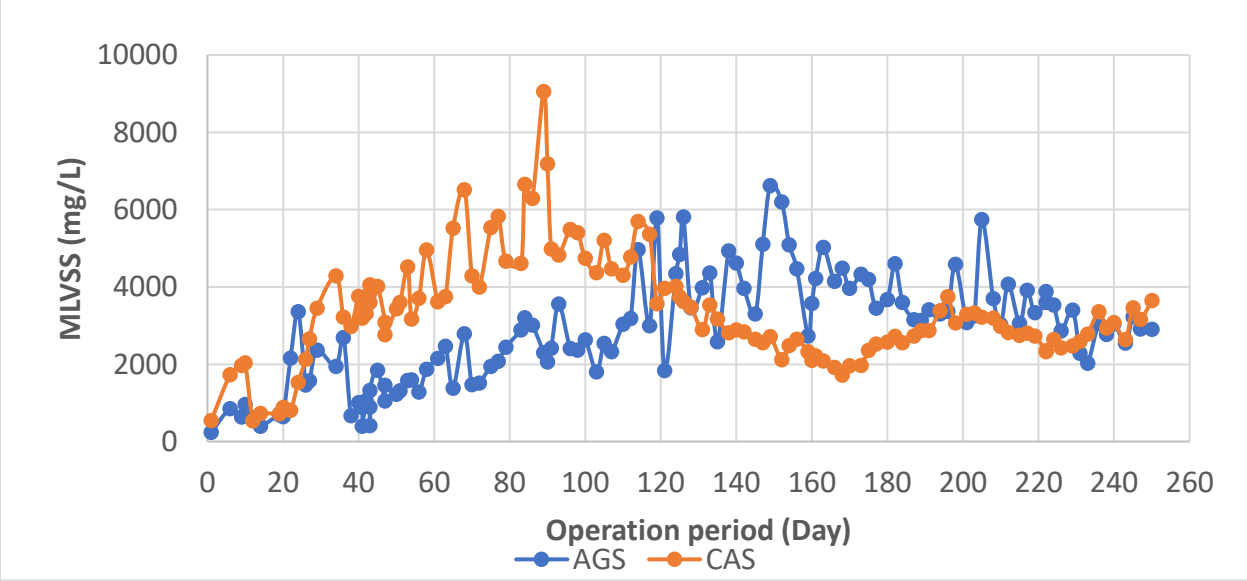

Figure 4-3: Concentrations of mixed liquor volatile suspended solids over duration of reactor operation for organic loading rate of 0.9 kg COD m^{-3} d^{-1}.

The SVI_5 for aggregates in CAS was generally higher than those measured in AGS throughout the operation period except in the last month (figure 4-4). The SVI reduced from 240 mL/g to 50 mL/g between days 36 and 100 in the CAS reactor. During the same time period, SVI measurements for AGS reduced from 160 mL/g to 35 mL/g indicating good settling of solids in both reactors. Between days 100 and 203, SVI_5 increased to 156 mL/g in CAS and 90 mL/g in AGS. During steady state, SVI_5 was maintained at about 81 mL/g in CAS and 93 mL/g in AGS.

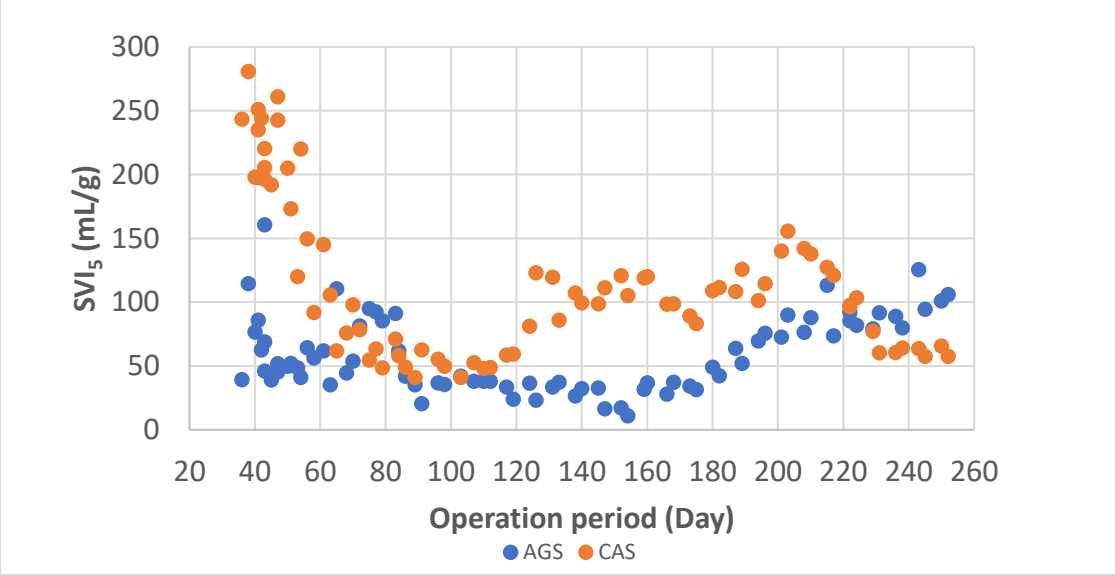

Figure 4-4: Sludge volume index (SVI at 5 min) measurements over duration of reactor operation for an organic loading rate of 0.9 kg COD m^{-3} d^{-1} for both reactors.

4.1.1.3 Chemical measurements – Reactor treatment efficiency

Weekly chemical analysis including total COD, ammonia, nitrite, nitrate and orthophosphate measurements were carried out during reactor operation. The purpose of this was to assess the treatment performance of aggregates in both CAS and AGS reactors. The COD removal efficiency for both reactors remained between 80 to 99% almost throughout the entire

duration of reactor operation (figure 4-5). During steady state operation, the average COD removal efficiency was 92% and 91% for AGS and CAS respectively.

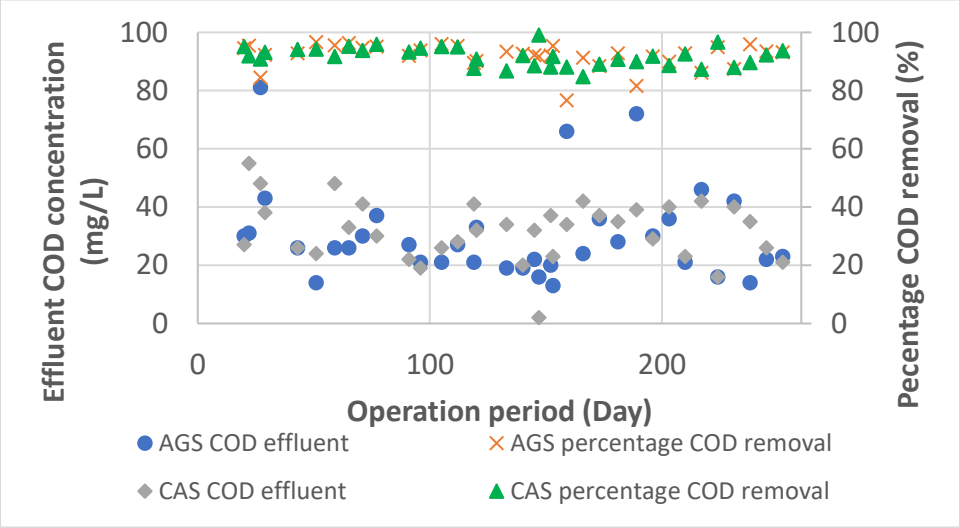

Figure 4-5: COD effluent measurements (primary y-axis) and the total percentage of COD removed (secondary y-axis) over duration of reactor operation for organic loading rate of 0.9 kg COD m^{-3} d^{-1}.

For both reactors, greater than 97% of ammonia was consistently removed in the SBR throughout reactor operation, which implies the occurrence of an almost complete nitrification (figure 4-6). Nitrate concentrations was mostly between 6 and 18 mg-N/L for both reactors throughout operation, while nitrite concentrations were below 5 mg-N/L throughout the duration of the experiment.

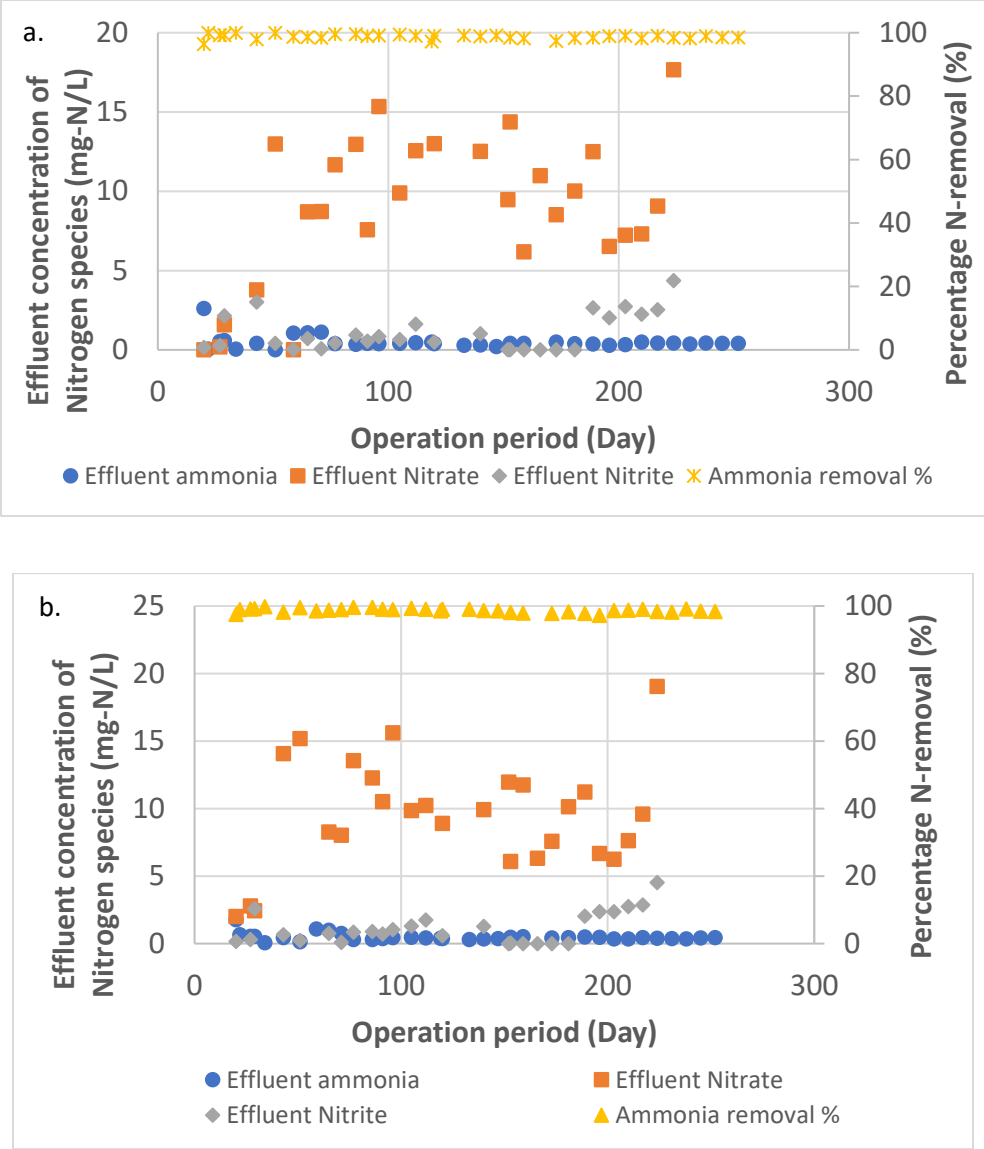

Figure 4-6: Effluent measurements of nitrogen species (primary y-axis) and the total percentage of ammonia removed (secondary y-axis) in (a) AGS and (b) CAS over duration of reactor operation for organic loading rate of 0.9 kg COD m^{-3} d^{-1}.

In AGS, total phosphate removal increased from 34% on day 43 to 94% on day 71 as shown in figure 4-7. Effluent phosphate concentration was below the detection limit of the ion chromatograph (0.5 mg-PO4/L) between days 77 and 133 which also corresponded to the period of increased biomass and low nitrite concentration. During the remaining days of operation,

phosphate removal concentration remained > 71%. During steady state, the average phosphate removal efficiency in AGS was 88%. On the other hand, CAS had a phosphate removal efficiency greater than 80% in the first 60 days of operation which corresponded to high biomass concentration and low nitrite and nitrate concentrations. However, between days 133 and 224, phosphate removal varied between 17% and 72% before increasing to 81% on day 231. The decline in phosphate removal can be attributed to the presence of residual nitrate concentration left in the SBR which inhibits the activity of phosphorus accumulating organisms (PAOs) during the anaerobic phase. During steady state operation, AGS and CAS had a phosphate removal efficiency of 86% and 60% respectively.

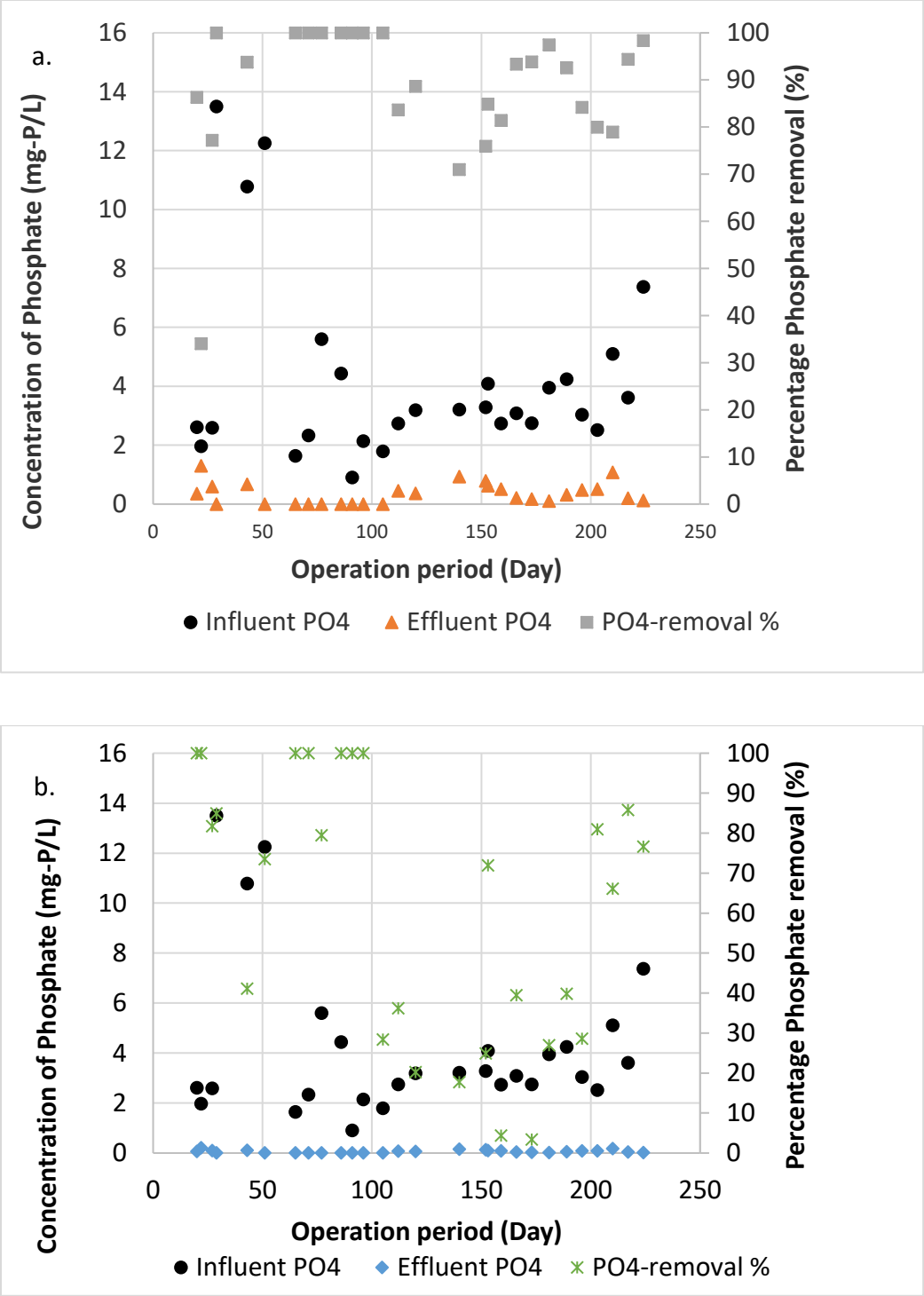

Figure 4-7: Measurement of orthophosphate concentrations (primary y-axis) and the total percentage of phosphate removed (secondary y-axis) in a) AGS and b) CAS over duration of reactor operation for organic loading rate of 0.9 kg COD m^{-3} d^{-1}.

Due to results from sludge characteristics and treatment performance two weeks before microplastics dosing, the reactors were determined as operating in steady-state condition. The summary of performance efficiencies during this period is reported in table 4-2. There was no significant difference ($p > 0.05$) between the reactors for all parameters during steady state except in the phosphate removal efficiency ($p < 0.05$).

Table 4-2: Steady state sludge properties for organic loading rate of 0.9 kg COD m^{-3} d^{-1}

	AGS±SD[1]	CAS±SD[1]
Volatile suspended solids concentration (mg VSS/L)	3100 ± 502	2900 ± 470
SVI 5min (mL/g)	93 ± 15	81 ± 25
NH4-Removal efficiency (%)	99±0.3	98±0.4
Total N-Removal efficiency (%)	63±9	63±8
P- Removal efficiency (%)	86±7	60±25
COD-Removal efficiency (%)	92±4	91±4

[1]SD is the standard deviation

4.1.2 Microplastics dosing and quantification

Two size fractions of mechanically produced polyethylene beads (40-90 μm and 100-150 μm) were dosed in influent synthetic wastewater for a three-week duration to assess removal performance of reactors.

4.1.2.1 Sludge size distribution during dosing

Sludge samples were taken weekly during the dosing period to evaluate if there was a change in sludge size and morphology. From image analysis results, the average diameter of aerobic granules reduced from 0.4 mm in the first week of dosing to 0.3 mm in the second week

and increased to 0.5 mm in the third week of microplastics dosing (figure 4-8). The aspect ratio however remained relatively constant throughout the three weeks of dosing. Conventional activated sludge solids reduced from an average size of 0.1 mm in the first week of dosing to 0.05 mm in the second week of dosing and remained at 0.05 mm in the third week (figure 4-8). The average aspect ratio varied between 1.5 and 1.7 within the period of dosing. The size distribution histograms for AGS and CAS with overlaying aggregate sizes before dosing and on the third week of dosing are presented in figure 4-9.

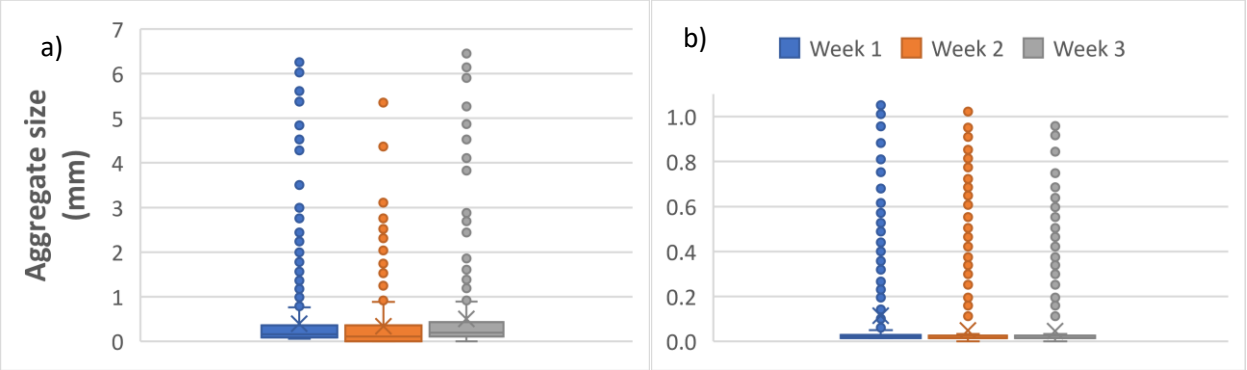

Figure 4-8: Box and whisker plots of aggregate size distribution during microplastics dosing in a) AGS and b) CAS for organic loading rate of 0.9 kg COD m^{-3} d^{-1}.

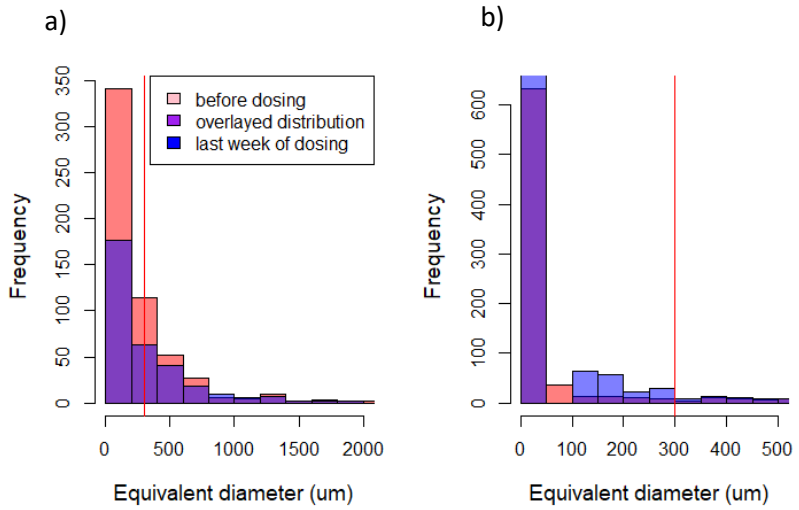

Figure 4-9: Overlapped size frequency distribution of sludge particles before dosing and on third week of dosing in (a) AGS and (b) CAS during 0.9 kg COD m^{-3} d^{-1} experimental phase, determined through image analysis. Red line shows the size limit of flocs (300 μm).

4.1.2.2 Microplastics removal efficiency

Influent and effluent samples were obtained three times each week, and the number of microplastics present was counted using epi-fluorescent microscope and image-j software. The samples collected were ran through a glass fiber filter and attached to a gridded sticker. The subsample area for analysis was determined by constructing a rarefaction curve to determine the minimum feasible sample area that would yield reasonable results. This curve was constructed using results from 8 samples (4 influent and 4 effluent samples). A Rarefaction curve constructed from an average of the total estimated microplastics concentration in all influent and effluent samples is shown in figure 4-10. The curve was found to converge at concentrations estimated from three to five grids which is one-fifth to one-third of the entire filter area. It was determined that five grids corresponding to one-third of the filter area would be used to estimate microplastics concentration in each sample. In addition, to avoid bias, a fixed cross-section of sample area shown in figure 4-11 was used for analysis in all prepared samples.

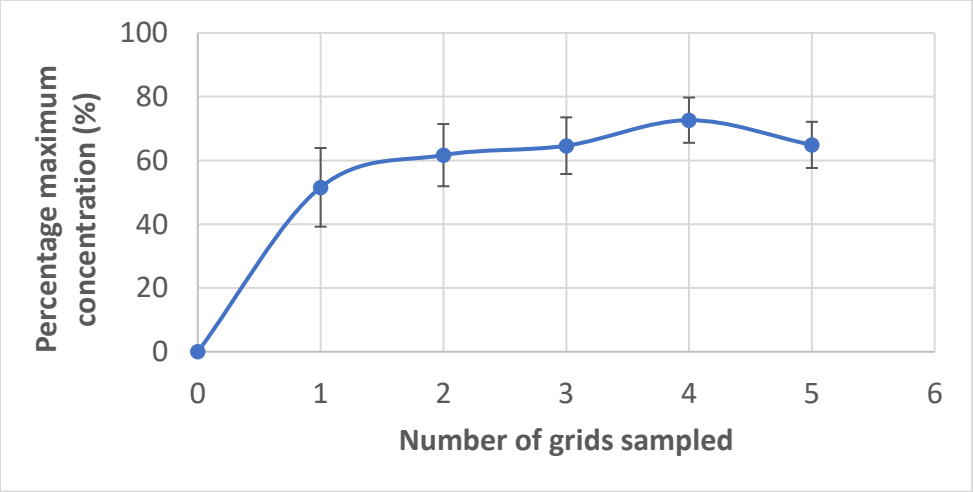

Figure 4-10: Rarefaction curve constructed with influent and effluent CAS samples. The curve presents the estimated percentage maximum concentration of plastics from a given subsample area. The error bars represent standard error.

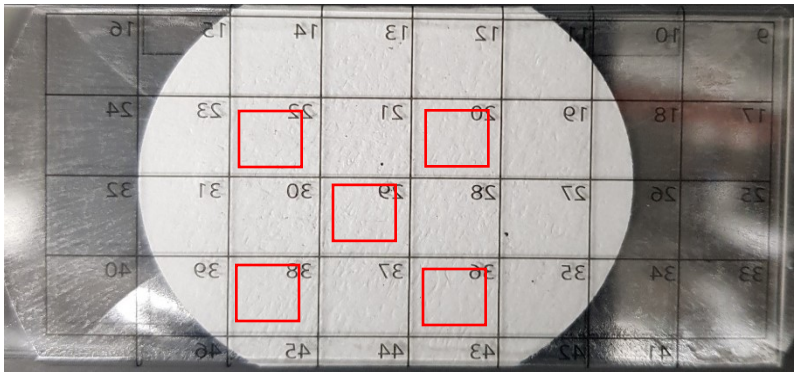

Figure 4-11: Cross-section of subsample area used for microplastics counts highlighted with red rectangle.

Microplastics removal efficiency of both reactors is shown in figure 4-12. The CAS reactor had 68% removal for the 40-90 µm size fraction and 73% removal for the 100-150 µm size fraction, giving a total microplastics removal of 69%. The AGS reactor had 77% removal for the 40-90 µm size fraction and 79% removal for the 100-150 µm size fraction, giving a total microplastics removal of 77%. Although, AGS had a higher removal than CAS in both size fractions, the results for both reactors were not statistically different ($p > 0.05$).

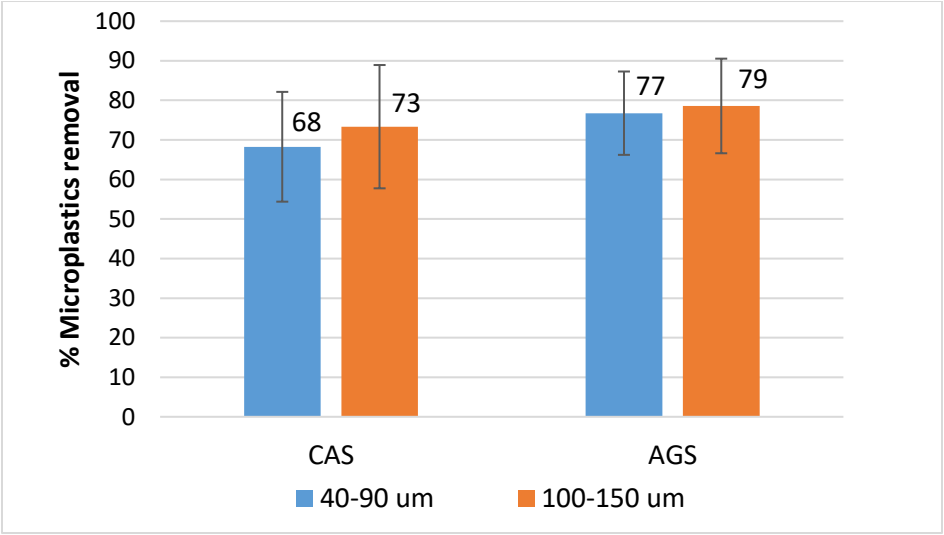

Figure 4-12: Percentage microplastics removal for the 1st experimental phase in which organic loading rate was 0.9 kg COD m^{-3} d^{-1} for both reactors.

4.1.2.3 Investigations into the loss of control microplastics coating

The quantity of fluorescent control microplastics in three effluent samples was compared with total stained microplastics in the same samples using Nile red stain. Many stained microplastics within the expected size range (40 – 150 µm) of control microbeads were present in the effluent samples (figure 4-13). However, when the expected size, aspect ratio (1.0 – 1.3) and roundness (0.8 – 1) of control microbeads was applied as cut-off, the quantity of microplastics counted were similar to that of the fluorescent beads counted before staining except in sample 3 (figure 4-13).

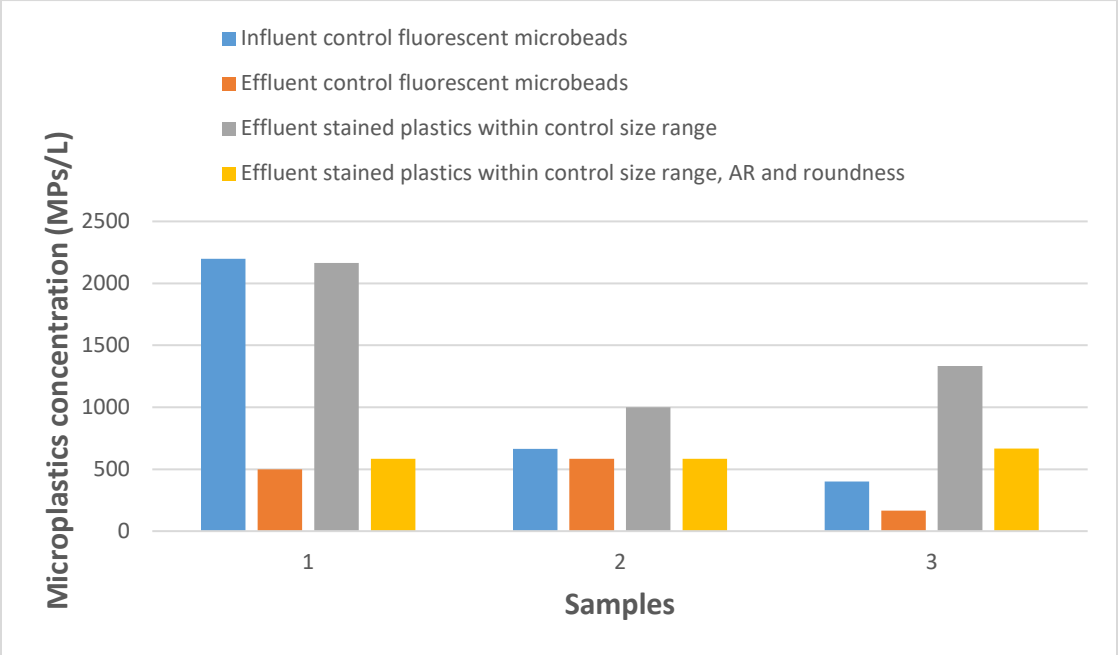

Figure 4-13: Bar chart showing results of quantified microplastics in effluent samples before and after Nile red staining

Microplastics identified in effluent sample 1 using FTIR included control fluorescent microplastics, polyester and polychloroprene. This indicates that other plastics apart from the dosed fluorescent microplastics were present in the effluent. This is understandable since the

reactors were not covered or controlled for plastics contamination throughout the experiment. While the results strongly suggested the presence of other microplastics in effluent wastewater, there was no absolute evidence to determine that the dosed fluorescent microbeads lost their coating as additional stained microplastics are very likely random microplastics that contaminated the reactor.

4.1.3 EPS staining – fate of microplastics in aggregates

During the experimental period, fixed floc samples and granule sections were stained with fluorescent dyes: Fluorescein-isothiocyanate (FITC) - proteins, Concanavalin A (ConA) - α-polysaccharides, and Wheat germ agglutinin (WGA) - glycoproteins. The purpose was to visualize microplastics attachment within the EPS structure of microbial aggregates. This can also provide insight into the mechanism of microplastics removal during biological treatment. A picture of an unstained whole granule is shown in figure 4-14. When unstained granules were viewed under fluorescent light in the Texas-red channel, fluorescent red beads were observed, which indicates the presence of control microbeads within granule structure. To determine if the plastics were within EPS structure, stained granule sections were also imaged. A total of approximately 25 granule sections with an area of 1 mm^2 were viewed under the confocal microscope. Figures 4-15, 4-16, and 4-17 show how the microplastics position were determined to avoid bias especially for sections not obtained at the surface of granule. In figure 4-16, the section shown was obtained at a depth between the outer layer and the middle of the granule. The microplastics in this section are positioned in region B i.e. a distance within one-tenth and three-tenth of the granule diameter. In figure 4-17, microplastics were attached in region A – a distance within the edge and one-tenth of the granule diameter.

A summary of section depth and microplastics' position within whole granules is reported in table 4-3. Region A was defined as the region between the granule surface and approximately one-tenth the depth of the whole granule, shown in figure 4-15. Of the Region A sections observed, 15% contained microplastics. Microplastics were observed in 33% of the sections obtained between the surface and the core, defined as region B in figure 4-15. For all sections obtained within the core of granules, defined as region C in figure 4-15, no microplastics were observed. An example of a section obtained at the core is shown in figure 4-18(b). A more comprehensive description of section depth and microplastics' positioning within whole granules for all sectioned samples observed is reported in appendix IV.

Figure 4-14: Picture of unstained whole granule viewed in (a) Texas-red channel, (b) bright field, and (c) combined channel overlay. Images were taken with a spinning disk confocal microscope using a 10x objective. Scale bar represents 100 µm.

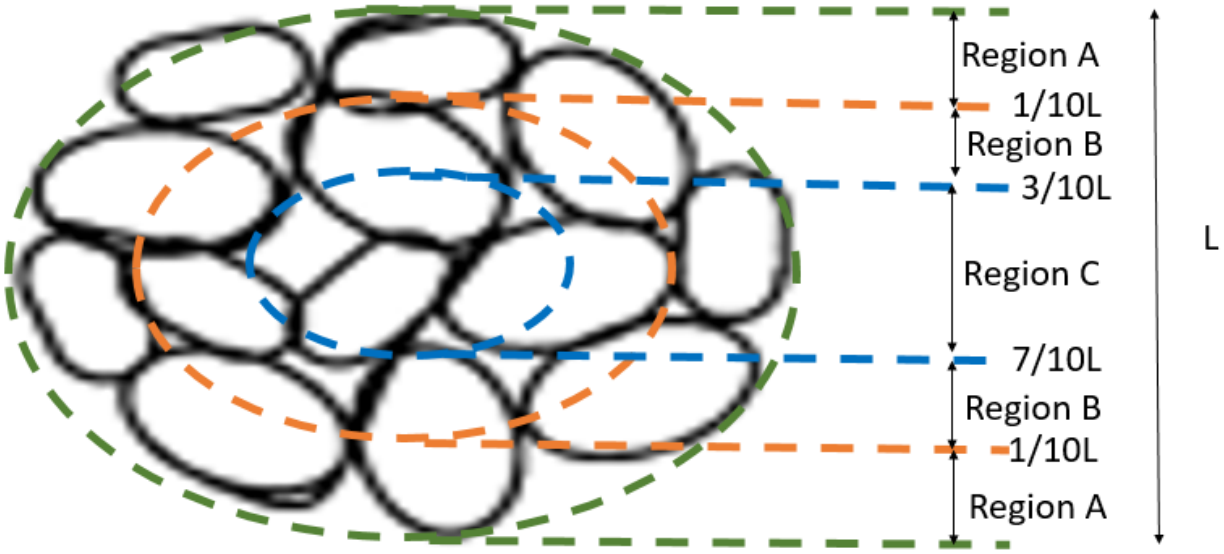

Figure 4-15: Depiction of granule showing defined regions of microplastics entrainment within granule section. Region A is defined as the granule surface, region B is defined as the region between the surface and the core, while region C is defined as the core. L connotes the length or diameter of the granule.

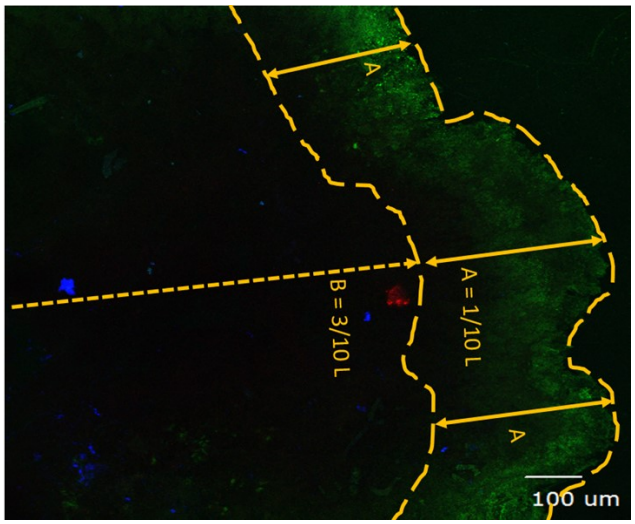

Figure 4-16: Picture of a 30 µm granule section obtained 270 µm from the surface of a 930 µm granule imaged in the texas-red (red), FITC (green) and ConA (blue) channels. L is the length of the granule. Images were taken with a Leica confocal microscope using a 10x objective. Scale bar represents 100 µm.

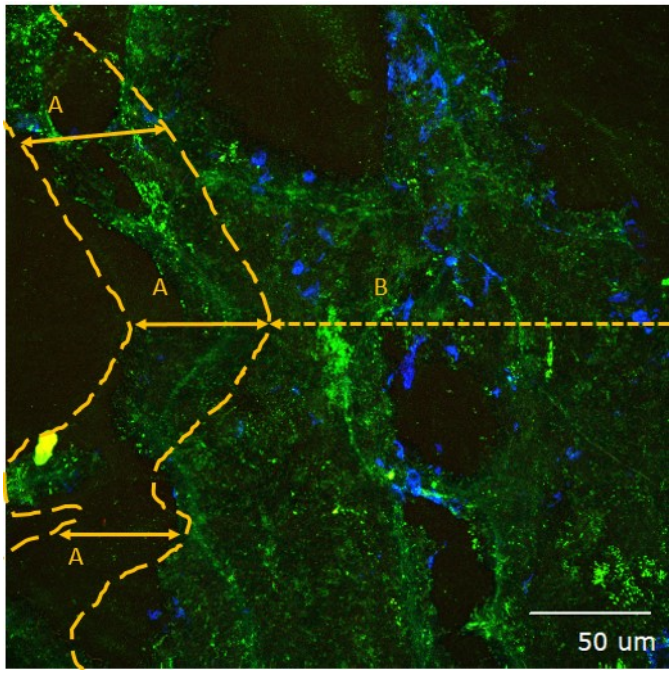

Figure 4-17: Picture of a 20 µm granule section obtained 100 µm from the surface of a 420 µm granule imaged in the texas-red (red), WGA (green) and ConA (blue) channels. L connotes the approximate diameter of granule. Images were taken with a Leica confocal microscope using a 40x objective. Scale bar represents 50 µm.

Table 4-3: Microplastics positioning within whole granule

Section depth	Number of sections imaged at region	Percentage of sections with microplastics present (%)
Region A	27	15
Region B	21	33
Region C	10	0

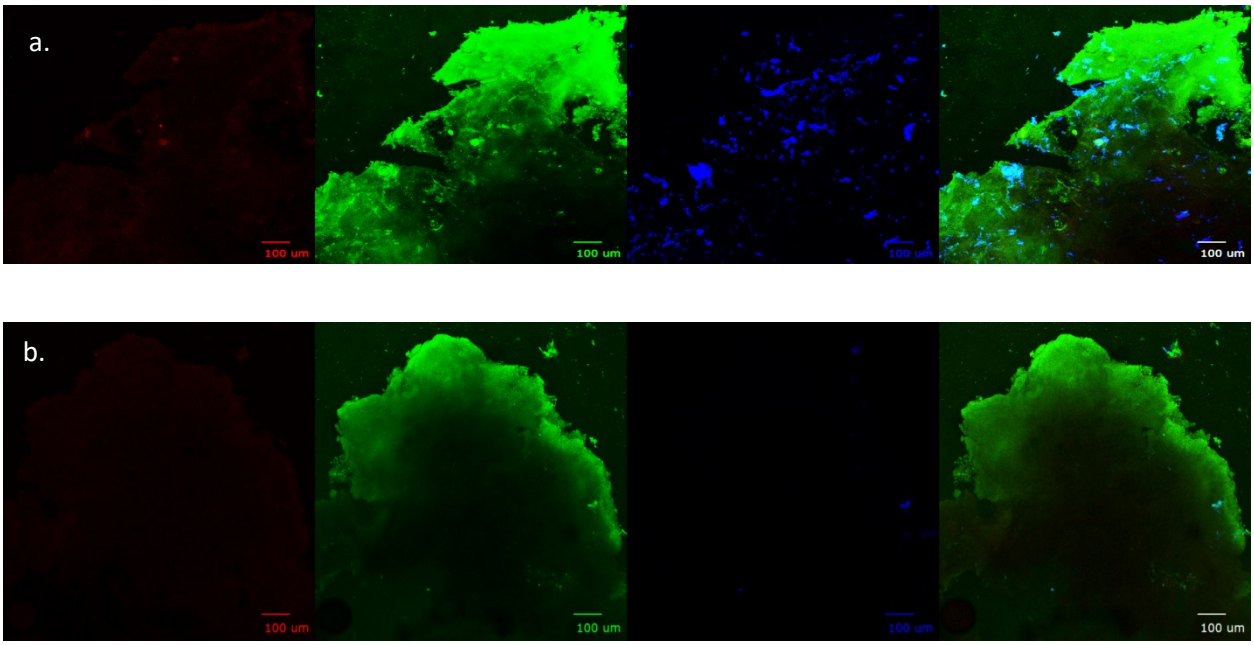

Figure 4-18: Pictures of 30 µm granule sections obtained (a) 150 µm (region B) and (b) 450 µm from the surface (region C) of an 870 µm granule imaged in the texas-red (red), FITC (green), ConA (blue) and combined overlay channels. Images were taken with a Leica confocal microscope using a 10x objective. Scale bar represents 100 µm.

Image analysis was carried out on specific spots where fluorescent red beads were observed to determine if plastics were distributed within the protein or carbohydrate structure. The intensities of fluorescent stains and plastic at the specific spot were determined through 4 µm optical stacks of a granule section and plotted. Examples of two spots analyzed from two stained granule sections are shown in figures 4-19(a) and (b). The intensity peaks of the Texas-red channel where plastics were found aligned with peaks of WGA and FITC channels but was not aligned with ConA, implying that plastics were attached within the protein and glycoproteins fraction of EPS.

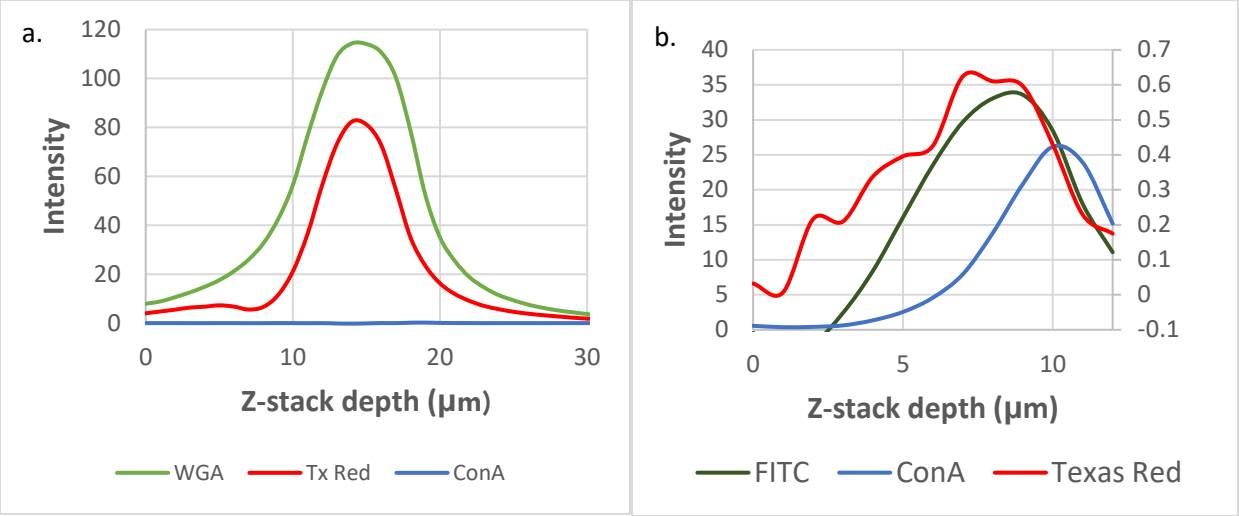

Figure 4-19: Intensity through optical Z-stacks at a point where microplastic was observed in a granule section stained with (a) WGA and ConA (b) FITC and ConA

4.1.4 Chemical identification of plastics within EPS structure

Some microplastics observed within aggregates did not have the perfect spherical shape of the dosed control microplastics as shown in figure 4-20. This shape distortion and shear of microplastics likely occurred due to hydrodynamic shear force during mixing in the SBRs. Nevertheless, fluorescent red microplastics observed in the EPS structure with the confocal microscope were verified with the aid of Fourier transform infrared spectroscopy (FTIR). The purpose of this was to confirm that fluorescent particles are the microplastics dosed in influent wastewater. Spectra extracted from samples were compared with control microplastics spectra. Figure 4-21 (a) and (b) show example spectra obtained from a granule section and floc sample respectively, matched with control microplastics spectra. A spectra match of up to 92% and 88% was obtained in floc samples and granule sections respectively confirming the presence of dosed microplastics within EPS structure.

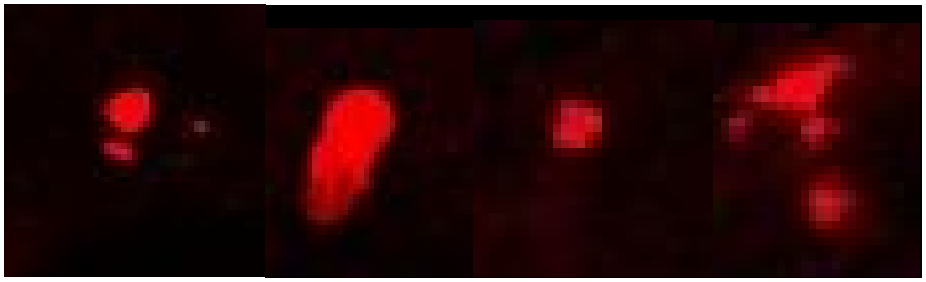

Figure 4-20: Cropped pictures of fluorescent red microplastics observed within granule sections in the texas-red channel. The original images were captured and observed using 40x objective of a confocal microscope.

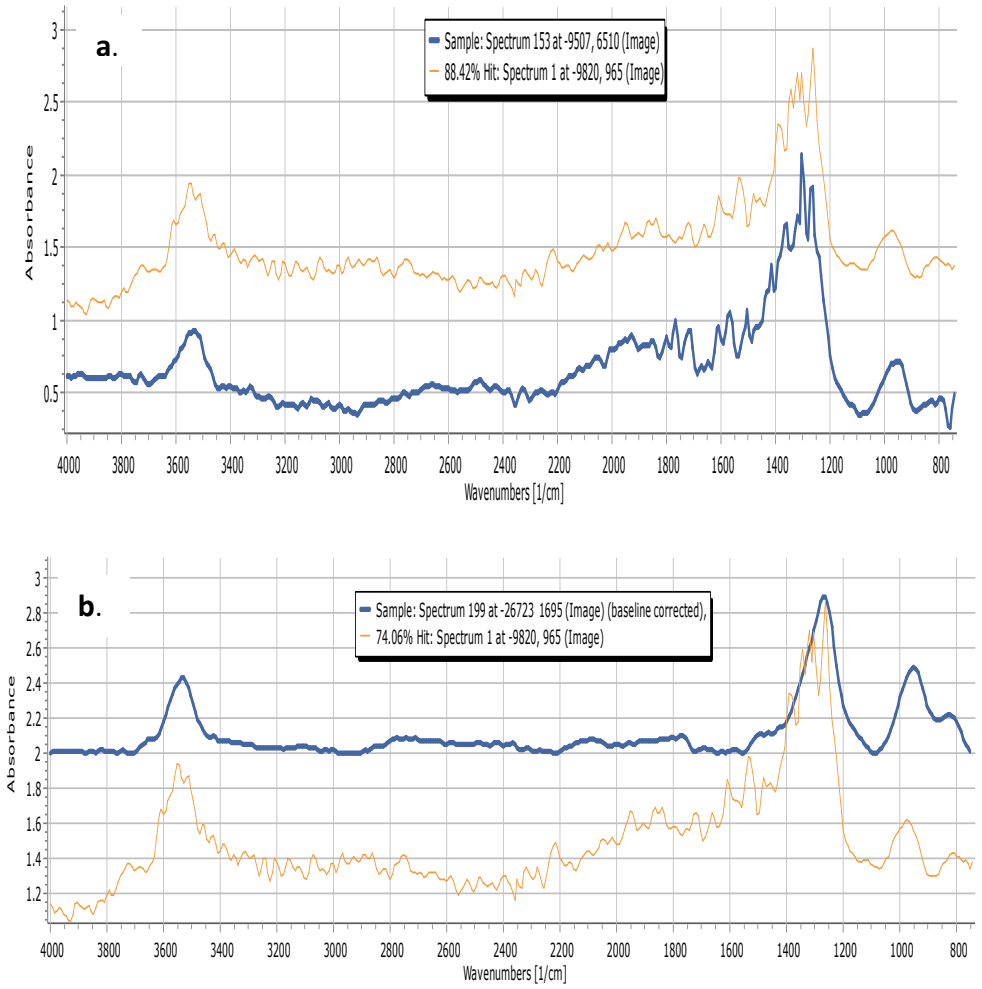

Figure 4-21: Fourier transform infrared spectra of observed microplastics in EPS structure (blue line) matched with control microplastics' spectra (orange line) in (a) granule section, and (b) floc sample

4.1.5 EPS quantification and distribution

At the end of the experiment, loosely-bound EPS (LB-EPS) and tightly-bound EPS (TB-EPS) fractions were extracted from microbial aggregates in CAS and AGS reactors. The extracted EPS was then analyzed for carbohydrate and protein content. Results showed that the EPS protein content was higher than carbohydrate content for both reactors as reported in figure 4-22. For the CAS reactor, the LB-EPS and TB-EPS fraction had carbohydrate content of 1 mg/ gVSS and 49 mg/ gVSS respectively, and a protein content of 120 mg/ gVSS and 429 mg/ gVSS respectively. While the LB-EPS and TB-EPS fractions of the aggregates in the AGS reactor had carbohydrate content of 1 mg/ gVSS and 47 mg/ gVSS respectively, and a protein content of 122 mg/ gVSS and 475 mg/ gVSS respectively. There was no significant difference ($p > 0.05$) in the EPS protein and carbohydrate content of aggregates developed in both reactors.

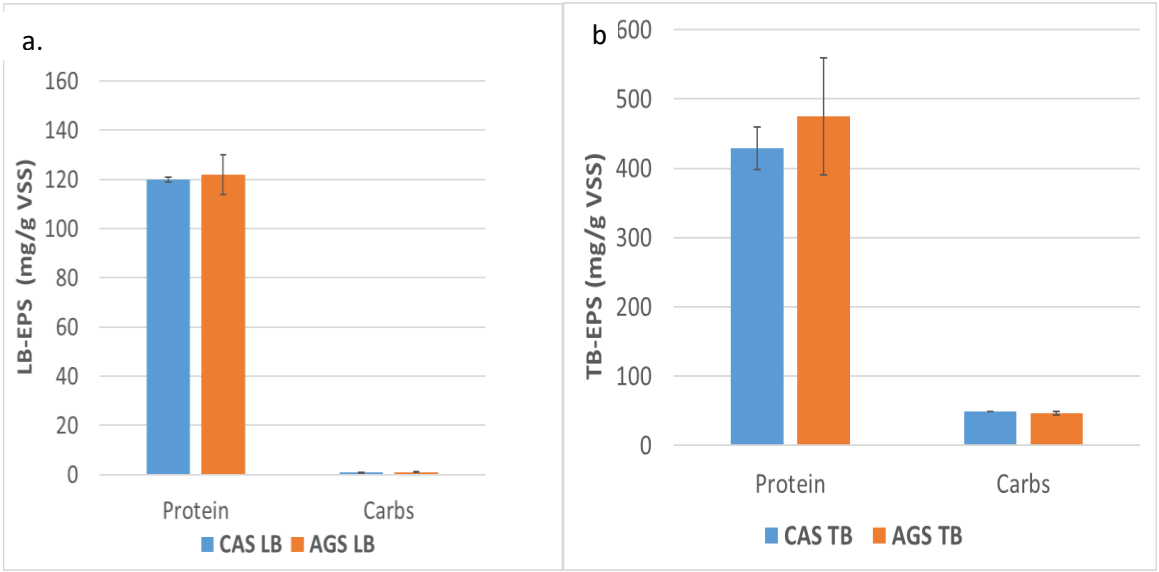

Figure 4-22: Protein and carbohydrate content of (a) loosely bound and (b) tightly bound EPS content of CAS and AGS reactors

4.2 Microplastics removal for organic loading rate of 0.6 kg COD m^{-3} d^{-1}

Conventional activated sludge reactors (CAS) and aerobic granular sludge (AGS) reactors were seeded with sludge from Kansas River WWTP and Wakarusa WWTP respectively. Both reactors were fed with sodium acetate as the only carbon source at a concentration of 200 mg O_2/L. The aim was to assess the microplastics removal performance at a lower organic loading rate (0.6 kg COD m^{-3} d^{-1}) than the first experimental phase (0.9 kg COD m^{-3} d^{-1}). Initially, the plan was to maintain the f/m ratio of both reactors at 0.18 g rbCOD / g VSS-day, but steady state could not be achieved at this low f/m ratio. During steady state operation, AGS maintained an f/m of 0.26±0.02 g rbCOD / g VSS-day, while CAS maintained an f/m of 0.44 ± 0.06 g rbCOD / g VSS-day.

4.2.1 Reactor operation

4.2.1.1 Sludge characteristics

Sludge samples were viewed under a stereomicroscope and images obtained were analyzed with image-j. Granule and floc structure after steady state has been achieved are shown in figure 4-23(a) and 4-23(b). Sludge samples were also passed through a 300 µm sieve weekly, and particles less than 300 µm were defined as flocs while particles retained on the sieve were defined as granules. A summary of results obtained from image analysis (including particle diameter, particle roundness and aspect ratio), and sieve analysis is shown in table 4-4. The size distribution of solids as measured from image analysis is displayed in figure 4-24. AGS contained mostly spherical compact granules, while CAS contained fluffy flocculent sludge.

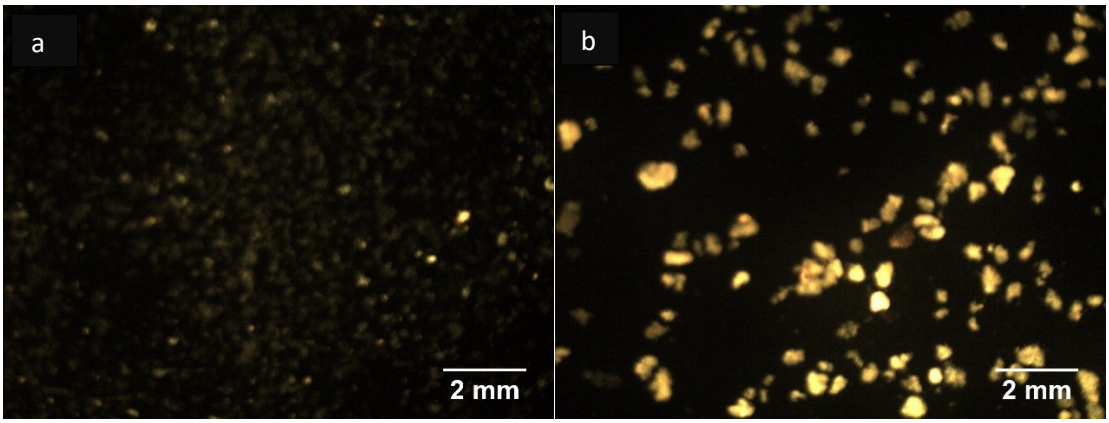

Figure 4-23: Steady state sludge structure in (a) CAS and (b) AGS during the 2nd experimental phase in which organic loading rate was 0.6 kg COD m^{-3} d^{-1}. Scale bar represents 2mm.

The average diameter of biomass particles in CAS (0.08 ± 0.1 mm) varied significantly ($p < 0.05$) from that in AGS (0.20 ± 0.3 mm). The granules developed in the AGS reactor were visibly smaller than those developed in the higher daily organic loading rate experimental phase. Results of sieve analysis showed that approximately 82% of the sludge particles in CAS were flocs, while AGS contained about 11% flocs.

Table 4-4: Average aggregate size analyzed on day 243 of the second experimental phase. Particles < 0.3 mm was estimated through sieve analysis carried out throughout reactor operation.

	CAS	AGS
Average diameter (mm)	0.08 ± 0.1	0.2 ± 0.3
Average aspect ratio (unitless)	2.1 ± 1.1	1.5 ± 0.6
Roundness	0.5 ± 0.2	0.7 ± 0.2
Number of particles	841	717
Percentage particles < 0.3 mm (From sieve analysis %)	82 ± 11	11 ± 8

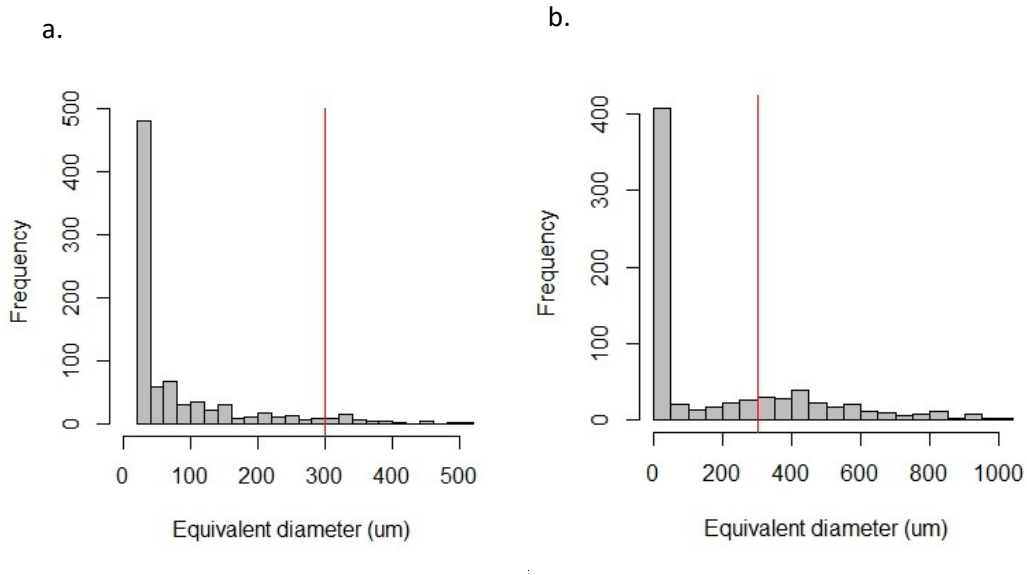

Figure 4-24: Steady state size frequency of sludge particles in (a) CAS and (b) AGS during low organic loading experimental phase, determined through image analysis. Red line shows the size limit of flocs.

4.2.1.2 Physical measurements

Solids measurements including MLSS, MLVSS, ESS and SVI_5 were carried out two to three times weekly. MLSS and MLVSS measures did not differ significantly ($p > 0.05$) between both reactors, but SVI_5 measurements differed significantly ($p < 0.05$) between reactors. A summary of the MLVSS measurements throughout the experimental period is shown in figure 4-25. Suspended solids declined in both reactors between days 50 and 150. Volatile solids in AGS decreased from 3600 to 1500 mg/L, while MLVSS in CAS decreased from about 4800 to 1350 mg/L. Between days 150 and 250, AGS biomass increased slowly and then became steady. In the same period, MLVSS in CAS also increased, then declined between days 176 and 200 before becoming steady.

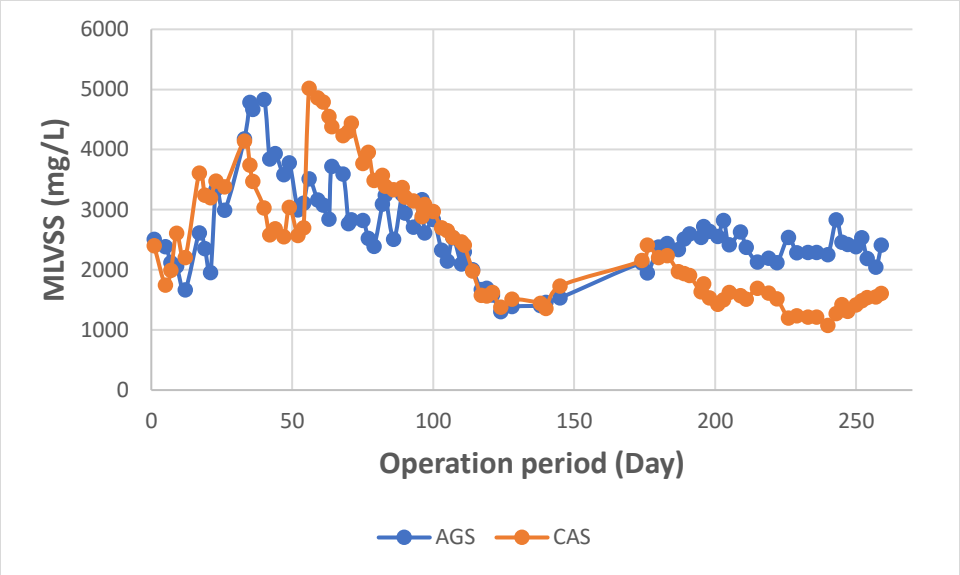

Figure 4-25: Concentrations of mixed liquor volatile suspended solids over duration of reactor operation during the 2nd experimental phase in which organic loading rate was 0.6 kg COD m^{-3} d^{-1}.

The SVI at 5 min was generally higher in CAS than in AGS as shown in figure 4-26 but much more in the last two months of reactor operation. The SVI_5 of sludge in CAS increased from 170 to about 760 ml/g between days 180 to 233 which corresponded to a decline in biomass, then SVI_5 decreased to 277 ml/g between days 233 and 259. In AGS, however, SVI_5 decreased from about 150 ml/g to 42 ml/g in the first three months of operation and remained below 55 ml/g throughout the last three months of reactor operation.

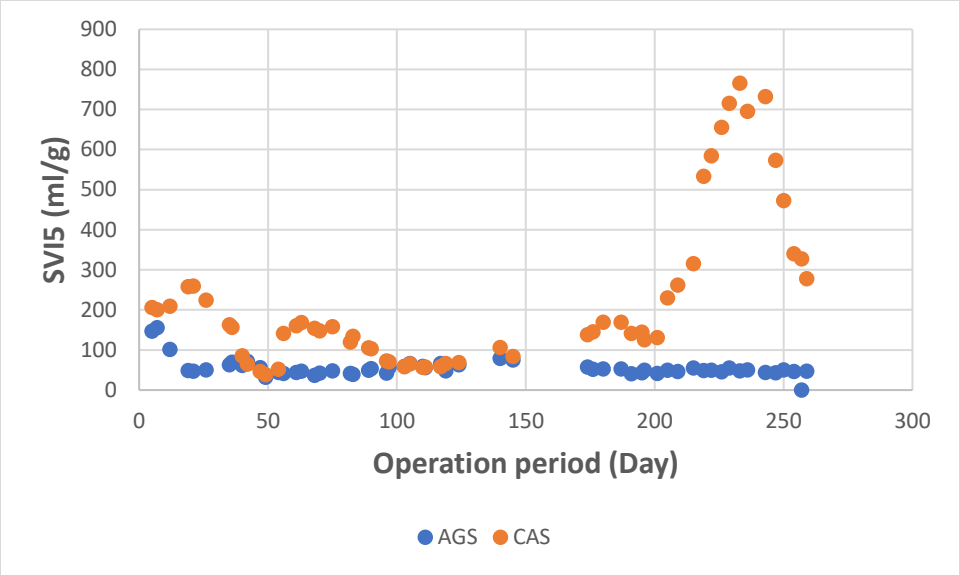

Figure 4-26: Sludge volume index at 5 min over duration of reactor operation during the 2nd experimental phase in which organic loading rate was 0.6 kg COD m^{-3} d^{-1}.

4.2.1.3 Chemical measurements – Treatment efficiency

Influent and effluent wastewater samples were taken periodically, and COD, ammonia, and phosphate removal performance was measured to monitor reactor treatment performance. The results of total COD removal and effluent COD for both reactors are reported in figure 4-27. Both CAS and AGS had a removal rate above 80% throughout the operation period similar to the results of the high organic loading experimental phase. Effluent COD in AGS varied between 8 and 40 mg/L during reactor operation, while effluent COD varied between 10 and 44 mg/L in CAS.

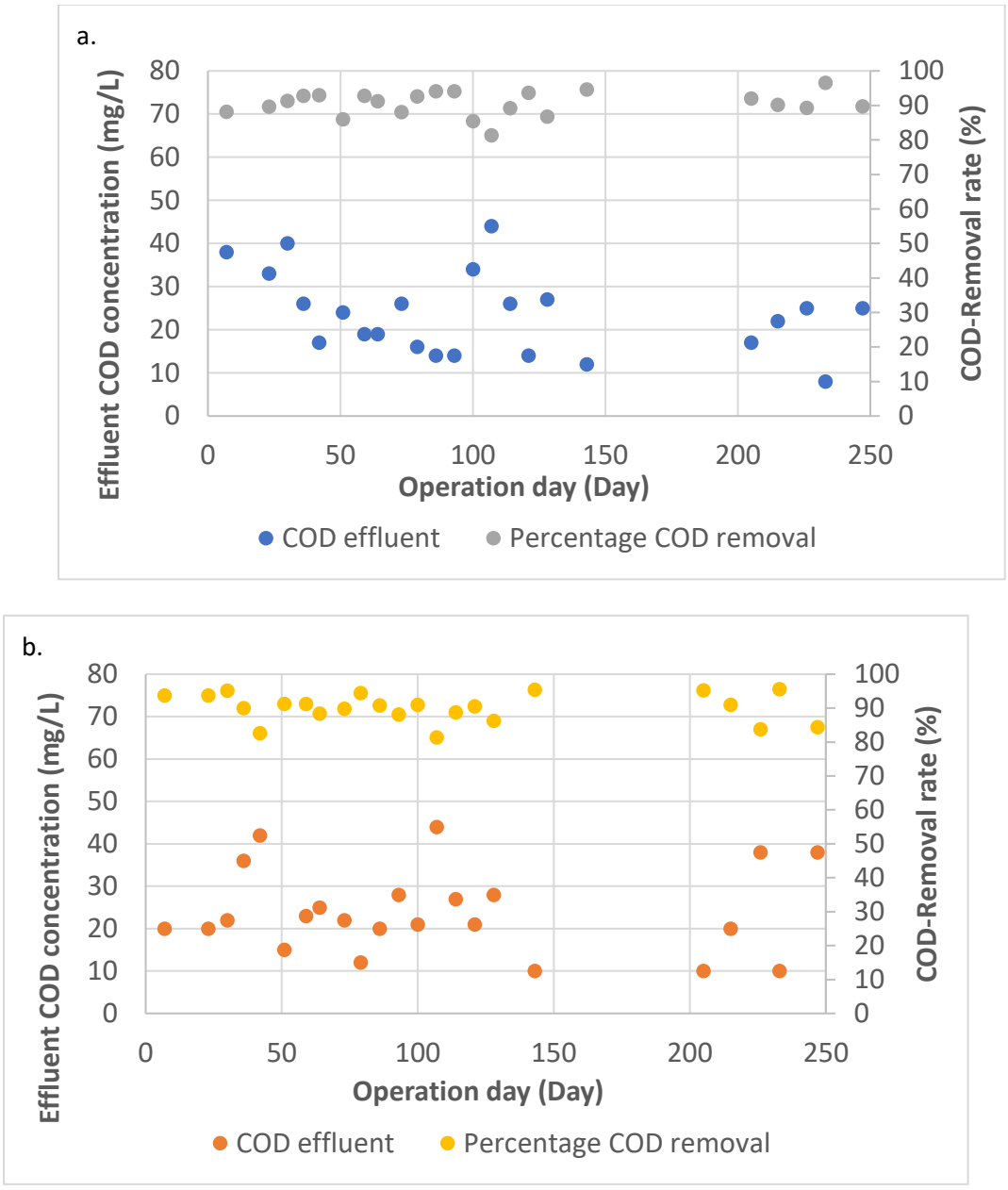

Figure 4-27: Effluent COD concentration (primary axis) and percentage COD removal rate (secondary axis) in a) AGS and b) CAS over duration of reactor operation for organic loading rate of 0.6 kg COD m^{-3} d^{-1}.

Ammonia removal rate was maintained above 98% in both reactors as shown in figure 4-28, indicating the occurrence of almost complete nitrification during the reaction process. This removal rate is similar ($p > 0.05$) to that recorded in the high organic loading rate experimental

phase. The denitrification rate increased in both reactors in the first three months of operation as shown in the decrease in nitrate concentration in the same period. Nitrite concentrations were mostly below 5 mg/L or below the detection limit for both reactors.

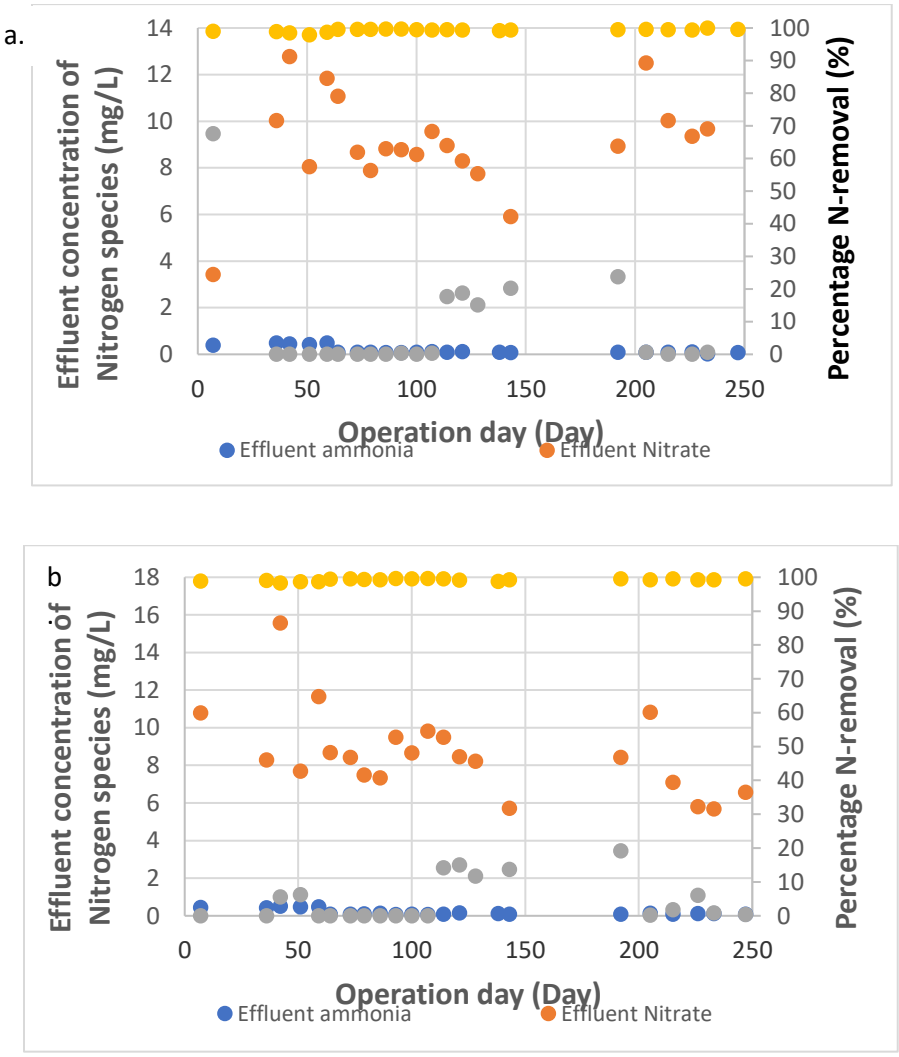

Figure 4-28: Effluent concentration of nitrogen species (primary axis) and percentage ammonia removal (secondary axis) in (a) AGS and (b) CAS during the 2nd experimental phase in which organic loading rate was 0.6 kg COD m^{-3} d^{-1}.

The percentage phosphate removal of aggregates in AGS decreased from 97% to 35% during the first four months of reactor operation. A decline from 95% to 34% in phosphate removal was also measured in CAS in the same time period as shown in figure 4-29. This corresponded to

a sharp decline in solids concentration in both reactors. In the last two months of operation, phosphate removal increased up to 81% in AGS and up to 58% in CAS.

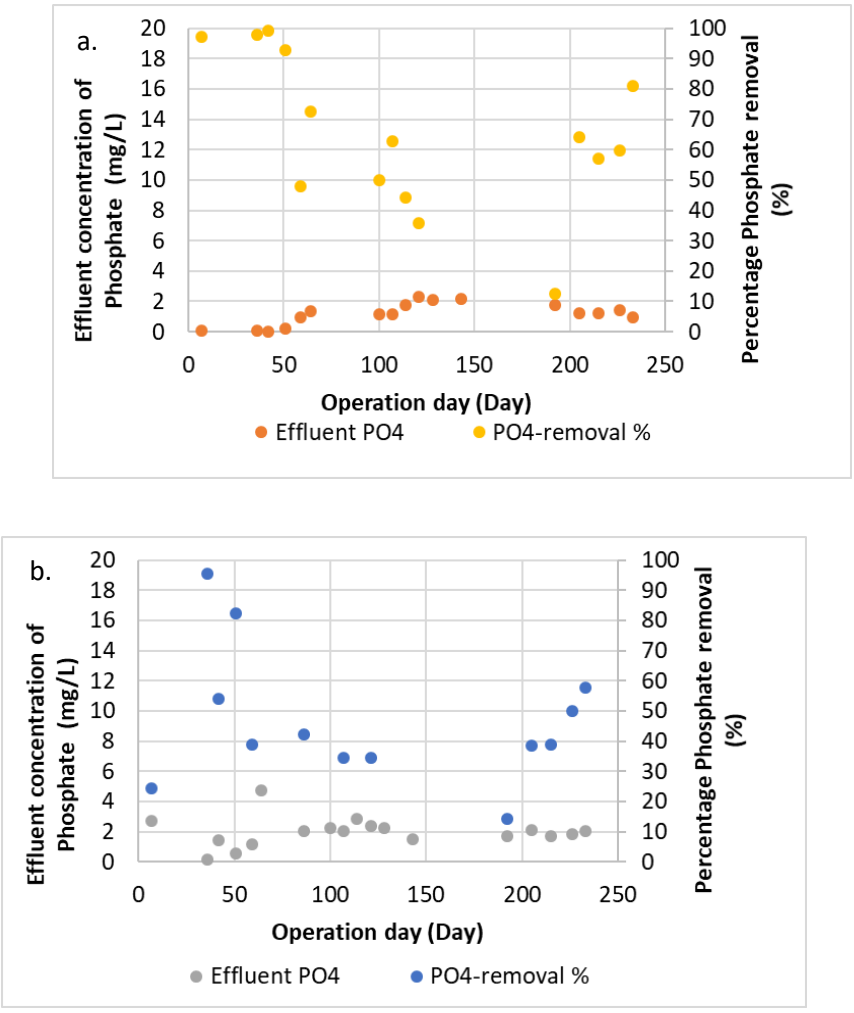

Figure 4-29: Effluent phosphate concentration (primary axis) and percentage phosphate removal (secondary axis) in a) AGS and b) CAS during the 2nd experimental phase in which organic loading rate was 0.6 kg COD m^{-3} d^{-1}.

The summary of reactor parameters during steady state operation is shown in table 4-5. There was no significant difference ($p > 0.05$) in COD, phosphate and ammonia removal rate between both reactors during steady state, but the VSS concentration and percentage total nitrogen removed differed significantly ($p < 0.05$).

Table 4-5: Steady state sludge properties for 2nd experimental phase in which organic loading rate was 0.6 kg COD m^{-3} d^{-1}

	AGS±SD[1]	CAS±SD[1]
Volatile suspended solids concentration (mg VSS/L)	2400 ± 181	1300 ± 130
SVI 5min (mL/g)	48 ± 5	660 ± 110
NH4-Removal efficiency (%)	99.6 ± 0.3	99.3 ± 0.1
Total N-Removal efficiency (%)	37 ± 2	56 ± 5
P- Removal efficiency (%)	66 ± 13	49 ± 10
COD-Removal efficiency (%)	92 ± 3	90 ± 6
Food to microorganism ratio (g rbCOD / gVSS-day)	0.26 ± 0.02	0.44 ± 0.06

4.2.2 Microplastics dosing and quantification

Influent microplastics dosing was carried out for three weeks in both reactors. Microplastics present in influent and effluent samples were counted using epi-fluorescent microscopy and image-J software.

4.2.2.1 Sludge properties during dosing

Sludge samples were observed with the stereomicroscope periodically during microplastics dosing to monitor the size distribution and morphology of aggregates during dosing. By the end of the first week of microplastics dosing, the average diameter of granules in the AGS reactor had increased from 0.2 mm to 0.34 mm but decreased back to 0.2 mm and 0.19mm by the second and third week respectively (figure 4-30). Flocs developed in CAS on the other hand, decreased a little

during the first week but remained at an average diameter of 0.08 mm by the end of the first week of dosing (figure 4-30b). The average diameter of flocs was then maintained at 0.06 mm during the second and third week of dosing. The aspect ratio of granules varied between 1.5 and 2.2 during dosing, while that of flocs varied between 2 and 2.2. An overlay of the size distribution of aggregates before dosing and on the third week of dosing is presented in figure 4-31.

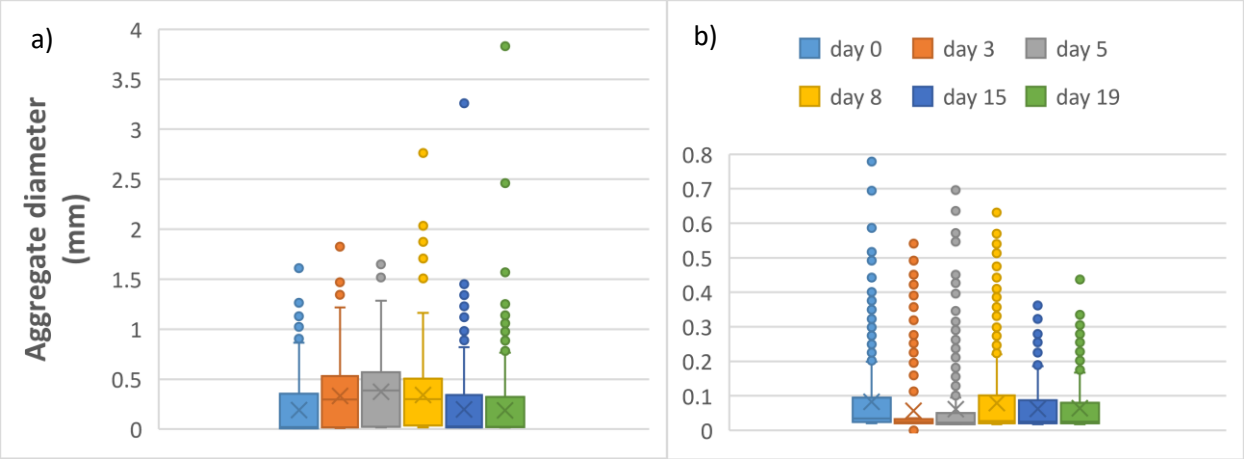

Figure 4-30: Box and whisker plots of aggregate size distribution in a) AGS and b) CAS during microplastics dosing for organic loading rate of 0.6 kg COD m^{-3} d^{-1}

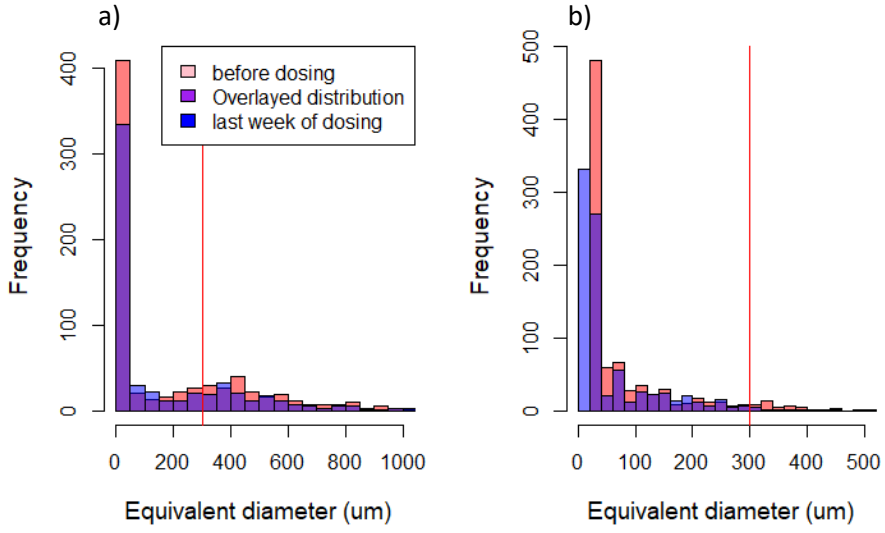

Figure 4-31: Overlapped size frequency distribution of sludge particles before dosing and on third week of dosing in (a) AGS and (b) CAS during 0.6 kg COD m^{-3} d^{-1} experimental phase, determined through image analysis. Red line shows the size limit of flocs (300 μm).

4.2.2.2 Microplastics removal performance

In counting the number of microplastics present in influent and effluent samples, the same subsample area (one-third of filter area) used for analysis in the high organic loading experimental phase was maintained during this low organic loading phase. The microplastics removal rate obtained in both reactors is shown in figure 4-32. A removal rate of 90% and 97% was recorded for the 40-90 µm and 100-150 µm sized particles respectively in the CAS reactor with a total microplastics removal rate of 96%. In the AGS reactor, a removal rate of 98% and 91% was measured for the 40-90 µm and 100-150 µm sized particles respectively, and an overall rate of 94% was recorded. There was no significant difference ($p > 0.05$) in the removal rates between both reactors. However, the removal rates obtained in this low organic loading rate experimental phase is higher than those of the first experimental phase in which a higher organic loading rate was employed.

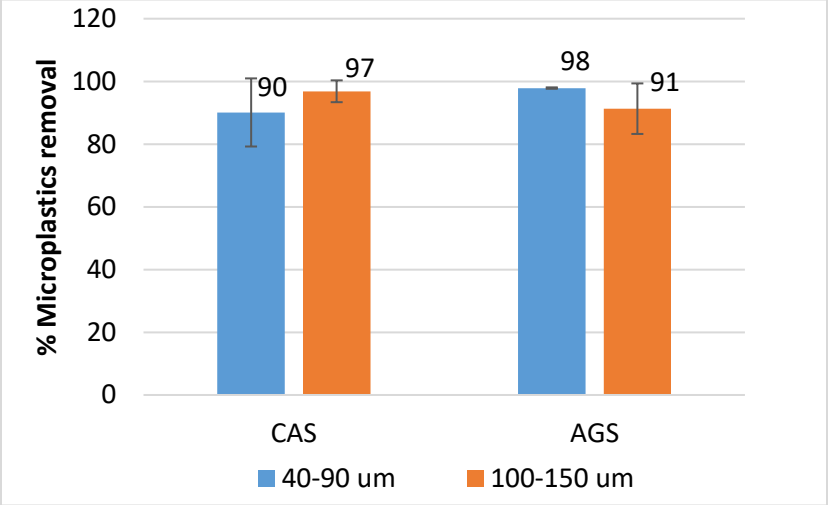

Figure 4-32: Percentage microplastics removal for the 2nd experimental phase in which organic loading rate was 0.6 kg COD m^{-3} d^{-1} and f/m ratio was 0.26 and 0.44 g rbCOD/g VSS-day for AGS and CAS reactors respectively. Error bars represents standard error.

4.2.3 EPS staining

Granule sections and floc samples obtained during microplastics dosing were fixed and stained with fluorescent dyes that probes extracellular polymeric substances (EPS). Stained samples were observed and imaged with the confocal microscope.

A total of 23 granule sections with an area of 1 mm^2 were viewed under the confocal microscope. A summary of microplastics' positioning within the granules is reported in table 4-6. Microplastics were present in 30% of the sections obtained at the granule surface described as region A in figure 4-15. Of the sections viewed at region B, 30% contained microplastics, while 22% of sections observed at the granule core (region C) contained microplastics. Figure 4-33 displays a granule section obtained in the middle of a granule and how the defined regions are determined. A granule section obtained at the surface (region A) is shown in figure 4-34. The position of microplastics within all sampled granule sections is reported in Appendix V. Microplastics found within floc structure were mostly positioned at the edge as shown in figure 4-35.

Table 4-6: Microplastics positioning within whole granule for organic loading rate of 0.6 kg COD m^{-3} d^{-1}

Section depth	Number of sections imaged at region	Percentage of sections with microplastics present (%)
Region A	23	30
Region B	19	30
Region C	10	22

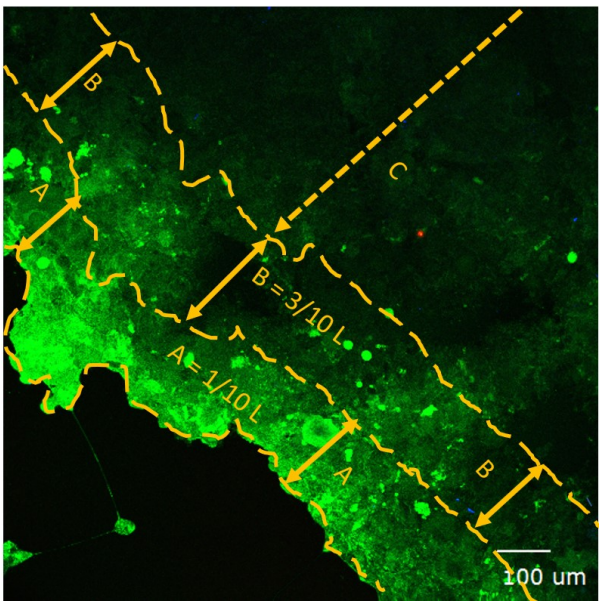

Figure 4-33: Picture of a 30 µm granule section obtained 150 µm from the surface of a 450 µm granule and imaged in the texas-red (red), FITC (green) and ConA (blue) channels. L connotes the approximate granule diameter. Yellow lines show defined regions of microplastic positioning within granules. Images were taken with a Leica confocal microscope using a 10x objective. Scale bar represents 100 µm.

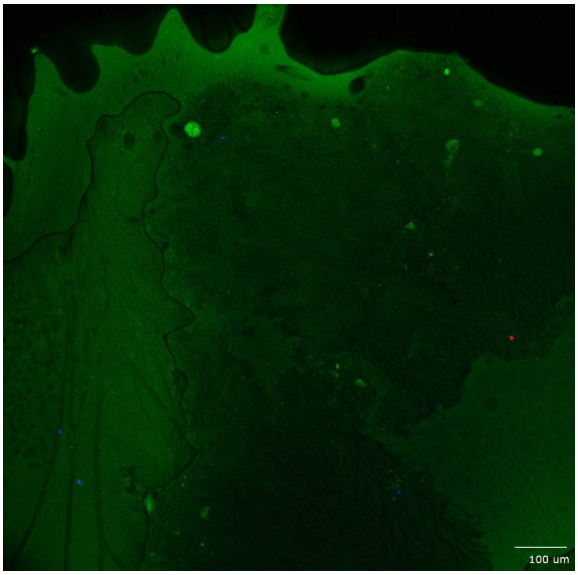

Figure 4-34: Picture of a 30 µm granule section obtained 30 µm from the surface of a 360 µm granule and imaged in the texas-red (red), FITC (green) and ConA (blue) channels. Images were taken with a Leica confocal microscope using a 10x objective. Scale bar represents 100 µm.

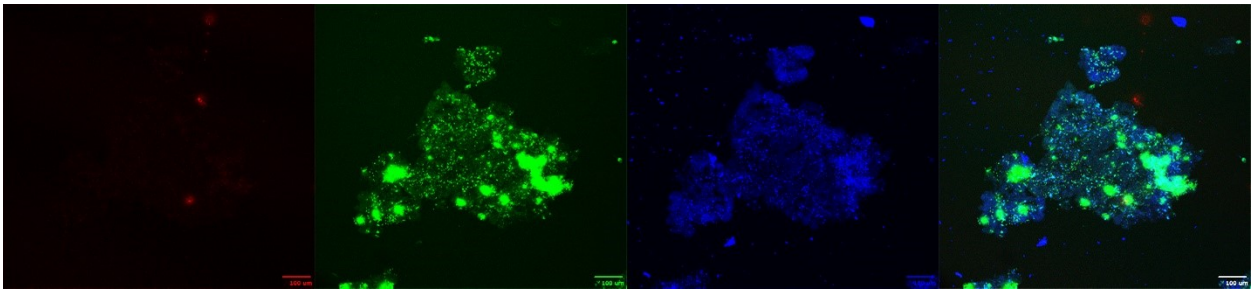

Figure 4-35: Picture of floc sample imaged in the texas-red (red), FITC (green), ConA (blue) and combined overlay channels. Images were taken with a Leica confocal microscope using a 10x objective. Scale bar represents 100 µm.

4.2.4 Chemical identification

Fluorescent red microplastics observed in EPS structure with the confocal microscope were verified with the aid of Fourier transform infrared spectroscopy (FTIR) to determine that fluorescent particles are the actual microplastics dosed in influent wastewater. Spectra extracted from samples were compared with control microplastics spectra. Figure 4-36(a) and (b) shows example spectra obtained from a granule section and floc sample respectively, matched with control microplastics spectra. A spectra match of up to 83% was obtained in both floc samples and granule section confirming the presence of dosed microplastics within EPS structure.

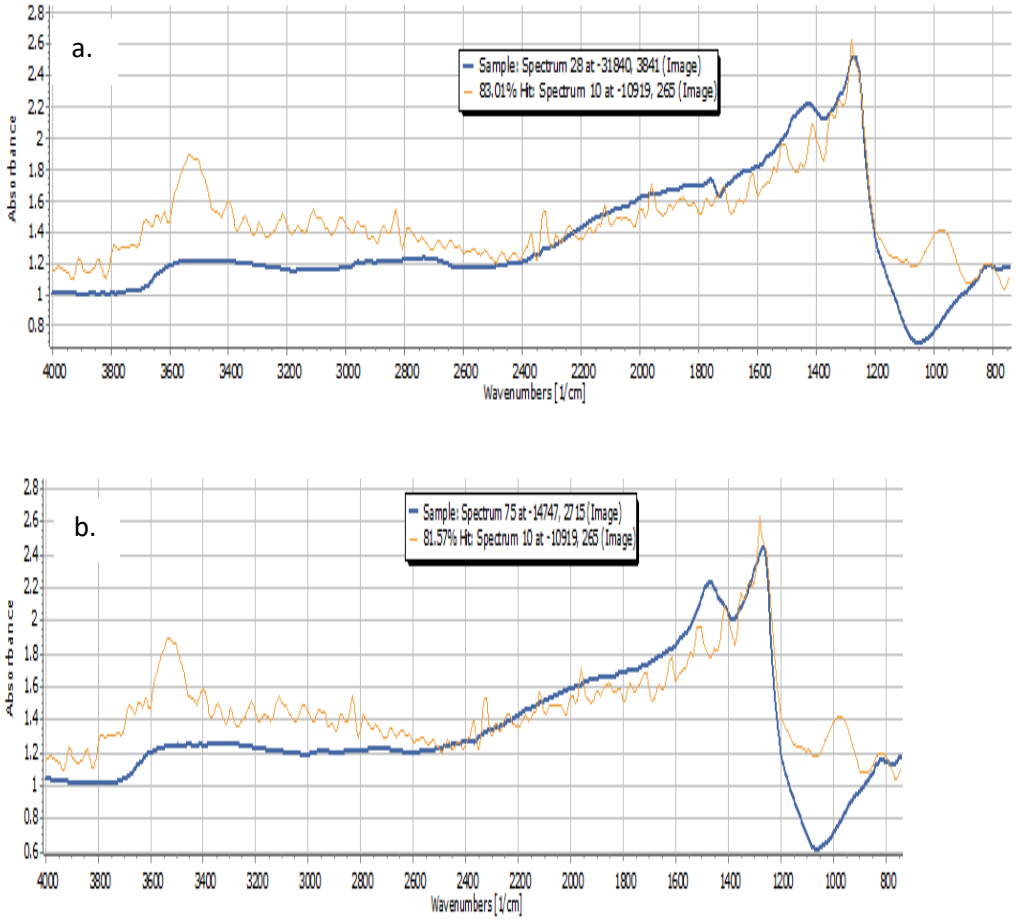

Figure 4-36: Fourier transform infrared spectra of observed microplastics in EPS structure (blue line) matched with control microplastics' spectra (orange line) in (a) granule section, and (b) floc sample

4.2.5 EPS extraction and quantification

At the end of the experiment, EPS was extracted from biomass in both reactors, and the carbohydrate and protein content was analyzed. Results of EPS content are shown in figure 4-37. The protein and carbohydrate content of loosely bound EPS extracted from CAS reactor was 137 and 17 mg LB-EPS / g VSS respectively, while 180 and 18 mg LB-EPS/g VSS was extracted from the AGS reactor respectively. The protein and carbohydrate content of tightly bound EPS extracted from CAS was 380 and 53 mg TB-EPS/g VSS respectively, while 358 and 57 mg TB-EPS/g VSS

was extracted from AGS respectively. The EPS carbohydrate content did not differ significantly ($p > 0.05$) between both reactors, but the EPS protein content differed significantly ($p < 0.05$).

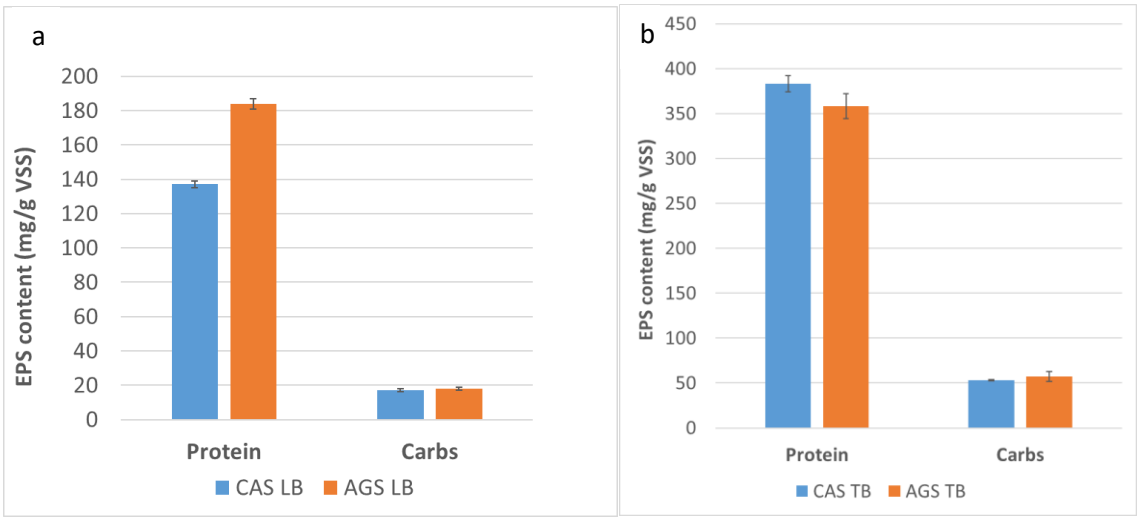

Figure 4-37: Protein and carbohydrate content of (a) loosely-bound EPS and (b) tightly-bound EPS at the end of the 2nd experimental phase in which organic loading rate was 0.6 kg COD m^{-3} d^{-1}

Comparison between EPS extracted in the high organic loading experimental phase and the low organic loading experimental phase is shown in figure 4-38. The low organic loading phase contained higher loosely bound EPS content than the high organic loading phase in both reactors. However, the reverse is the case for the tightly bound EPS fractions in both reactors. The protein content was lower for tightly bound EPS fractions during the low organic loading phase compared to the high organic loading phase in both reactors. The protein and carbohydrate content of loosely bound and tightly bound EPS fractions (except TB-EPS of flocs) were statistically different ($p<0.05$) between the high organic loading phase and the low organic loading phase.

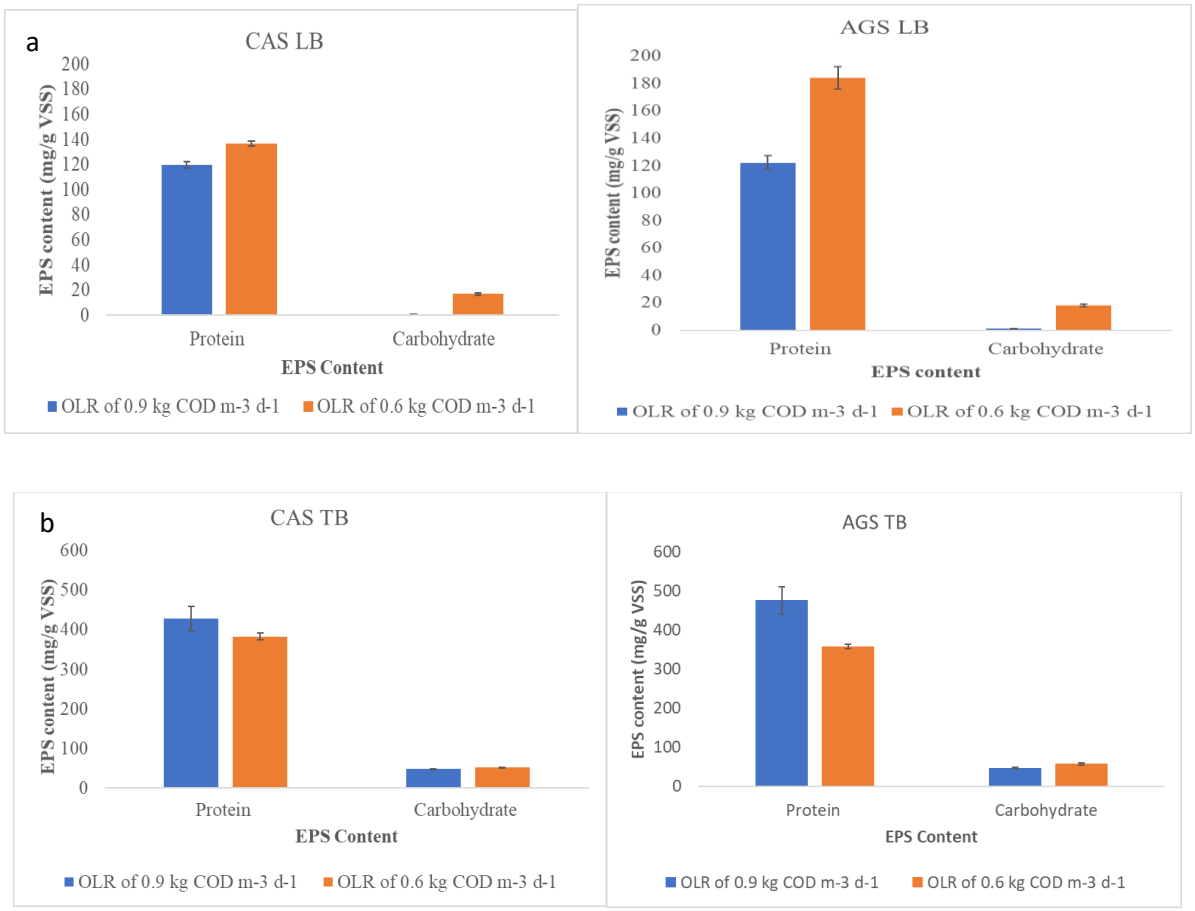

Figure 4-38: Comparison between protein and carbohydrate content of (a) loosely-bound EPS and (b) tightly-bound EPS extracted at an organic loading rate of 0.9 kg COD m^{-3} d^{-1} and organic loading phase of 0.6 kg COD m^{-3} d^{-1}.

5. DISCUSSION

5.1 Organic loading rate of 0.9 kg COD m^{-3} d^{-1}

5.1.1 Aggregate characteristics

Solids greater than 0.3 mm are generally described as granules (de Kreuk, Heijnen, and van Loosdrecht 2005). The aerobic granular sludge reactor contained large compact granules which were also spherical as determined from the average roundness of granules (0.6 ± 0.2). A roundness value of 1 describes a perfectly spherical granule, so values close to 1 would mean the granule is relatively regular and spherical. The compactness and size of the granules provided for good settling properties as determined by the steady state sludge volume index of 93 ± 15 ml/g.

Although the average size (0.1mm) of sludge solids developed in the conventional activated sludge (CAS) reactor were within the size range of flocs found in literature (Pochana and Keller 1999; Jin, Wilén, and Lant 2003), solids contained a proportion of sludge particles greater than 0.3 mm. The solids developed in the CAS reactor were also spherical (roundness of 0.8 ± 0.2). The implication of this was that solids in CAS also had good settling properties (sludge volume index of 81 ± 21 mL/g). In literature, the shape of aggregates have been found to influence settleability (Amaral 2003). Good settling was however only observed in both reactors after about two months of reactor operation when sludge solids were fully developed, and biomass concentration increased. The performance of the activated sludge process is susceptible to an effective solid-liquid separation, which is subsequently determined by the settling properties of sludge.

5.1.2 Treatment efficiency

An almost complete COD and ammonia removal of greater than 95% and 96%, respectively, was measured in both reactors after about three weeks of reactor operation. This

implies that the bacteria responsible for nitrification (*Nitrosomonas* and *Nitrobacter*) were present and fully active. Denitrification however was not as efficient as there were elevated effluent nitrate concentrations (between 6 – 19 mg-N/L) between the second month and the end of reactor operation. For denitrification to occur, an organic carbon source and an anaerobic/anoxic environment must be present. Studies have related aggregate size to simultaneous nitrification/denitrification (SND) in microbial aggregates developed in SBRs (Pochana and Keller 1999; de Kreuk, Heijnen, and van Loosdrecht 2005). SND requires an anoxic zone inside the aggregate for heterotrophic denitrification as a result of limitations in oxygen diffusion. The implication of this is that smaller-sized aggregates will not have a sufficient anoxic region, eventually leading to poor denitrification. Since the dissolved oxygen level for this study was not controlled and was near saturation (about 8 mg O_2/L), it is likely that an excessive penetration of oxygen occurred in aggregates thereby limiting the anoxic volume for nitrate reduction. The steady state total N-removal was 63% in both reactors, higher than results obtained in a full-scale SBR study by Fernandes et al. (2013).

In the CAS reactor, the phosphate removal was low between the 2nd month and the 5th month of reactor operation which corresponded to the period when there was a sharp decline in biomass. The presence of high levels of nitrate during the anoxic period also limited enhanced biological phosphorus removal since organisms using nitrate as electron acceptors (such as denitrifiers) will grow preferentially, thus reducing the VFAs available for storage by the PAOs. In the last month of reactor operation when biomass increased in concentration, phosphate removal increased up to 85% in CAS. The AGS reactor however maintained a phosphate removal between 70 and 98% throughout reactor operation because biomass concentration in the AGS did not undergo any drastic decline compared to CAS.

5.1.3 Microplastics removal at organic loading rate of 0.9 kg COD m^{-3} d^{-1}

During microplastics dosing, the morphology of aggregates changed slightly as seen in the increase in average aspect ratio of both CAS and AGS from 1.5 and 1.9 to 1.7 and 2.0, respectively, by the 2nd week of dosing. However, the aspect ratio reduced back to 1.6 and 1.9, respectively, during the third week of dosing. This may be due to the adjustment of aggregates to the alien particles (microplastics).

5.1.3.1 Evaluation of EPS content as a possible influence on microplastics removal

For both microplastics size fractions used in this study, the AGS reactor performed slightly better than the CAS reactor in microplastics removal efficiency. Similarly, the extracted EPS content of aggregates in AGS was slightly higher. Extracellular proteins were the dominant extracted EPS component in this study, similar to results gotten by Zhu et al. (2012); (Wang et al. 2006; McSwain et al. 2005). EPS has been found to play a significant role in bio-aggregation, aggregate hydrophobicity, adsorption of pollutants, and mass transfer in and out of bacteria cells (Liu et al. 2003; Liu, Liu, and Tay 2004; Wang, Liu, and Tay 2005). Since more EPS is required to form compact granules compared to flocs, it is possible that AGS will have more sites for microplastics adsorption.

5.1.3.2 Evaluation of microplastics positioning within microbial aggregates

Results of EPS staining and FTIR confirmed the presence of microplastics within the EPS structure but an interesting observation was that microplastics were mostly found at a region between the granule surface and the core. This means that the microplastics were possibly more entrained within the outer layers of granules which is the loosely bound EPS matrix. Microplastics observed within floc samples were also positioned at the edge or close to the edge of aggregate structure. This can be explained in terms of the ease of microplastics diffusion through the loosely

bound EPS fraction and adsorption (attachment) within the EPS matrix. From Fick's first law of diffusion (Fick 1855), ideally microplastics would move from the bulk liquid where the concentration of plastics is high to the aggregate structure where there is little or no concentration of microplastics. The aggregate structure however consists of bacteria cells embedded in EPS matrix, and bound EPS is a two-layer model consisting of loosely bound and tightly bound EPS (Nielsen and Jahn 1999). The loosely bound EPS are disperse and not tightly bonded together thereby making it easy for microplastics diffusion and attachment within the region. Wang, Liu, and Tay (2005) in their study of the distribution of EPS and cell surface hydrophobicity in aerobic granules found that the outer shell of aerobic granule was much more hydrophobic than the core.

Results of image analysis of stained aggregates in this study also suggested that microplastics might be attached mostly to the protein fraction of EPS. Studies like Jorand, Boué-Bigne, et al. (1998) discovered that proteins were mostly hydrophobic and carbohydrates were mostly hydrophilic. Given the hydrophobicity of the microplastics used in this study, it is likely that they will be preferentially attached to the protein fraction rather than the carbohydrate fraction of EPS.

5.2 Organic loading rate of 0.6 kg COD m^{-3} d^{-1}

5.2.1 Aggregate characteristics

In this low organic loading phase, the granules developed in the AGS reactor were small (average size of 0.2 mm) and spherical (roundness of 0.7), while flocs developed in the CAS reactor were not regular (roundness of 0.5) compared to flocs developed during the high organic loading phase (roundness of 0.8). Flocs were mostly loose and amorphous containing pin or filamentous flocs, and due to this, settleability was poor. Granules on the other hand possessed good settling properties. The small size of granules and irregular shape of flocs were a direct

consequence of the low daily organic loading rate. Other studies (Tay et al. 2004; Kim, Kim, and Jang 2008; Peyong et al. 2012) also found that smaller aerobic granules were developed at lower organic loading rates. Peyong et al. (2012) successfully grew compact, non-filamentous aerobic granules at an OLR of 0.6 kg/m3 day.

5.2.2 Treatment efficiency

After one month of reactor operation, a COD and ammonia removal of greater than 90% and 98% respectively was measured in both reactors implying that nitrifiers were successfully selected. These results are similar to removal efficiencies recorded in SBR reactors (Fernandes et al. 2013; Orhon et al. 2005; Ni et al. 2009). Effluent nitrate concentrations ranged between 3 – 12 mg/L in AGS, and 5 – 15 mg/L in CAS during reactor operation, giving a steady state total nitrogen removal of 37% in AGS and 56% in CAS. This removal rate was even lower than that recorded for the higher organic loading phase. Granules in this phase are small and the dissolved oxygen level for this study was near saturation (about 8 mg O_2/L), so the anoxic volume generated within the core of aggregates due to oxygen diffusion limitation (Pochana and Keller 1999; de Kreuk, Heijnen, and van Loosdrecht 2005) is either very small or nonexistent, thereby leading to poor denitrification. The lower substrate concentration likely contributed to the poor denitrification since sufficient organic carbon source is required for denitrification to occur. Since this study was focused on microplastics removal, strategies to optimize nitrate removal as found in literature (de Kreuk, Heijnen, and van Loosdrecht 2005; Beun, Heijnen, and Van Loosdrecht 2001) was not carried out.

Phosphate removal in both reactors were greater than 95% after the first month of reactor operation. However, the efficiency declined between the 2^{nd} and 6^{th} month in the period when biomass concentration also declined rapidly. Removal in both reactors were about 34% on day

120. Previous studies have reported that phosphate uptake is directly related to biomass concentration (Bosch 1992). When biomass increased slightly in concentration and became stable, a gradual increase in phosphate removal up to 81% in AGS and 58% in CAS occurred.

5.2.3 Microplastics dosing

As observed during the first experimental phase, the size of aggregates changed slightly during the first and second week of dosing before becoming constant at the start of the third week. While the aspect ratio remained relatively constant during dosing in CAS, the morphology of AGS changed. The roundness reduced from 0.7 on the first day of dosing to 0.5 and 0.47 in the second and third week of dosing. This means that the granules became more irregularly shaped during the experiment. The settling properties of granules remained below 50 ml/g during the experiment, implying that the presence of filamentous granules was not excessively abundant. The change in morphology is likely due to the reaction of aggregate EPS to the presence of microplastics.

5.2.3.1 Comparison of microplastics removal in both experimental phases.

For the smaller sized microplastics (40 – 90 μm), the AGS reactor performed considerably better than the CAS reactor in microplastics removal efficiency (98% and 90% for AGS and CAS respectively). This trend is similar to the removal obtained in the high organic loading phase for this size range. However, the CAS reactor performed slightly better for the larger sized microplastics (91% and 97% for AGS and CAS respectively). Overall, the removal efficiencies recorded in this 2nd phase were higher than those recorded during the high organic loading phase. A look at the results showed that between these experimental phases, the extracted EPS were significantly different and the size and morphology of aggregates during the experiment were also different.

Size and morphology:

The smaller the size of aggregates, the higher the surface area for microplastics attachment (Clark 2011). Hence, the higher removal efficiency in the smaller sized granules is explained. The presence of filamentous flocs and granules during the experiment in the low organic loading phase might also make for an easier capture of microplastics compared to the compact spherical structure of aggregates present during the high organic loading phase. The disperse aggregates would have a much higher surface area than the completely spherical regular-shaped aggregates (Clark 2011), hence providing better microplastics capture than the later.

EPS content:

From the results of extracted EPS content, significantly higher TB-extracellular protein content was recorded in the high organic loading phase. It is likely that TB-EPS fractions was used by bacteria as carbon and energy source during the low organic loading phase. Wang, Liu, and Tay (2005) discovered that under starvation condition, EPS located in the core of aerobic granules could be biodegraded, while EPS located at the outer shell remained intact (nonbiodegradable). In the same study, the authors found that the outer shell of aerobic granule was much more hydrophobic than the core. In this study, the LB-EPS content in the low organic loading phase was significantly higher than those in the high organic loading phase which means aggregates would have more adsorption sites in the former given the disperse structure of the LB-EPS. This would explain why more microplastics were removed during the low organic loading phase. This suggestion is also supported by the results of EPS staining and image analysis in both experimental phases as microplastics were mostly found in the outer layers of granules and at the edge of flocs. In the second experimental phase, microplastics were found within the core probably due to the large surface area of granules.

6. CONCLUSIONS AND FUTURE RECOMMENDATIONS

6.1 Conclusions

This study was carried out to assess the performance of conventional activated sludge and aerobic granular sludge treating synthetic wastewater containing microplastics at two organic loading rates: 0.9 and 0.6 kg COD m^{-3} d^{-1}. An attempt at evaluating the mechanism of microplastics removal was also conducted through granule sectioning and EPS staining.

When the aggregates were fed at an organic loading rate of 0.9 kg COD m^{-3} d^{-1}, dense granules and good-settling flocs were formed ($SV1_5$ of 93±15 and 81±25 mL/g in both reactors). The aggregates removed COD and ammonia efficiently (91-92% and 98-99% respectively). In addition, a total nitrogen removal of 63% and a phosphorus removal of 60-86% was achieved during steady state for both reactors. AGS had a higher total microplastics removal efficiency than CAS (74% and 64% respectively) in this phase. The extracted EPS from both reactor systems comprised mostly of proteins which possibly influenced the adsorption of microplastics within the EPS structure because of the hydrophobicity of proteins. Image analysis also suggested that microplastics were possibly attached within the protein fraction of EPS.

When an organic loading rate of 0.6 kg COD m^{-3} d^{-1} was used to feed the aggregates, smaller compact granules and irregular flocs with a more porous structure than that developed during the first experimental phase were formed. This was a result of the lower readily biodegradable COD fed into the reactors in this phase which also led to a decrease in total EPS production from aggregates. The steady state settling properties for the flocs were especially poor (SVI_5 of 659 mL/g and SVI_{30} of 278 mL/g). However, COD and ammonia was removed efficiently by aggregates in both reactors (90-92% and 99% respectively). Total microplastics removal was considerably higher in this phase compared to the first phase (93% and 95% in CAS and AGS

respectively) possibly because of the larger surface area of aggregates available for microplastics attachment. The higher concentration of loosely bound EPS fractions present in this phase also suggests a higher ease of microplastics diffusion and adsorption within aggregate structure. Image analysis of aggregates in both experimental phases suggested that microplastics were attached to the outer layers of granules, further corroborating the theory of the loosely bound EPS microplastics attachment.

In this study, it was determined that the aggregate morphology influenced by the EPS composition plays an important role in the effective removal of microplastics in activated sludge and aerobic granular sludge treatment systems. Full-scale wastewater treatment plants can optimize the use of irregular aggregates with large surface area for the effective capture of microplastics.

6.2 Future recommendations

Fluorescent red microbeads were used for investigations in this study. The data obtained might be affected if the fluorescent coating of microbeads is lost. Future studies should determine if the coating is indeed lost over time by carrying out a controlled jar study to test fluorescence loss over time while strictly avoiding contamination from open air.

In this study, microplastics' dosing was carried out for a period of three weeks because of the limited duration of the research. Considering the fact that granules break up after a while during mixing to form smaller granules, microplastics removal efficiency might decrease after a certain period since attached microplastics would be released back into the bulk liquid when this happens. Hence, it might be important to conduct this experiment for an extended period of time for future studies in order to investigate the influence of time on microplastics removal. Investigations of

microplastics removal by sampling full-scale wastewater treatment plants might also consolidate the results obtained in this study.

Moreover, in this study, microplastics removal was carried out at an organic loading rate of 0.6 and 0.9 kg COD m^{-3} d^{-1}. Further studies at an even lower organic loading rate or a very low food to microorganism ratio should be conducted to have a clear picture of how aggregate structure and EPS production influenced by low substrate concentration might affect microplastics removal efficiency.

REFERENCES

Ab Halim, Mohd Hakim, Aznah Nor Anuar, Nur Syahida Abdul Jamal, Siti Izaidah Azmi, Zaini Ujang, and Mustafa M. Bob. 2016. 'Influence of high temperature on the performance of aerobic granular sludge in biological treatment of wastewater', *Journal of Environmental Management*, 184: 271-80.

Adav, Sunil S, Duu-Jong Lee, Kuan-Yeow Show, and Joo-Hwa Tay. 2008. 'Aerobic granular sludge: recent advances', *Biotechnology advances*, 26: 411-23.

Adav, Sunil S., and Duu-Jong Lee. 2008. 'Extraction of extracellular polymeric substances from aerobic granule with compact interior structure', *Journal of Hazardous Materials*, 154: 1120-26.

Adav, Sunil S., Duu-Jong Lee, and J. Y. Lai. 2007. 'Effects of aeration intensity on formation of phenol-fed aerobic granules and extracellular polymeric substances', *Applied Microbiology and Biotechnology*, 77: 175-82.

Ahmed, Mohammad Boshir, John L. Zhou, Huu Hao Ngo, Wenshan Guo, Nikolaos S. Thomaidis, and Jiang Xu. 2017. 'Progress in the biological and chemical treatment technologies for emerging contaminant removal from wastewater: A critical review', *Journal of Hazardous Materials*, 323: 274-98.

Amaral, AL. 2003. 'Image analysis in biotechnological processes: applications to wastewater treatment'.

Andrady, Anthony L. 2011. 'Microplastics in the marine environment', *Marine Pollution Bulletin*, 62: 1596-605.

AWWA, APHA. 2005. 'Wef', *Standard Methods for the Examination of Water & Wastewater, 21st ed., American Public Health Association*, 23.

Baird, Fiona J., Marilyn P. Wadsworth, and Jane E. Hill. 2012. 'Evaluation and optimization of multiple fluorophore analysis of a Pseudomonas aeruginosa biofilm', *Journal of Microbiological Methods*, 90: 192-96.

Bassin, J. P., D. C. Tavares, R. C. Borges, and M. Dezotti. 2019. 'Development of aerobic granular sludge under tropical climate conditions: The key role of inoculum adaptation under reduced sludge washout for stable granulation', *Journal of Environmental Management*, 230: 168-82.

Basuvaraj, Mahendran, Jared Fein, and Steven N. Liss. 2015. 'Protein and polysaccharide content of tightly and loosely bound extracellular polymeric substances and the development of a granular activated sludge floc', *Water research*, 82: 104-17.

Beech, Iwona B, CW Sunny Cheung, D Barrie Johnson, and James R Smith. 1996. 'Comparative studies of bacterial biofilms on steel surfaces using atomic force microscopy and environmental scanning electron microscopy', *Biofouling*, 10: 65-77.

Benefield, Larry D, and Clifford W Randall. 1981. 'Biological process design for wastewater treatment.' in, *Prentice Hall Series in Environmental Sciences* (prentice hall).

Beun, JJ, JJ Heijnen, and MCM Van Loosdrecht. 2001. 'N-removal in a granular sludge sequencing batch airlift reactor', *Biotechnology and Bioengineering*, 75: 82-92.

Blackall, Linda L, Gregory R Crocetti, Aaron M Saunders, and Philip L Bond. 2002. 'A review and update of the microbiology of enhanced biological phosphorus removal in wastewater treatment plants', *Antonie Van Leeuwenhoek*, 81: 681-91.

Bosch, Marlene. 1992. 'Phosphorus uptake kinetics of Acinetobacter in activated sludge mixed liquor'.

Bradford, Marion M. 1976. 'A rapid and sensitive method for the quantitation of microgram quantities of protein utilizing the principle of protein-dye binding', *Analytical Biochemistry*, 72: 248-54.

Browne, Mark Anthony, Phillip Crump, Stewart J. Niven, Emma Teuten, Andrew Tonkin, Tamara Galloway, and Richard Thompson. 2011. 'Accumulation of Microplastic on Shorelines Woldwide: Sources and Sinks', *Environmental Science & Technology*, 45: 9175-79.

Bura, R, M Cheung, B Liao, J Finlayson, BC Lee, IG Droppo, GG Leppard, and SN Liss. 1998. 'Composition of extracellular polymeric substances in the activated sludge floc matrix', *Water Science and Technology*, 37: 325-33.

Buttiglieri, Gianluigi, and TP Knepper. 2007. 'Removal of emerging contaminants in wastewater treatment: conventional activated sludge treatment.' in, *Emerging Contaminants from Industrial and Municipal Waste* (Springer).

Carr, Steve A, Jin Liu, and Arnold G Tesoro. 2016. 'Transport and fate of microplastic particles in wastewater treatment plants', *Water research*, 91: 174-82.

Chen, Chunmao, Jie Ming, Brandon A. Yoza, Jiahao Liang, Qing X. Li, Hongqiao Guo, Zhiyuan Liu, Jingmin Deng, and Qinghong Wang. 2019. 'Characterization of aerobic granular sludge used for the treatment of petroleum wastewater', *Bioresource technology*, 271: 353-59.

Chen, Ming-Yuan, Duu-Jong Lee, Joo-Hwa Tay, and Kuan-Yeow Show. 2007. 'Staining of extracellular polymeric substances and cells in bioaggregates', *Applied Microbiology and Biotechnology*, 75: 467-74.

Chien, Chih-Ching, Bo-Chou Lin, and Chun-Hsien Wu. 2013. 'Biofilm formation and heavy metal resistance by an environmental Pseudomonas sp', *Biochemical Engineering Journal*, 78: 132-37.

Claessens, Michiel, Lisbeth Van Cauwenberghe, Michiel B Vandegehuchte, and Colin R Janssen. 2013. 'New techniques for the detection of microplastics in sediments and field collected organisms', *Marine pollution bulletin*, 70: 227-33.

Clark, Mark M. 2011. *Transport modeling for environmental engineers and scientists* (John Wiley & Sons).

Cole, Matthew, Pennie Lindeque, Claudia Halsband, and Tamara S. Galloway. 2011. 'Microplastics as contaminants in the marine environment: A review', *Marine Pollution Bulletin*, 62: 2588-97.

Comte, S., G. Guibaud, and M. Baudu. 2006. 'Relations between extraction protocols for activated sludge extracellular polymeric substances (EPS) and EPS complexation properties: Part I. Comparison of the efficiency of eight EPS extraction methods', *Enzyme and Microbial Technology*, 38: 237-45.

de Kreuk, M.K., J.J. Heijnen, and M.C.M. van Loosdrecht. 2005. 'Simultaneous COD, nitrogen, and phosphate removal by aerobic granular sludge', *Biotechnology and Bioengineering*, 90: 761-69.

Derraik, Jose GB. 2002. 'The pollution of the marine environment by plastic debris: a review', *Marine pollution bulletin*, 44: 842-52.

Dubois, M., K. A. Gilles, J. K. Hamilton, P. A. Rebers, and F. Smith. 1956a. 'Colorimetric method for determination of sugars and related substances', *Analytical Chemistry*, 28: 350-56.

Dubois, Michel, K Ao Gilles, J Ko Hamilton, PA t Rebers, and Fred Smith. 1956b. 'Colorimetric method for determination of sugars and related substances', *Analytical chemistry*, 28: 350-56.

Durmaz, B, and FD Sanin. 2001. 'Effect of carbon to nitrogen ratio on the composition of microbial extracellular polymers in activated sludge', *Water Science and Technology*, 44: 221-29.

Dutta, Kasturi, Cheng-Yu Tsai, Wen-Hsing Chen, and Jih-Gaw Lin. 2014. 'Effect of carriers on the performance of anaerobic sequencing batch biofilm reactor treating synthetic municipal wastewater', *International Biodeterioration & Biodegradation*, 95: 84-88.

Eerkes-Medrano, Dafne, Richard C Thompson, and David C Aldridge. 2015. 'Microplastics in freshwater systems: a review of the emerging threats, identification of knowledge gaps and prioritisation of research needs', *Water research*, 75: 63-82.

Felz, Simon, Salah Al-Zuhairy, Olav Andreas Aarstad, Mark CM van Loosdrecht, and Yue Mei Lin. 2016. 'Extraction of structural extracellular polymeric substances from aerobic granular sludge', *JoVE (Journal of Visualized Experiments)*: e54534.

Fendall, Lisa S., and Mary A. Sewell. 2009. 'Contributing to marine pollution by washing your face: Microplastics in facial cleansers', *Marine pollution bulletin*, 58: 1225-28.

Fernandes, Heloísa, Mariele K. Jungles, Heike Hoffmann, Regina V. Antonio, and Rejane H. R. Costa. 2013. 'Full-scale sequencing batch reactor (SBR) for domestic wastewater: Performance and diversity of microbial communities', *Bioresource Technology*, 132: 262-68.

Fick, Adolph. 1855. 'V. On liquid diffusion', *The London, Edinburgh, and Dublin Philosophical Magazine and Journal of Science*, 10: 30-39.

Frias, JPGL, P Sobral, and AM Ferreira. 2010. 'Organic pollutants in microplastics from two beaches of the Portuguese coast', *Marine pollution bulletin*, 60: 1988-92.

Frølund, Bo, Rikke Palmgren, Kristian Keiding, and Per Halkjær Nielsen. 1996. 'Extraction of extracellular polymers from activated sludge using a cation exchange resin', *Water research*, 30: 1749-58.

Gallagher, Anthony, Aldous Rees, Rob Rowe, John Stevens, and Paul Wright. 2016. 'Microplastics in the Solent estuarine complex, UK: an initial assessment', *Marine pollution bulletin*, 102: 243-49.

Gaudy, AF. 1962. 'Colorimetric determination of protein and carbohydrate', *Ind. Water Wastes.*, 7: 17-22.

Goldstein, Irwin J, and Colleen E Hayes. 1978. 'The lectins: carbohydrate-binding proteins of plants and animals.' in, *Advances in carbohydrate chemistry and biochemistry* (Elsevier).

Goodship, Vannessa. 2007. *Introduction to plastics recycling* (iSmithers Rapra Publishing).

Gregory, Murray R. 1996. 'Plastic 'scrubbers' in hand cleansers: a further (and minor) source for marine pollution identified', *Marine pollution bulletin*, 32: 867-71.

Hammer, Jort, Michiel HS Kraak, and John R Parsons. 2012. 'Plastics in the marine environment: the dark side of a modern gift.' in, *Reviews of environmental contamination and toxicology* (Springer).

Heijnen, J, and M Van Loosdrecht. 1998. 'Method for acquiring grain-shaped growth of a microorganism in a reactor', *Biofutur*, 183: 50.

Imhof, Hannes K, Johannes Schmid, Reinhard Niessner, Natalia P Ivleva, and Christian Laforsch. 2012. 'A novel, highly efficient method for the separation and quantification of plastic particles in sediments of aquatic environments', *Limnology and oceanography: methods*, 10: 524-37.

Janga, Namjung, Xianghao Ren, Geontae Kim, Changhyo Ahn, Jaeweon Cho, and In S Kim. 2007. 'Characteristics of soluble microbial products and extracellular polymeric substances in the membrane bioreactor for water reuse', *Desalination*, 202: 90-98.

Jenkins, David, Michael G Richard, and Glen T Daigger. 2003. *Manual on the causes and control of activated sludge bulking, foaming, and other solids separation problems* (Crc Press).

Jin, Bo, Britt-Marie Wilén, and Paul Lant. 2003. 'A comprehensive insight into floc characteristics and their impact on compressibility and settleability of activated sludge', *Chemical Engineering Journal*, 95: 221-34.

Jorand, F, F Boue-Bigne, JC Block, and V Urbain. 1998. 'Hydrophobic/hydrophilic properties of activated sludge exopolymeric substances', *Water Science and Technology*, 37: 307-15.

Jorand, F., F. Boué-Bigne, J. C. Block, and V. Urbain. 1998. 'Hydrophobic/hydrophilic properties of activated sludge exopolymeric substances', *Water Science and Technology*, 37: 307-15.

Keiding, Kristian, Lisbeth Wybrandt, and Per Halkjær Nielsen. 2001. 'Remember the water-a comment on EPS colligative properties', *Water Science and Technology*, 43: 17-23.

Kim, In S., Sung-Min Kim, and Am Jang. 2008. 'Characterization of aerobic granules by microbial density at different COD loading rates', *Bioresource technology*, 99: 18-25.

Klatt, Christian G., and Timothy M. LaPara. 2003. 'Aerobic biological treatment of synthetic municipal wastewater in membrane-coupled bioreactors', *Biotechnology and bioengineering*, 82: 313-20.

Lenz, Robin, Kristina Enders, Colin A. Stedmon, David M. A. Mackenzie, and Torkel Gissel Nielsen. 2015. 'A critical assessment of visual identification of marine microplastic using Raman spectroscopy for analysis improvement', *Marine Pollution Bulletin*, 100: 82-91.

Li, X. Y., and S. F. Yang. 2007. 'Influence of loosely bound extracellular polymeric substances (EPS) on the flocculation, sedimentation and dewaterability of activated sludge', *Water Research*, 41: 1022-30.

Li, Xu, and Bruce E Logan. 2004. 'Analysis of bacterial adhesion using a gradient force analysis method and colloid probe atomic force microscopy', *Langmuir*, 20: 8817-22.
Liu, Hong, and Herbert H. P. Fang. 2002. 'Extraction of extracellular polymeric substances (EPS) of sludges', *Journal of biotechnology*, 95: 249-56.
Liu, Yan, and Herbert HP Fang. 2003. 'Influences of extracellular polymeric substances (EPS) on flocculation, settling, and dewatering of activated sludge'.
Liu, Yong-Qiang, Yu Liu, and Joo-Hwa Tay. 2004. 'The effects of extracellular polymeric substances on the formation and stability of biogranules', *Applied Microbiology and Biotechnology*, 65: 143-48.
Liu, Yu, and Joo-Hwa Tay. 2001. 'Detachment forces and their influence on the structure and metabolic behaviour of biofilms', *World Journal of Microbiology and Biotechnology*, 17: 111-17.
Liu, Yu, Shu-Fang Yang, Qi-Shan Liu, and Joo-Hwa Tay. 2003. 'The role of cell hydrophobicity in the formation of aerobic granules', *Current microbiology*, 46: 0270-74.
Lowry, Oliver H, Nira J Rosebrough, A Lewis Farr, and Rose J Randall. 1951. 'Protein measurement with the Folin phenol reagent', *Journal of biological chemistry*, 193: 265-75.
Magnusson, Kerstin, and Fredrik Norén. 2014. 'Screening of microplastic particles in and down-stream a wastewater treatment plant'.
Mason, Sherri A., Danielle Garneau, Rebecca Sutton, Yvonne Chu, Karyn Ehmann, Jason Barnes, Parker Fink, Daniel Papazissimos, and Darrin L. Rogers. 2016. 'Microplastic pollution is widely detected in US municipal wastewater treatment plant effluent', *Environmental Pollution*, 218: 1045-54.
Masura, Julie, Joel E. Baker, Gregory D. Foster, Courtney Arthur, and Carlie Herring. 2015. 'Laboratory methods for the analysis of microplastics in the marine environment : recommendations for quantifying synthetic particles in waters and sediments'.
Mayer, Christian, Ralf Moritz, Carolin Kirschner, Werner Borchard, Ralf Maibaum, Jost Wingender, and Hans-Curt Flemming. 1999. 'The role of intermolecular interactions: studies on model systems for bacterial biofilms', *International Journal of Biological Macromolecules*, 26: 3-16.
McCormick, Amanda, Timothy J. Hoellein, Sherri A. Mason, Joseph Schluep, and John J. Kelly. 2014. 'Microplastic is an abundant and distinct microbial habitat in an urban river', *Environmental science & technology*, 48: 11863-71.
McSwain, BS, RL Irvine, M Hausner, and PA Wilderer. 2005. 'Composition and distribution of extracellular polymeric substances in aerobic flocs and granular sludge', *Appl. Environ. Microbiol.*, 71: 1051-57.
Michielssen, Marlies R, Elien R Michielssen, Jonathan Ni, and Melissa B Duhaime. 2016. 'Fate of microplastics and other small anthropogenic litter (SAL) in wastewater treatment plants depends on unit processes employed', *Environmental Science: Water Research & Technology*, 2: 1064-73.
Mikkelsen, Lene Haugaard, and Per Halkjær Nielsen. 2001. 'Quantification of the bond energy of bacteria attached to activated sludge floc surfaces', *Water Science and Technology*, 43: 67-75.
Mintenig, SM, Ivo Int-Veen, Martin GJ Löder, Sebastian Primpke, and Gunnar Gerdts. 2017. 'Identification of microplastic in effluents of waste water treatment plants using focal plane array-based micro-Fourier-transform infrared imaging', *Water Research*, 108: 365-72.
Miranda, Daniele de A, and Gustavo Freire de Carvalho-Souza. 2016. 'Are we eating plastic-ingesting fish?', *Marine pollution bulletin*, 103: 109-14.
Mishima, K, and M Nakamura. 1991. 'Self-immobilization of aerobic activated sludge–a pilot study of the aerobic upflow sludge blanket process in municipal sewage treatment', *Water Science and Technology*, 23: 981-90.
Murphy, Fionn, Ciaran Ewins, Frederic Carbonnier, and Brian Quinn. 2016. 'Wastewater treatment works (WwTW) as a source of microplastics in the aquatic environment', *Environmental science & technology*, 50: 5800-08.

Neu, Thomas R, and John R Lawrence. 2014. 'Advanced techniques for in situ analysis of the biofilm matrix (structure, composition, dynamics) by means of laser scanning microscopy.' in, *Microbial Biofilms* (Springer).

Ni, Bing-Jie, Wen-Ming Xie, Shao-Gen Liu, Han-Qing Yu, Ying-Zhe Wang, Gan Wang, and Xian-Liang Dai. 2009. 'Granulation of activated sludge in a pilot-scale sequencing batch reactor for the treatment of low-strength municipal wastewater', *Water Research*, 43: 751-61.

Nielsen, Per H, and Andreas Jahn. 1999. 'Extraction of EPS.' in, *Microbial extracellular polymeric substances* (Springer).

Nizzetto, Luca, Martyn Futter, and Sindre Langaas. 2016. "Are Agricultural Soils Dumps for Microplastics of Urban Origin?" In.: ACS Publications.

Nouha, K, NV Hoang, Yan Song, Rajeshwar Dayal Tyagi, and Rao Surampalli. 2016. 'Characterization of extracellular polymeric substances (eps) produced by Cloacibacterium normanense isolated from wastewater sludge for sludge settling and dewatering'.

Nouha, Klai, Ram Saurabh Kumar, Sellamuthu Balasubramanian, and Rajeshwar Dayal Tyagi. 2018. 'Critical review of EPS production, synthesis and composition for sludge flocculation', *Journal of Environmental Sciences*, 66: 225-45.

Nuelle, Marie-Theres, Jens H Dekiff, Dominique Remy, and Elke Fries. 2014. 'A new analytical approach for monitoring microplastics in marine sediments', *Environmental Pollution*, 184: 161-69.

Orhon, Derin, Ozlem Karahan, GE Zengin, Oliver Olsson, and Melanie Bauer. 2005. *Mechanism and design of sequencing batch reactors for nutrient removal* (Iwa Publishing).

Peyong, Yet Nee, Yan Zhou, Ahmad Zuhairi Abdullah, and Vel Vadivelu. 2012. 'The effect of organic loading rates and nitrogenous compounds on the aerobic granules developed using low strength wastewater', *Biochemical Engineering Journal*, 67: 52-59.

Pochana, Klangduen, and Jürg Keller. 1999. 'Study of factors affecting simultaneous nitrification and denitrification (SND)', *Water Science and Technology*, 39: 61-68.

Quarmby, J., and C. F. Forster. 1995. 'An examination of the structure of UASB granules', *Water research*, 29: 2449-54.

Rao, Pragna, and Thillaisthanam N Pattabiraman. 1989. 'Reevaluation of the phenol-sulfuric acid reaction for the estimation of hexoses and pentoses', *Analytical Biochemistry*, 181: 18-22.

Raunkjær, Kamma, Thorkild Hvitved-Jacobsen, and Per Halkjær Nielsen. 1994. 'Measurement of pools of protein, carbohydrate and lipid in domestic wastewater', *Water research*, 28: 251-62.

Rocha-Santos, Teresa, and Armando C Duarte. 2015. 'A critical overview of the analytical approaches to the occurrence, the fate and the behavior of microplastics in the environment', *TrAC Trends in Analytical Chemistry*, 65: 47-53.

Rochman, Chelsea M, Sara M Kross, Jonathan B Armstrong, Michael T Bogan, Emily S Darling, Stephanie J Green, Ashley R Smyth, and Diogo Veríssimo. 2015. 'Scientific evidence supports a ban on microbeads', *Environmental science & technology*, 49: 10759-61.

Rochman, Chelsea M, Akbar Tahir, Susan L Williams, Dolores V Baxa, Rosalyn Lam, Jeffrey T Miller, Foo-Ching Teh, Shinta Werorilangi, and Swee J Teh. 2015. 'Anthropogenic debris in seafood: Plastic debris and fibers from textiles in fish and bivalves sold for human consumption', *Scientific Reports*, 5: 14340.

Schmid, Markus, Antoine Thill, Ulrike Purkhold, Marion Walcher, Jean Yves Bottero, Philippe Ginestet, Per Halkjær Nielsen, Stefan Wuertz, and Michael Wagner. 2003. 'Characterization of activated sludge flocs by confocal laser scanning microscopy and image analysis', *Water Research*, 37: 2043-52.

Schmidt, JEE, and Birgitte Kiær Ahring. 1994. 'Extracellular polymers in granular sludge from different upflow anaerobic sludge blanket (UASB) reactors', *Applied Microbiology and Biotechnology*, 42: 457-62.

Setälä, Outi, Vivi Fleming-Lehtinen, and Maiju Lehtiniemi. 2014. 'Ingestion and transfer of microplastics in the planktonic food web', *Environmental Pollution*, 185: 77-83.

Seviour, Thomas, Nicolas Derlon, Morten Simonsen Dueholm, Hans-Curt Flemming, Elisabeth Girbal-Neuhauser, Harald Horn, Staffan Kjelleberg, Mark CM van Loosdrecht, Tommaso Lotti, and Robert Nerenberg. 2018. 'Extracellular polymeric substances of biofilms: suffering from an identity crisis', *Water research*.

Seviour, Thomas, Zhiguo Yuan, Mark C. M. van Loosdrecht, and Yuemei Lin. 2012. 'Aerobic sludge granulation: A tale of two polysaccharides?', *Water Research*, 46: 4803-13.

Sheng, Guo-Ping, Han-Qing Yu, and Xiao-Yan Li. 2010. 'Extracellular polymeric substances (EPS) of microbial aggregates in biological wastewater treatment systems: A review', *Biotechnology Advances*, 28: 882-94.

Shim, Won Joon, Young Kyoung Song, Sang Hee Hong, and Mi Jang. 2016. 'Identification and quantification of microplastics using Nile Red staining', *Marine pollution bulletin*, 113: 469-76.

Smith, P. K., R. I. Krohn, G. T. Hermanson, A. K. Mallia, F. H. Gartner, M. D. Provenzano, E. K. Fujimoto, N. M. Goeke, B. J. Olson, and D. C. Klenk. 1985. 'Measurement of protein using bicinchoninic acid', *Analytical Biochemistry*, 150: 76-85.

Smolders, G. J. F., M. C. M. van Loosdrecht, and J. J. Heijnen. 1995. 'A metabolic model for the biological phosphorus removal process', *Water Science and Technology*, 31: 79-93.

Song, Young Kyoung, Sang Hee Hong, Mi Jang, Gi Myung Han, Manviri Rani, Jongmyoung Lee, and Won Joon Shim. 2015. 'A comparison of microscopic and spectroscopic identification methods for analysis of microplastics in environmental samples', *Marine pollution bulletin*, 93: 202-09.

Späth, R., H. C. Flemming, and S. Wuertz. 1998. 'Sorption properties of biofilms', *Water Science and Technology*, 37: 207-10.

Strathmann, Martin, Jost Wingender, and Hans-Curt Flemming. 2002. 'Application of fluorescently labelled lectins for the visualization and biochemical characterization of polysaccharides in biofilms of Pseudomonas aeruginosa', *Journal of Microbiological Methods*, 50: 237-48.

Sun, Jing, Xiaohu Dai, Qilin Wang, Mark C. M. van Loosdrecht, and Bing-Jie Ni. 2019. 'Microplastics in wastewater treatment plants: Detection, occurrence and removal', *Water Research*, 152: 21-37.

Sutton, Rebecca, Sherri A. Mason, Shavonne K. Stanek, Ellen Willis-Norton, Ian F. Wren, and Carolynn Box. 2016. 'Microplastic contamination in the San Francisco Bay, California, USA', *Marine pollution bulletin*, 109: 230-35.

Talvitie, Julia, Mari Heinonen, Jari-Pekka Pääkkönen, Emil Vahtera, Anna Mikola, Outi Setälä, and Riku Vahala. 2015. 'Do wastewater treatment plants act as a potential point source of microplastics? Preliminary study in the coastal Gulf of Finland, Baltic Sea', *Water Science and Technology*, 72: 1495-504.

Talvitie, Julia, Anna Mikola, Outi Setälä, Mari Heinonen, and Arto Koistinen. 2017. 'How well is microlitter purified from wastewater?–A detailed study on the stepwise removal of microlitter in a tertiary level wastewater treatment plant', *Water research*, 109: 164-72.

Tay, J-H, Q-S Liu, and Y Liu. 2001a. 'Microscopic observation of aerobic granulation in sequential aerobic sludge blanket reactor', *Journal of Applied Microbiology*, 91: 168-75.

———. 2001b. 'The role of cellular polysaccharides in the formation and stability of aerobic granules', *Letters in Applied Microbiology*, 33: 222-26.

Tay, Joo-Hwa, Shun Pan, Yanxin He, and Stephen Tiong Lee Tay. 2004. 'Effect of organic loading rate on aerobic granulation. II: Characteristics of aerobic granules', *Journal of Environmental Engineering*, 130: 1102-09.

Tchobanoglous, G, HD Stensel, R Tsuchihashi, F Burton, M Abu-Orf, G Bowden, and W Pfrang. 2014. "Waterwater Engineering: Treatment and Resource Recovery, Metcalf and Eddy Inc." In.: McGraw-Hill, New York.

Teuten, Emma L, Jovita M Saquing, Detlef RU Knappe, Morton A Barlaz, Susanne Jonsson, Annika Björn, Steven J Rowland, Richard C Thompson, Tamara S Galloway, and Rei Yamashita. 2009. 'Transport and release of chemicals from plastics to the environment and to wildlife', *Philosophical Transactions of the Royal Society B: Biological Sciences*, 364: 2027-45.

Tsuneda, S, S Park, H Hayashi, J Jung, and A Hirata. 2001. 'Enhancement of nitrifying biofilm formation using selected EPS produced by heterotrophic bacteria', *Water Science and Technology*, 43: 197-204.

Van Cauwenberghe, Lisbeth, Ann Vanreusel, Jan Mees, and Colin R Janssen. 2013. 'Microplastic pollution in deep-sea sediments', *Environmental Pollution*, 182: 495-99.

Van der Roest, HF, LMM De Bruin, G Gademan, and F Coelho. 2011. 'Towards sustainable waste water treatment with Dutch Nereda® technology', *Water Practice and Technology*, 6.

van Dijk, Edward J. H., Mario Pronk, and Mark C. M. van Loosdrecht. 2018. 'Controlling effluent suspended solids in the aerobic granular sludge process', *Water research*, 147: 50-59.

Wagner, Martin, Christian Scherer, Diana Alvarez-Muñoz, Nicole Brennholt, Xavier Bourrain, Sebastian Buchinger, Elke Fries, Cécile Grosbois, Jörg Klasmeier, and Teresa Marti. 2014. 'Microplastics in freshwater ecosystems: what we know and what we need to know', *Environmental Sciences Europe*, 26: 12.

Wang, Zhi-Wu, Yu Liu, and Joo-Hwa Tay. 2005. 'Distribution of EPS and cell surface hydrophobicity in aerobic granules', *Applied Microbiology and Biotechnology*, 69: 469.

Wang, Zhiping, Lili Liu, Jie Yao, and Weimin Cai. 2006. 'Effects of extracellular polymeric substances on aerobic granulation in sequencing batch reactors', *Chemosphere*, 63: 1728-35.

Wei, Yuansong, Renze T. Van Houten, Arjan R. Borger, Dick H. Eikelboom, and Yaobo Fan. 2003. 'Minimization of excess sludge production for biological wastewater treatment', *Water research*, 37: 4453-67.

Zhang, Tong, and Herbert HP Fang. 2001. 'Quantification of extracellular polymeric substances in biofilms by confocal laser scanning microscopy', *Biotechnology letters*, 23: 405-09.

Zhu, Liang, Mei-le Lv, Xin Dai, Yan-wen Yu, Han-ying Qi, and Xiang-yang Xu. 2012. 'Role and significance of extracellular polymeric substances on the property of aerobic granule', *Bioresource technology*, 107: 46-54.

Ziajahromi, Shima, Peta A Neale, and Frederic DL Leusch. 2016. 'Wastewater treatment plant effluent as a source of microplastics: review of the fate, chemical interactions and potential risks to aquatic organisms', *Water Science and Technology*, 74: 2253-69.

Ziajahromi, Shima, Peta A Neale, Llew Rintoul, and Frederic DL Leusch. 2017. 'Wastewater treatment plants as a pathway for microplastics: development of a new approach to sample wastewater-based microplastics', *Water Research*, 112: 93-99.

APPENDIXES

Appendix I: Trace metals solution recipe used in the preparation of synthetic wastewater

Compound	Concentration(g/L)
$FeCl_3*6H_2O$	1.5
H_3BO_3	0.15
$CuSO_4*5H_2O$	0.03
KI	0.03
$MnCL_2*4H_2O$	0.12
$Na_2MoO_4*2H_2O$	0.06
$ZnSO_4*7H_2O$	0.12
$CoCl_2*6H_2O$	0.15

Appendix II: Ion Chromatography operating conditions employed for the measurement of nitrite, nitrate and phosphate concentrations of influent and effluent wastewater samples

Columns	IonPac AS18 4 × 250 mm Analytical Column (Dionex P/N 060549)
	IonPac AG18 4 × 250 mm Guard Column (Dionex P/N 060551)
Eluent source	ICS-2000
Eluent concentration	26 Mm KOH
Flow rate	1 mL/min
Temperature	30 ºC
Injection volume	5 mL
Sample run time	18
Suppresser current	75 mA
Detection	Suppressed conductivity, ASRS® ULTRA, 4 mm (Dionex P/N 053947) AutoSuppression®

Appendix III: Standard operating procedure for phenol sulfuric acid assay for carbohydrate analysis

Prepare Glucose Standards

1. When preparing glucose standards, prepare in batches, aliquot into 2 mL centrifuge tubes (400 µL per tube), and freeze at -20°C for storage.

2. Add 2.500 g of dextrose (D-glucose) powder to a 500 mL volumetric flask and dilute to 500 mL with Nanopure water to achieve a final concentration of 5 $g \cdot L^{-1}$. Mix well, and label this Flask A.

3. Using a volumetric pipette, pull out 10 mL from Flask A and add it to a 100 mL volumetric flask. Dilute to 100 mL with Nanopure water to achieve a final concentration of 500 $mg \cdot L^{-1}$ glucose solution. This will be the first point on the standard curve. Label this as Flask B.

4. Prepare 6 more standards using the combination of glucose stock and diluent (Nanopure water) as shown in the table below. Make sure flasks are well-mixed before pipetting to the next flask.

Flask	Volume and Source of Glucose	Volume of Diluent (Nanopure water)	Glucose Concentration [$mg \cdot L^{-1}$]
B	10 mL of Flask A	90 mL	500
C	50 mL of Flask B	50 mL	250
D	50 mL of Flask C	50 mL	125
E	**40 mL** of Flask D	**60 mL**	50
F	50mL of Flask E	50mL	25
G	50mL of Flask F	50mL	12.5
H	-	100 mL	0 - Blank

5. Mix standards again and transfer to pre-labeled 50 mL centrifuge tubes.

6. Pipette 400 µL of each standard solution into each of fifteen 2 mL screw cap centrifuge tubes.

7. Freeze centrifuge tubes at -20°C immediately.

Procedure

1. Digest Samples

1.1. In a fume hood, add 10 µL of phenol to each 2 mL centrifuge tube.

1.2. Next, add 1,000 µL of concentrated sulfuric acid to all centrifuge tubes. The reaction between the acid and the sample increases the temperature of the centrifuge tube rapidly. Handle all tubes carefully after the acid has been added. Make sure the cap is sealed tightly, then vortex. This achieves the sample: sulfuric acid: phenol ratio of 40:1:100 (Dubois et al. 1956a).

1.3. Confirm all caps are tightly sealed.

1.4. Place tubes in an aluminum rack within an aluminum pan (do not use plastic racks – they will melt).

1.5. Place all tubes in the thermoblock and allow them to bake at 90 °C for 5 minutes.

1.6. After baking, vortex tubes briefly and place tubes in a dark cabinet all allow them to cool to room temperature for 30 minutes (be consistent with the timing of all steps).

2. Read Absorbance (perform these steps in a fume hood)

2.1. For each cooled sample, vortex the microcentrifuge tube.

2.2. In a fume hood, pipette 150 µL of sample into each of three microplate wells (150 µL per well). (Note: Do NOT use UV-transparent microplates. The sulfuric acid will degrade the walls of the microplate. Use the less expensive plates identified in the Equipment and Materials list above.)

2.3. Read the microplate absorbance at 490 nm using the microplate reader.

2.4. Save data obtained for reading in Microsoft Excel for later reference.

Waste & Clean-Up

- Contaminated pipette tips should be thrown in the dry waste container
- Ensure all liquid waste is placed in the liquid waste container

Appendix IV: Image analysis of stained aggregates observed using a confocal microscope during phase 1

Table IV-a: Results of microplastics presence and positioning within granule sections observed with a confocal microscope during high organic loading experimental phase

Section sample	Sample date	Section area visible under microscope objective (mm^2)	Section distance from surface of granule (μm)	Diameter of whole granule (um)	Section location region within granule defined in figure 4-13	Microplastics present?	Microplastics location on section
1	11/11/18	0.93	0-20	420	A	no	
2	11/11/18	0.05	20-40	420	A	yes	edge
3	11/11/18	0.06	40-60	420	A	yes	edge
4	11/11/18	0.08	100-120	420	B	yes	center
5	11/11/18	0.06	100-120	420	A	yes	edge
6	11/11/18	1.13	100-120	420	B	yes	center
7	11/26/18	0.32	150-180	870	B	yes	center
8	11/9/2018	1.29	360-380	1000	C	no	
9	11/09/2018	1.24	120-140	1000	B	no	
10	11/09/2018	1.29	260-280	1000	B	no	
11	11/16/2018	1.31	160-180	700	B	yes	center
12	11/16/2018	1.23	220-240	700	C	no	
13	11/16/18	1.29	160-180	700	B	no	
14	11/16/2018	1.18	120-140	700	B	yes	center
15	11/19/2018	1.18	240-260	640	C	no	
16	11/16/2018	1.20	280-300	700	C	no	
17	11/19/2018	0.99	220-240	640	C	no	
18	11/23/2018	1.12	540-570	1080	C	no	
19	11/26/2018	0.91	420-450	870	C	no	
20	11/26/2018	0.96	360-390	870	C	no	
21	11/26/2018	0.99	180-210	870	B	no	
22	11/26/2018	0.88	120-150	870	B	yes	close to edge
23	11/26/2018	1.09	30-60	870	A	no	

24	11/30/2018	0.71	30-60	930	A	yes	center
25	11/30/2018	1.02	270-300	930	B	yes	close to edge
26	11/30/2018	1.04	360-390	930	C	no	
27	11/30/2018	0.93	420-450	930	C	no	
	Total sample area	24.46					

Table IV-b: Results of microplastics presence and positioning within stained floc samples observed with a confocal microscope during high organic loading experimental phase

Sample number	Sample date	Area of floc viewed under the microscope (mm^2)	Microplastics present?	Microplastics location within floc
1	11/30/18	0.28	no	
2	11/30/18	0.29	yes	edge
3	11/19/2018	0.01	no	
4	11/19/2018	0.29	no	
5	11/19/2018	0.08	yes	close to edge
6	11/26/18	0.16	no	
7	11/12/2018	0.59	no	
8	11/19/2018	0.12	no	
9	11/26/2018	1.08	yes	center
	Total area =	2.91		

Appendix V: Image analysis of stained aggregates observed using a confocal microscope during phase 2

Table V-a: Results of microplastics presence and positioning within granule sections observed with a confocal microscope during low organic loading experimental phase

Section sample	Sample date	Section area under microscope objective (mm^2)	Section distance from surface of granule (μm)	diameter of whole granule (μm)	Section location region within granule defined in figure 4-13	Microplastics present?	Microplastics location on section
1	8/31/19	0.76	90-120	450	B	yes	close to edge
2	8/31/19	1.09	210-240	450	C	no	
3	8/31/19	1.05	210-240	450	C	no	
4	8/31/19	1.13	150-180	450	A	yes	edge
5	8/31/19	0.97	150-180	450	C	yes	center
6	8/31/19	0.97	180-210	450	C	no	
7	8/31/19	1.08	0-30	450	A	no	
8	9/06/19	1.18	80-100	280	C	yes	center
9	9/06/19	1.24	100-120	280	B	yes	close to edge
10	8/30/2019	0.99	60-80	400	B	yes	center
11	8/31/2019	1.01	30-60	450	A	no	
12	9/16/2019	1.11	0-30	360	A	yes	close to edge
13	9/16/2019	1.03	0-30	360	A	no	
14	9/16/2019	0.53	90-120	360	B	yes	center
15	9/16/2019	0.91	90-120	360	B	no	
16	9/16/2019	1.08	150-180	360	A	yes	edge
17	9/16/2019	0.93	150-180	360	A	yes	edge
18	9/16/2019	0.94	150-180	360	C	no	
19	9/16/2019	1.20	120-150	360	C	no	
20	9/16/2019	0.98	150-180	360	C	no	
21	9/16/2019	0.89	150-180	360	C	no	
22	9/16/2019	1.06	120-150	360	B	yes	close to edge
23	9/16/2019	1.03	120-150	360	B	yes	close to edge
Total area =		23.15					

Table V-b: Results of microplastics presence and positioning within stained floc samples observed with a confocal microscope during high organic loading experimental phase

Sample number	Sample date	Area of floc viewed under the microscope (mm^2)	Microplastics present?	Microplastics location within floc
1	08/28/19	0.31	yes	edge
2	08/28/19	0.02	yes	edge
3	08/28/19	0.35	no	
4	09/02/19	0.28	yes	edge
5	09/02/19	0.27	no	
6	09/16/19	0.06	yes	edge
7	09/16/19	0.16	no	
8	08/30/19	0.24	yes	edge
9	08/30/19	0.41	yes	edge
10	08/30/19	0.04	yes	edge
11	09/06/19	0.15	no	
12	09/06/19	0.22	no	
13	09/13/19	0.07	no	
14	09/13/19	0.16	no	
Total area =		2.74		